

**RAB GTPASE REGULATION OF APICAL CYSTIC FIBROSIS TRANSMEMBRANE
CONDUCTANCE REGULATOR RECYCLING IN POLARIZED INTESTINAL
EPITHELIAL CELLS**

by

Mark Robert Silvis

B.S. Biology, Geneva College, 1999

Submitted to the Graduate Faculty of
the Department of Cell Biology & Physiology in partial fulfillment
of the requirements for the degree of
Doctor of Philosophy

University of Pittsburgh

2009

UNIVERSITY OF PITTSBURGH

School of Medicine

This dissertation was presented

by

Mark Robert Silvis

It was defended on

September 3, 2009

and approved by

Daniel C. Devor, Ph.D., Associate Professor, Cell Biology and Physiology
Committee Chair

Gerard L. Apodaca, Ph.D., Professor, Medicine

John P. Johnson, M.D., Professor, Medicine

Neil A. Bradbury, Ph.D., Associate Professor, Physiology and Biophysics, Rosalind Franklin
University of Science and Medicine, Chicago, IL
(Dissertation Director)

Ray A. Frizzell, Ph.D., Professor, Cell Biology and Physiology
(Dissertation Director)

Copyright © by Mark Robert Silvis

2009

**RAB GTPASE REGULATION OF APICAL CFTR RECYCLING IN POLARIZED
INTESTINAL EPITHELIAL CELLS**

Mark Robert Silvis, Ph.D.

University of Pittsburgh, 2009

The regulated recycling of endocytosed membrane proteins at the plasma membrane is an important intracellular trafficking process that can regulate the copy number of proteins at the membrane and thereby modulate their function and the physiology of the tissue as a whole. The Cystic Fibrosis Transmembrane conductance Regulator (CFTR), a cAMP/PKA-activated anion channel, undergoes rapid and efficient recycling at the apical plasma membrane in polarized epithelial cells. The cellular mechanisms that facilitate CFTR recycling are understood poorly, especially in polarized cell systems, yet this process ensures the proper channel copy number at the apical membrane, and it is defective in the common CFTR mutant, $\Delta F508$. Using a physiologically relevant model that recapitulates the *in vivo* secretory functions of the intestinal epithelia, I tested the hypothesis that distinct members of the Rab family of GTPases mediate the recycling of CFTR at the apical plasma membrane and that this process facilitates transepithelial anion secretion by maintaining a physiologically functional surface density of CFTR channels. The role of the Rab11 isoforms in CFTR recycling was investigated using the colonic epithelial cell line, T84, and rat intestine for *in vivo* studies. Immuno-isolation of Rab11 vesicles revealed endogenous CFTR within both the Rab11a and Rab11b compartments; however, only perturbing Rab11b expression or function attenuated the CFTR-mediated, cAMP-activated anion efflux. In

polarized epithelial monolayers, mutant Rab11b inhibited the forskolin-stimulated transepithelial anion secretion by reducing the apical membrane density of CFTR. Biotin protection assays revealed a dependence of CFTR recycling on functional Rab11b, not Rab11a, demonstrating the selective requirement for the Rab11b isoform. Therefore, apical CFTR copy number is regulated by Rab11b-mediated recycling, which facilitates the agonist-stimulated, transepithelial anion response in polarized intestinal epithelial cells. The identification of Rab11b as a mediator of recycling reveals an apical recycling itinerary unidentified previously and emphasizes the importance of elucidating the membrane recycling itineraries in polarized epithelial cell models, which mimic the normal physiology of tissue. Understanding these processes within relevant models have direct implications for understanding normal cell biology and tissue physiology and form a foundation for future clinical therapies designed to correct disease processes arising from improper membrane recycling.

TABLE OF CONTENTS

PREFACE.....	xii
ABBREVIATIONS.....	xiii
1.0 INTRODUCTION.....	1
1.1 OVERVIEW.....	1
1.2 POLARIZED EPITHELIAL CELLS.....	2
1.2.1 Epithelia morphology.....	2
1.2.2 Epithelia function.....	5
1.3 POLARIZED MEMEBRANE TRAFFICKING AND RECYCLING.....	5
1.4 RAB FAMILY OF GTPASES.....	7
1.4.1 Brief history of the Rab family of GTPases.....	7
1.4.2 Rab GTPases.....	9
1.4.3 Rabs function as molecular switches.....	11
1.4.4 Rab effectors.....	13
1.4.5 Rab function in membrane traffic.....	14
1.4.5.1 Rabs as vesicle bud initiators.....	16
1.4.5.2 Rabs as transport mediators.....	17
1.4.5.3 Rabs as tethering factors.....	18
1.4.5.4 Rabs as fusion regulators.....	18
1.4.6 Rabs decipher compartment identity.....	19
1.4.7 Rab11 family of GTPases.....	22
1.4.7.1 Rab11a and Rab11b localization.....	22
1.4.7.2 Rab11a and Rab11b function.....	26
1.5 CYSTIC FIBROSIS.....	29
1.6 CFTR.....	30
1.6.1 CFTR Structure.....	30

1.6.2	CFTR localization in native tissue and endogenous expression systems.....	32
1.6.3	CFTR biosynthesis in polarized epithelial cells.....	33
1.6.4	CFTR endocytosis and recycling in polarized epithelial cells.....	34
1.6.5	Constitutive recycling of CFTR in polarized epithelia.....	35
1.6.6	Regulated recycling of CFTR in polarized epithelia.....	36
1.7	COLONIC EPITHELIAL T84 CELLS.....	37
1.7.1	Morphology.....	37
1.7.2	Functional Studies.....	38
1.7.3	T84 cells as a model of intestinal physiology.....	40
1.8	GOALS OF THIS DISSERTATION.....	44
2.0	RAB11B REGULATION OF APICAL CFTR REYCLCING IN POLARIZED INTESTINAL EPITHELIAL CELLS.....	46
2.1	INTRODUCTION.....	46
2.2	RESULTS.....	48
2.2.1	Endogenous CFTR Localizes to Punctate Vesicles at the Apical Pole of Polarized T84 Cells.....	48
2.2.2	CFTR colocalizes with both Rab11a and Rab11b in polarized T84 cells.....	49
2.2.3	CFTR and Rab11 colocalize <i>in vivo</i>	51
2.2.4	Immuno-magnetic isolation of Rab11-positive vesicles reveals the presence of CFTR.....	55
2.2.5	Rab11b S25N selectively impairs CFTR function in SPQ halide efflux assays.....	58
2.2.6	Rab11b Q70L increases CFTR-mediated anion efflux.....	65
2.2.7	Dominant negative Rab11b expression inhibits CFTR chloride secretion across polarized T84 monolayers.....	68
2.2.8	Dominant negative Rab11b expression decreases CFTR protein expression at the apical membranes of polarized T84 monolayers....	72
2.2.9	Dominant negative Rab11b inhibits apical recycling of CFTR in polarized intestinal epithelial cells.....	75
2.2.10	shRNA-mediated knockdown of Rab11b inhibits CFTR-mediated	

increases in SPQ fluorescence in T84 cells.....	78
2.3 DISCUSSION.....	81
2.3.1 Rab11 Isoform Comparisons.....	83
2.3.2 Cell type-dependent recycling pathways.....	84
3.0 CONCLUSIONS.....	87
3.1 CFTR TRAFFIC IN POLARIZED EPITHELIAL CELLS.....	88
3.2 LOCALIZATION OF ENDOGENOUS CFTR.....	91
3.3 ROLE OF RAB11A IN CFTR TRAFFIC.....	95
3.4 REGULATION OF STIMULATED AND CONSTITUTIVE CFTR TRAFFIC BY RAB11B.....	99
3.5 RAB11A AND RAB11B.....	103
3.6 RECYCLING MECHANISMS.....	110
3.6.1 Rab11 Trafficking	110
3.6.2 Agonist-dependent recycling by Rab11s and their effectors	112
3.6.3 Rab-cargo interactions and recycling motifs.....	113
3.7 IMPORTANCE FROM A CF PERSPECTIVE.....	114
4.0 MATERIALS AND METHODS.....	115
4.1 Cell culture, electroporation, and adenoviral transduction.....	115
4.2 Antibodies.....	116
4.3 DNA constructs, RT-PCR, and Rab11a- & b-S25N Adenoviruses.....	117
4.4 Immunoisolation of Rab11-positive endosomes.....	119
4.5 Immunofluorescence labeling.....	120
4.6 SPQ fluorescence assays.....	121
4.7 Ussing Chamber Experiments.....	122
4.8 Cell Surface Biotinylation & Apical Recycling Assays.....	122

4.9 Statistical analysis.....	123
5.0 APPENDIX.....	124
Figure A.1: SPQ fluorescence assays measure CFTR function.....	124
Figure A.2: Dose effect of GFP-Rab11b-S25N expression levels on CFTR-mediated SPQ fluorescence response.....	126
Figure A.3: Endocytosis of CFTR from the apical plasma membrane in polarized T84 cells.....	127
Figure A.4: Immunoisolation of Rab11a and Rab11b vesicles reveals the overlap of each isoform.....	129
Figure A.5: Comparison of the apical membrane CFTR density in the Rab11a- and Rab11b-S25N-expressing T84 monolayers with or without cAMP/PKA stimulation.....	130
6.0 BIBLIOGRAPHY.....	132

LIST OF FIGURES

Figure 1.1: Morphology of a polarized epitheliamonolayer.....	4
Figure 1.2: The small G protein superfamily.....	8
Figure 1.3: Structure of Rab GTPases.....	10
Figure 1.4: The Rab GTPase cycles.....	12
Figure 1.5: Overview of the membrane trafficking process.....	15
Figure 1.6: Rabs decipher membrane identity.....	21
Figure 1.7: Model depicting the proposed structure of CFTR.....	31
Figure 1.8: Transmission Electron Micrograpy of a polarized T84 cell monolayer.....	39
Figure 1.9: Schematic representation of Cl ⁻ secretion in colonic epithelial cells.....	41
Figure 1.10: Model of chloride secretion in the colon	43
Figure 2.1: Localization of endogenous CFTR in polarized T84 cells.....	50
Figure 2.2: Rab11a and Rab11b are expressed in T84 cells and co-localize with CFTR.....	52
Figure 2.3: CFTR and Rab11 colocalize in rat intestinal crypts <i>in vivo</i>	54
Figure 2.4: CFTR is present within Rab11 immuno-isolated vesicles.....	56
Figure 2.5: Dominant negative Rab11b impairs CFTR-mediated increases in halide permeability.....	59
Figure 2.6: Dominant active Rab11b accelerates the CFTR-mediated halide permeability response to agonist.....	66
Figure 2.7: Dominant negative Rab11b expression inhibits short circuit current (I _{SC}) in polarized T84 cell monolayers.....	70
Figure 2.8: Dominant negative Rab11b overexpression decreases apical membrane CFTR in polarized T84 cells.....	73
Figure 2.9: Dominant negative Rab11b inhibits the apical recycling of endogenous CFTR in polarized T84 cells.....	76
Figure 2.10: shRNA knockdown of Rab11b inhibits CFTR-mediated halide efflux from T84 cells.....	79
Figure 3.1: Two potential interrelationships for Rab11a and Rab11b.....	94
Figure 3.2: A potential role for Rab11a in recycling of CFTR.....	98

Figure 3.3: The roles of Rab11b in CFTR recycling at the apical plasma membrane.....	102
Figure 3.4: Two potential interrelationships of the Rab11a and Rab11b recycling itineraries.....	106
Figure A.1: SPQ fluorescence assays measure CFTR function.....	124
Figure A.2: Dose effect of GFP-Rab11b-S25N expression levels on CFTR-mediated SPQ fluorescence response.....	126
Figure A.3: Endocytosis of CFTR from the apical plasma membrane in polarized T84 cells.....	127
Figure A.4: Immunisation of Rab11a and Rab11b vesicles reveals the overlap of each isoform.....	129
Figure A.5: Figure A.5: Comparison of the apical membrane CFTR densities in Rab11a-S25N- and Rab11b-S25N-expressing T84 monolayers with or without cAMP/PKA stimulation.....	130

PREFACE

First and foremost, I am deeply indebted to my parents, Mr. and Mrs. Robert A. Silvis, who have always supported me in every way possible. Mom and Dad, I am blessed to be your son and I am very thankful for all you've done to help me earn this degree. Your belief in me and what I can do has been a constant inspiration. I am also thankful for my sister and brother and their support. Misty and Ross, you have been with me through this and I thank you for all the times you have encouraged me to push through when things were difficult.

I would also like to thank my dissertation advisors, Dr. Neil Bradbury and Dr. Ray Frizzell. Your guidance and mentorship has helped me mature as a scientist and I look forward to utilizing the skills I have learned under your direction. Dr. Frizzell, I especially appreciate all the revising and editing of my manuscripts as this has taught me to be a better writer. I would also like to thank the members of my thesis committee, Drs. Dan Devor, John Johnson, and Gerry Apodaca, for all of their helpful suggestions and support throughout my graduate work.

Finally, I would like to thank all of the members of the Frizzell lab for their camaraderie and support. Each of you made my time as a graduate student a positive, memorable experience. I especially thank Drs. Bela Schmidt, Carol Bertrand, Kathi Peters, and Michael Butterworth for contributing to my training as a scientist. You each took time to give me your support, knowledge, and experience and to teach me the skills that it takes to be an excellent researcher.

ABBREVIATIONS

ARE	Apical Recycling Endosomes
ATP	Adenosine Triphosphate
BHK	Baby Hamster Kidney
cAMP	cyclic Adenosine Monophosphate
CCV	Clathrin-coated Vesicle
CF	Cystic Fibrosis
CFBE	Cystic Fibrosis Bronchial Epithelia
CFTR	Cystic Fibrosis Transmembrane conductance Regulator
CHO	Chinese Hamster Ovary
CT	Carboxyl-terminus
DIC	Differential Interference Contrast
dIgA	dimeric immunoglobulin A
EE	Early Endosomes
EM	Electron Microscopy
ER	Endoplasmic Reticulum
ERAD	ER-associated Degradation
FIP	Rab11 Family of Interacting Protein
GAP	GTPase Activating Protein
GDF	GDI Displacement Factor
GDI	GDP Dissociation Inhibitor
GDP	Guanine Diphosphate
GEF	Guanine nucleotide Exchange Factors
GFP	Green Fluorescent Protein

GTP	Guanine Triphosphate
HEK	Human Epithelial Kidney
Isc	Short Circuit Current
MDCK	Madin-Darby Canine Kidney
NBD	Nucleotide Binding Domains
NKCC1	Na⁺-K⁺-2Cl⁻ cotransporter
NSF	N-ethyl-maleimide-sensitive factor
NT	Amino-terminus
P_i	Inorganic Phosphate
pIgR	poly-Immunoglobulin Receptor
PKA	Protein Kinase A
PM	Plasma Membrane
PNS	Post-nuclear Supernatant
RD	regulatory domain
REP	Rab Escort Proteins
RER	rough endoplasmic reticulum
RT-PCR	Reverse Transcriptase Polymerase Chain Reaction
ROI	Region of Interest
SEM	Standard Error of the Mean
shRNA	Short Hairpin RNA
SNAP	soluble NSF attachment proteins
SNARE	SNAP receptor
SPQ	6-methoxy-N-(3-sulfopropyl) quinolinium
TEM	Transmission Electron Microscopy
TER	Transepithelial Resistance

TfR	Transferrin Receptor
TGN	<i>trans</i> Golgi network
TJ	Tight Junction
VIP	Vasoactive Intestinal Peptide
WT	Wild Type
ZO-1	Zona Occludin

1.0 INTRODUCTION

1.1 OVERVIEW

The recycling of integral membrane proteins between the myriad of intracellular compartments and the cell surface, which is necessary for maintaining the appropriate copy numbers of receptors, transporters, and ion channels within the plasma membrane, is an important biological function of cells. In fact, the physiological functions of tissues are supported by the efficient, specific, and complex trafficking pathways that are inherent to the individual cells that comprise the tissue as a whole. The purpose of this work is to contribute to the general understanding of the apical membrane recycling pathways within a relevant, tissue-specific cell model that simulates the *in vivo* physiological mechanisms of the intestine. In this dissertation, I focused on investigating the recycling pathways that mediate the membrane turnover of a physiologically and clinically important ion channel within the apical subdomain of a polarized epithelial intestinal cell model. This work demonstrates the complexity of the apical recycling itineraries by revealing two disparate, non-redundant trafficking functions for two highly homologous protein isoforms within a physiologically relevant polarized epithelial cell model. Furthermore, it begins to elucidate a distinction between the constitutive, non-stimulated and the regulated, agonist-stimulated recycling of this channel, which contributes to the general understanding of the apical recycling pathways in modulating the cell surface density of an integral membrane protein that functions in the normal physiology of tissue.

1.2 POLARIZED EPITHELIAL CELLS

The polarized epithelia that line the cavities and surface of the body perform crucial physiological functions that are necessary for the survival of the individual. For example, in addition to forming the protective cellular lining that separates the underlying tissues from the outside world, these specialized cell sheets form a selective barrier that enables transepithelial ion transport, and secretion or absorption of molecules to or from the mucosal surface, respectively. The polarized epithelial cell model, established *in vitro* from isolated epithelia, serves as an invaluable tool for understanding the cell biology and molecular physiology of these complex cell types. Specifically, the relative ease with which these cells can be cultured and manipulated *in vitro*, and the phenotypic mimicking of the *in vivo* tissues from which they originate, allow for careful experimentation to elucidate the underlying molecular mechanisms that execute the physiological functions inherent to the epithelia. In the immediate sections below, I will introduce the general characteristics of the polarized epithelial cell model, followed by an introduction of their complex intracellular membrane trafficking routes, with particular focus on apical membrane recycling, which is relevant for the studies performed within this dissertation.

1.2.1 Epithelia Morphology

Epithelia are tissues composed of interconnected cells that form sheets and line the internal and external surfaces of the body. Individual epithelial cells are connected to each other with junctional complexes, including tight junctions, adherens junctions, gap junctions, and desmosomes, which can produce a mono-, stratified, or pseudostratified layer of interconnected cells [1]. The cellular positioning of the tight junction complexes, which form the narrow belts that circumferentially surround the apical-most domain of the lateral surfaces of adjacent epithelial cells [2], morphologically divides polarized epithelial cells into two distinct domains,

the apical and basolateral plasma membranes [3] (See Figure 1.1). While the basolateral domain contacts the basement membrane and adjacent cells within the monolayer, the apical domain faces the lumen of organs or the external surface of the body. This unique cell morphology, formed by the bordering tight junction complexes, prevents the intramembrane diffusion of lipids and proteins and enables the apical and basolateral domains to have unique compositions. Furthermore, as will be discussed in Section 1.3, the targeted delivery of proteins that emerge from the biosynthetic pathway, in addition to the subsequent post-endocytic recycling of these proteins to specific membrane domains, generates and maintains the idiosyncratic nature of these membranes.

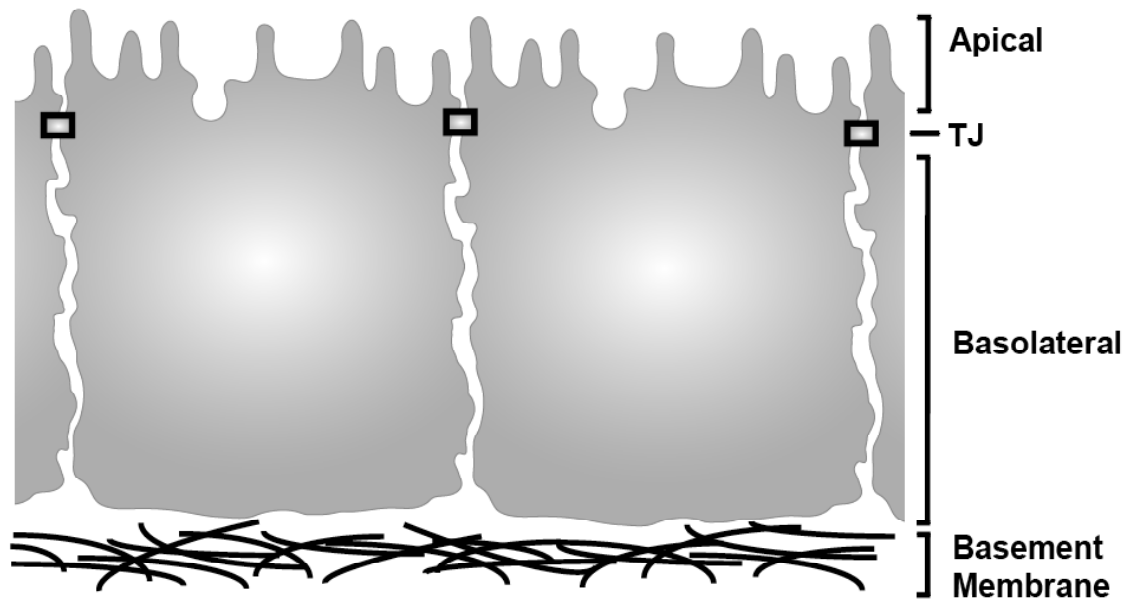


Figure 1.1: Morphology of a polarized epithelial cell monolayer.

Polarized epithelial cells are structurally and functionally divided into the apical and basolateral domains by tight junctions (TJ). The apical plasma membranes face the lumen of organs or the external world and are studded with microvilli. The basolateral membranes face adjacent cells and adhere to the underlying basement membrane.

1.2.2 Epithelia Function

Epithelia perform crucial functions, including: protection against invasion by toxins and pathogens, absorption or secretion of nutrients, and ion transport [4]. Their ability to form selectively permeable barriers between two compartments of the body, whereby they direct the transport of ions and solutes, is especially relevant for the work contained here (For a specific example, see Section 1.7.3: “T84 cells as a model of intestinal physiology”). This vectorial ion transport, which is performed by secretory and absorptive epithelia, requires the polarized distribution of ion channels and transporters between the structurally and functionally unique apical and basolateral plasma membranes [5]. In addition, the selectively permeable nature of the intercellular tight junctions, which is specified by the protein components of these junctional complexes and is unique to the physiology of the tissue in which they are found, allow for the paracellular movement of water and solutes [6, 7]. Therefore, polarized epithelial monolayers perform functions necessary for the normal physiology of the tissue they line, such as mediating the vectorial transport of fluids or solutes against concentration gradients in a secretory or absorptive fashion in the intestine [8].

1.3 POLARIZED MEMBRANE TRAFFICKING AND RECYCLING

The spatial and temporal distribution of lipids and proteins that is characteristic of the eukaryotic cell necessitates highly regulated transport mechanisms for the trafficking of cargo-carrying vesicles between distinct membrane-bound organelles localized at specific intracellular locations. In 1975, the pioneering work of George Palade revealed the earliest evidence for what is today known as “vesicular transport” when he described the presence of newly synthesized proteins within the membrane-enclosed organelles of the secretory pathway en route to the extracellular

milieu [9]. Palade's work remains the foundation for a sub-specialty of the field of cell biology: membrane trafficking. Membrane trafficking through the cell is a highly dynamic process in which intracellular compartments communicate via membrane-enclosed vesicular structures that shuttle cargo molecules to their appropriate destinations.

In polarized epithelial cells, the establishment of a polarized distribution of membrane proteins to their site of function requires the active targeting of proteins to distinct apical and basolateral surfaces by elaborate intracellular sorting and trafficking events [10]. For instance, the targeted delivery of proteins that are selected and sorted by their cognate receptors as they emerge from the biosynthetic pathway functions to generate and then maintain the unique membrane composition of each cellular domain [11]. In addition, numerous studies have demonstrated that ion channels and transporters that are required for the absorptive or secretory functions of the intestines are not stable components of the plasma membrane, but commute between the plasma membrane and intracellular storage compartments [12-14]. Of particular relevance to this work is the process of membrane protein recycling; whereby post-endocytic intracellular trafficking mechanisms recognize, sort, and return proteins to the correct plasma membrane domain where they function. The efficient recycling of membrane proteins between the intracellular, membrane-bound compartments and the cell surface serves to regulate the copy number and therefore the availability of functional molecules at the plasma membrane. Thus, in addition to regulating the activation states of transport proteins localized to the cell surface by agonists and secretagogues, the membrane trafficking mechanisms that manipulate their cell surface densities also enables polarized cells to precisely modulate their physiological functions [15].

1.4 RAB FAMILY OF GTPASES

Key to the efficient and specific nature of membrane trafficking pathways, including membrane recycling, are the Rab family of small GTPases, which are central regulators of the complex orchestration of membrane traffic. In the sections below, I will discuss the discovery of the Rab GTPases; the distinct steps of membrane traffic that they regulate; and how their intrinsic GTPase activity enables them to function as regulators of membrane traffic. Finally, I will narrow the focus on Rab GTPases by discussing the Rab11 family and give insight in to how this particular subset of Rabs function to regulate the apical membrane recycling in polarized epithelial cells.

1.4.1 Brief history of the Rab Family of GTPases

An ortholog of the Rab family of GTPases was discovered originally in 1986 by Gallwitz and colleagues when they found that the 23.5kDa protein product of the ras-related *YPT1* gene from *Saccharomyces cerevisiae* was essential for cell growth [16, 17]. A year later, Salminen and Novick reported that a GTP-binding protein, Sec4, controlled a late stage of the secretory pathway in yeast: fusion of post-Golgi secretory vesicles to the plasma membrane [18]. Subsequently, the protein product of *YPT1*, Ypt1, was demonstrated to be necessary for the secretory processes of endoplasmic reticulum (ER) to Golgi transport as its deletion caused accumulation of small transport vesicles in yeast cytosol [19, 20].

Within a year, four mammalian orthologs of the *YPT* genes were cloned from rat brain cDNA and termed 'Rab', for 'Ras-related in brain' [21, 22]. Like Ypt1 and Sec4, Rab proteins were shown to be necessary for eukaryotic cell trafficking pathways analogous to those in yeast

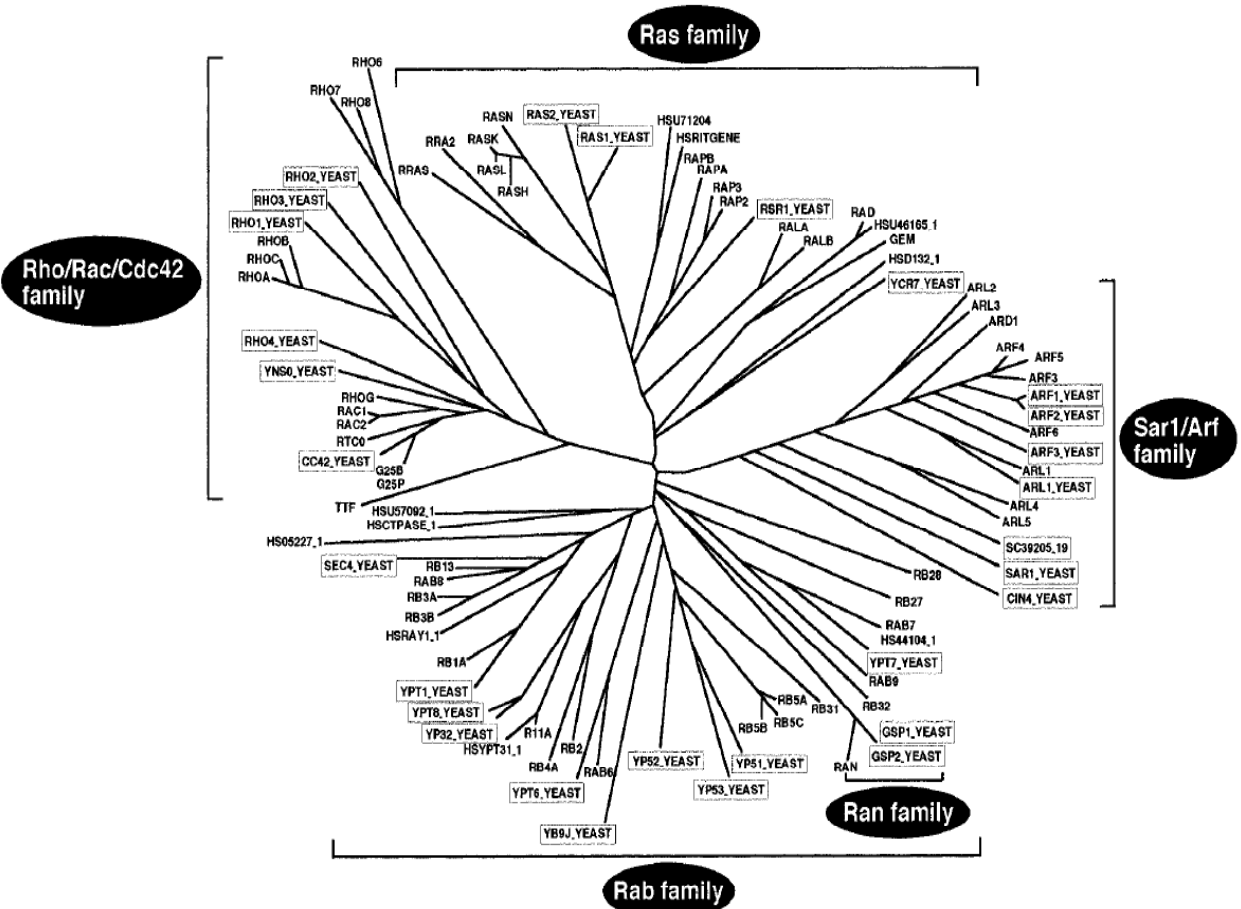


Figure 1.2: The small G protein superfamily [29].

Dendrogram of all known yeast (boxes) and human sequences of the ras superfamily.

[23]. Furthermore, several of the yeast Ypt proteins were found to have one or more putative mammalian homologs that enabled the functional replacement of a mammalian Rab for its yeast counterpart, which pointed to the conserved nature of Rabs across eukaryotic cell types [24, 25]. Since the early documentations of Ypt1 and Sec4, eleven additional Rab genes have been found in yeast (*YPT*). The mammalian genome encodes more than sixty Rabs [26-28], which reflects the increased complexity of intracellular trafficking events within higher eukaryotes.

1.4.2 Rab GTPases

The mammalian Rabs belong to and comprise the largest family of monomeric, GTP-binding proteins within the Ras superfamily of small GTPases, which includes five structurally classified families: ras, rho/rac, rab, arf, and ran [29] (See Figure 1.2). The Rab family members share approximately 30% amino acid homology with the Ras proteins. Rab gene sequences are distributed widely over the human chromosomes and have been found in all eukaryotes investigated including yeast, plants, and mammals, which emphasizes their importance in eukaryotic cell biology [30].

Most Rabs are expressed ubiquitously in all human tissues; however, some are tissue-specific, such as the neuronally expressed Rab3a [31] or Rab17 and Rab25, which are only expressed in epithelial cells [32]. Within the Rab family exists several Rab subfamilies, which contain closely related isoforms that share 75-95% sequence identity and have potentially overlapping functions [26]. Known subfamilies include: Rab1, 3, 4, 5, 6, 8, 11, 22, 27, and 40; however, a number of Rab proteins cannot be grouped into these subfamilies.

The amino acid sequences for Rabs encode small (20-29kDa) soluble proteins. Like all GTP-binding proteins, the Rabs have conserved amino acid residues that mediate guanine triphosphate



Figure 1.3: Structure of Rab GTPases (modified from [29]).

The Rab consensus sequences responsible for binding to GTP and GDP, in addition to the GTPase activities, are shown above (I-IV). The Switch I and II regions (SwI, SwII), responsible for effector binding, are highlighted with solid black bars, while the carboxyl terminally-located lipid modification site is noted with a C.

(GTP) and guanine diphosphate (GDP) nucleotide binding, as well as sequences that encode the GTPase domain, which hydrolyzes bound GTP to GDP (See Figure 1.3). Rabs also contain two active regions, termed Switch I and Switch II, which undergo large conformational changes upon GTP binding or GTP hydrolysis and enable interactions with downstream effectors in their GTP-bound state. Cysteine-based consensus sequences within the Rab carboxyl termini are prenylated post-translationally with geranylgeranyl lipid moieties, which enable Rabs to associate reversibly with the cytosolic face of discrete intracellular membranes. The main sequence divergences among Rabs are found within their hypervariable carboxyl termini, which are thought to be responsible for differences in their subcellular localization. In the section below, I will introduce how these structural and functional intricacies of Rab GTPases make them specialized regulators of membrane trafficking processes.

1.4.3 Rabs function as molecular switches

Like other GTPases within the Ras superfamily, Rab proteins bind to guanine nucleotides and are capable of hydrolyzing GTP to GDP [29]. GTP-bound Rabs are regarded as being in an ‘active’ state while GDP-bound Rabs are considered ‘inactive’. Rabs undergo multiple rounds of activation/inactivation and this transient, reversible conversion between the two distinct structural conformations epitomizes their ability to act as molecular switches (See Figure 1.4). Activation of Rabs by GTP binding is facilitated by Guanine nucleotide Exchange Factors (GEFs) [33], which enable downstream trafficking processes through the coordinated recruitment of effector proteins to the GTP-bound Rabs (step c, d). In addition, active Rabs are bound to the membrane, which is necessary for specifying the correct subcellular location for the localized recruitment of trafficking machinery [34]. Rabs have a slow GTP hydrolysis rate inherently and rely upon the activation of their GTPase activity by GTPase Activating Proteins

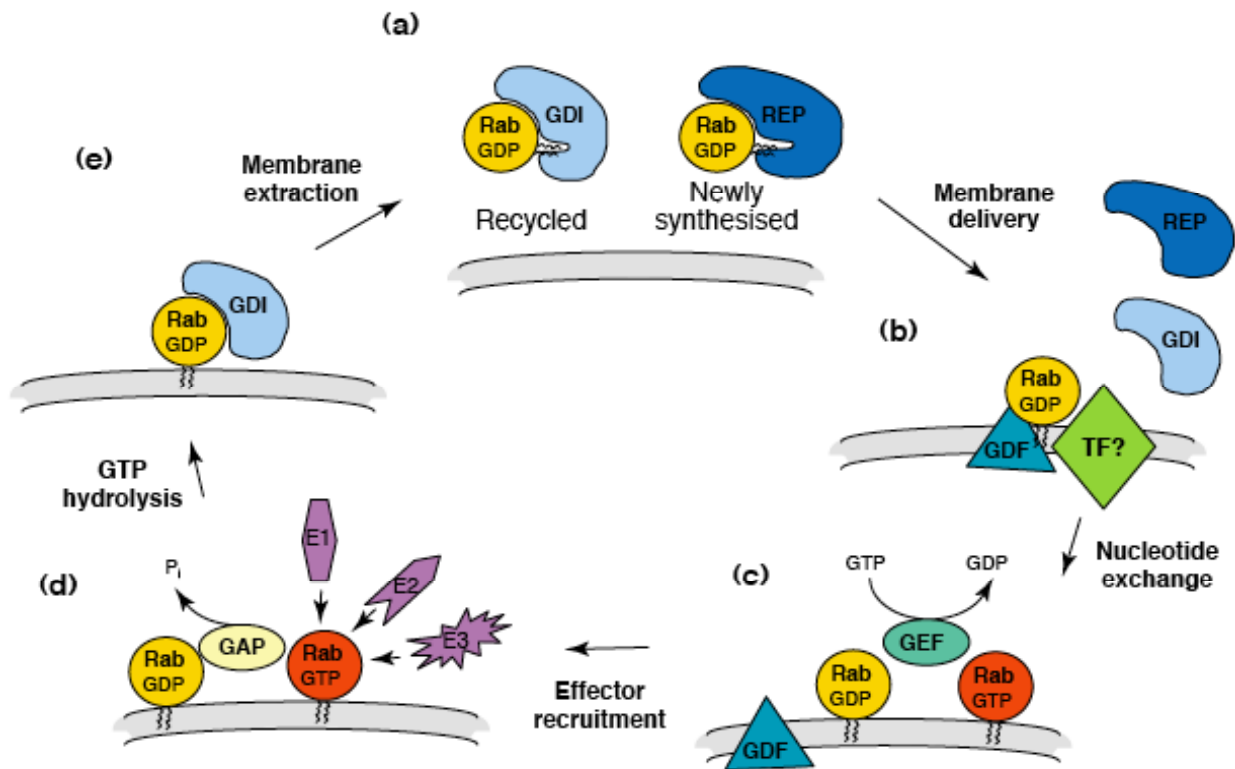


Figure 1.4: The Rab GTPase cycles [39].

The diagram above depicts the Rab GTPase cycles of membrane insertion/extraction by GDF/GDI, respectively; and the activation/inactivation by GEF/GAP, respectively, as described in detail in the text.

(GAPs) [35], which cause the release of inorganic phosphate (P_i) and inactivate the Rab (step d). GDP-bound Rab is then extracted from the membrane and bound by cytosolic Rab GDP Dissociation Inhibitor (GDI) (step e & a), which retains the GDP-Rab in the cytosol by masking its geranylgeranyl moiety [36]. Recycled Rab proteins are delivered to specific membranous sites by GDIs and require a GDI Displacement Factor (GDF) to transfer the prenylated Rab from the GDI to the membrane [37]. Similarly, newly synthesized Rab proteins are bound to Rab Escort Proteins (REPs) in the GDP-bound form and are also displaced by GDFs (step a & b) [38]. After membrane binding, GEFs catalyze the exchange of GDP for GTP and activate membrane-bound Rabs for another round of effector recruitment (step b & c). Thus, Rab GTPases cycle through rounds of activation/inactivation and membrane insertion/extraction at discrete subcellular locations to coordinate and regulate membrane trafficking process. In the section below, I will explain how the molecular switching capability of Rabs enables them to control the complex processes of membrane traffic through the regulated interactions with downstream effector proteins.

1.4.4 Rab Effectors

Rab effector proteins are defined operationally by their ability to bind selectively to a specific Rab in its GTP-bound state. Effectors are termed thus as they are recruited to an activated Rab at a discrete subcellular localization where they mediate at least one element of its downstream effects [40]. Inactivation of Rabs by GAPs initiates a conformational change in the switch regions that causes the release of effectors from the Rab, thereby halting the downstream trafficking events. Rab effectors have been identified by a variety of techniques, including genetic screens, yeast two hybrid, and affinity purification. In contrast to the high degree of

conservation within the Rab GTPase family, the effectors documented to date are unrelated, which is indicative of the diversity of downstream actions that they perform. A single Rab can have more than one effector, for example, Rab5 has been shown to bind to 22 different proteins in its GTP-bound form [41]. Rabs are able to signal through a variety of different effectors that translate the signal from one Rab protein to several diverse aspects of membrane transport. Therefore, a specific Rab GTPase, in concert with its specific effectors, is capable of mediating multiple steps in the membrane trafficking itinerary, as I will discuss in detail in the following section.

1.4.5 Rab functions in membrane traffic

Cells utilize lipid bilayer-enclosed vesicles for the transport of molecules from one subcellular location to another by a multi-step process. The diagram in Figure 1.5 outlines the four basic steps in membrane trafficking, which include: (1) budding, (2) movement (or trafficking), (3) tethering, and (4) docking and fusion. The selective recruitment of cargo to a bud site within the donor compartment comprises the earliest stage of the budding vesicle. In addition, budding components including adaptor and coat proteins are recruited to the site of the forming transport intermediate. After budding and scission, the cargo-carrying vesicle is moved through the intracellular space by targeted transport. This requires the coordinated mobilization of vesicles by motor proteins, which rely upon the cytoskeletal framework for the directional movement of vesicles. Arrival of vesicles at a specific target site initiates tethering to vesicle-recognition molecules that ensure specificity at the appropriate acceptor membrane. Finally, tethered vesicles are brought within close proximity to the destination compartment, dock, and then fusion releases the vesicular contents either at a new intracellular location or at the plasma

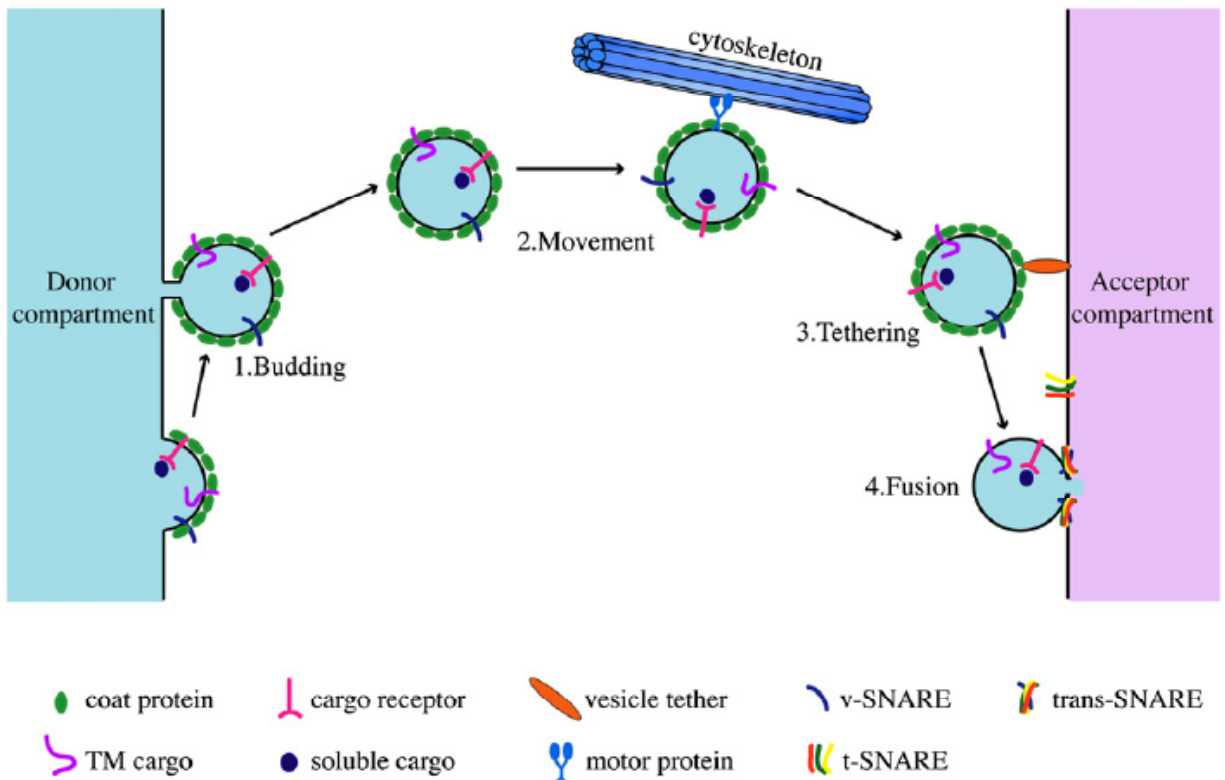


Figure 1.5: Overview of the membrane trafficking process [42].

The schematic above depicts the general trafficking itinerary described in the text. Soluble cargo molecules, bound to their cognate transmembrane-bound receptors, in addition to transmembrane cargo molecules (TM cargo) are recruited to sites of vesicle bud formation, which is initiated by the binding of coat proteins to the donor compartment. Coat and accessory proteins mediate the scission and release of cargo-containing vesicles (1) that undergo directed movement through the intracellular space via interactions with the cytoskeleton-associated motor proteins (2). The arrival of vesicles at the acceptor compartment is met by the tethering of vesicles (3), which allows for the site-specific interactions of cognate t- and v-SNAREs to form trans-SNARE bundles. The formation of trans-SNARE pairs mediates the fusion of the trafficked vesicle with the acceptor compartment (4), thus completing the trafficking itinerary with the delivery of cargo from the donor to the acceptor site.

membrane where the cargo is released into the extracellular milieu. Each step in the membrane trafficking progression requires the spatial and temporal regulation of specific trafficking machinery to perform the functions required for the appropriate movement of membrane proteins and lipids between discrete subcellular locations. In the following four sections, I will overview briefly the role that Rab GTPases, with their unique effectors, play in each of the aforementioned steps, thus explaining why Rabs are considered the central regulators of membrane traffic.

1.4.5.1 Rabs as vesicle bud initiators

Vesicle budding requires the recruitment of specific cargo molecules, adaptor proteins, and coat accessories to the site of vesicle formation within the donor compartment. Various reports have demonstrated a role for some Rab proteins in this process. For instance, *in vitro* studies uncovered a critical function for Rab5 in the recruitment and sequestration of cargo molecules (transferrin receptors) to newly formed clathrin-coated pits at the plasma membrane of human epithelial carcinoma A431 cells [43]. Furthermore, inactivation of Rab5 by its GAP, RN-tre, inhibited clathrin-coated vesicle formation and receptor internalization [44]. Thus, Rab5 appears to be critical for both cargo recruitment and modulation of the adaptor or coat proteins necessary for vesicle formation from the PM. An additional example is the requirement for Rab4 expression to mediate the formation of recycling vesicles containing asialoglycoprotein receptor H1 from the recycling compartment in permeabilized, cytosol-reconstituted MDCK cells [45]. These data suggest that particular Rabs are capable of initiating the earliest step of the trafficking pathway by recruiting specific cargo and budding machinery to the sites of vesicle formation.

1.4.5.2 Rabs as transport mediators

Vesicles containing cargo originating from the donor compartment are moved through the intracellular space by active transport, which requires actin-dependent motors (myosins) or microtubule-dependent motors (kinesins or dyneins) [46]. Rabs confer a directional motility to their bound vesicles by recruiting effectors that mediate binding to the cytoskeleton motors [39], or in some cases Rabs bind cytoskeleton specific motors directly [47]. Thus, the microtubule and actin cytoskeletons serve as rails for Rab-bound vesicles to travel to the targeted destination site. In a well-described example, GTP-bound Rab27a recruits the actin motor, myosin-Va, to pigment containing melanosomes within melanocytes [48]. This recruitment is dependent upon a Rab27a effector, melanophilin, which links Rab27a-positive melanosomes to myosin-Va [49]. Thus, the Rab27a-regulated linkage between the melanosomes and the actin cytoskeleton, via the effectors melanophilin and myosin-Va, mediates the transfer of pigment-containing melanosomes to neighboring keratinocytes that is required for proper skin pigmentation [50]. In a similar example, active Rab11a recruits the effector, Rab11-FIP2 (Rab11 Family of Interacting Proteins 2), to recycling endosomes where it mediates binding to myosin-Vb, thereby linking recycling endosomes with the actin cytoskeleton [39]. These examples demonstrate the functional requirement of Rabs for the recruitment of motor and motor-binding effectors for the active transport of vesicles between subcellular compartments.

1.4.5.3 Rabs as tethering factors

The initial connection, or tethering, between the incoming cargo-carrying vesicle and the target membrane occurs prior to the fusion of the two membranous organelles. Rab GTPases also regulate this event. In general, GTP-bound Rabs localized to incoming transport vesicles recruit effector proteins, which often contain highly extended, coiled-coil domains [51]. These tethering proteins form extended rod structures that bridge proximal membranes, thereby priming the vesicle for the subsequent docking and fusion with the acceptor site [52]. For instance, the intra-Golgi transport of vesicles through the biosynthetic, secretory pathway requires the Rab1-regulated p115 tethering factor, which tethers giantin-containing vesicles to the *cis*-Golgi localized GM130 protein [53, 54]. After tethering, acceptor membrane-bound vesicles dock and fuse by the actions of SNARE proteins, as I have discussed below.

1.4.5.4 Rabs as fusion regulators

The final step of vesicular transport is assigned traditionally to a family of conserved membrane proteins termed SNAREs (SNAREs, defined as SNAP receptors; SNAP, as soluble NSF attachment proteins; and NSF, as N-ethyl-maleimide-sensitive factor) [55]. SNARE proteins localized to vesicles, or v-SNAREs, bind their cognate target membrane SNAREs (t-SNAREs) and form complexes that drive membrane fusion [51]. However, recent *in vitro* work on homotypic fusion of early endosomes indicates that Rabs and their effectors are required for the formation of SNARE complexes and the efficient fusion of donor/acceptor membranes [56].

1.4.6 Rabs decipher compartment identity

Recognizing discreet intracellular locations demands a remarkable degree of specificity by Rab proteins and this is crucial for their ability to act as key cellular regulators of distinct membrane trafficking events simultaneously. It is from their localization to compartments that Rabs coordinate the temporal and spatial organization of downstream effectors for each step necessary for accurate and specific cargo transport [37]. Furthermore, the intracellular trafficking systems of eukaryotic cells are a highly pleomorphic, asynchronous network of interconnected and interchanging compartments. This complexity requires an amazing level of distinction between subcellular sites by Rabs, yet the mechanisms responsible for this specificity are understood poorly.

Some evidence suggests that GDFs, such as the small, integral membrane Yip proteins, localize to specific intracellular organelles where they recognize a cognate GDI-bound Rab, displace GDI, and mediate the membrane insertion of a particular Rab at the correct location [57]. However, with only 16 mammalian Yips for more than 60 Rabs and several that recognize more than one Rab, it is unlikely that they mediate all of the detailed specificity required for Rab targeting [34]. Other, as of yet, unidentified GDF families may contribute to the required level of target specificity. Some reports have suggested that Rab hypervariable domains target Rabs to the correct sites. For instance, transplantation of the C-terminal hypervariable domain of Rab5 or Rab2 with that of Rab7 relocalized Rab5 or Rab2 to Rab7-positive late endosomes [58]. Other work has suggested the geranylgeranyl groups act as a possible targeting mechanism [59, 60]. Thus, it may be a combined effect of GDFs that decipher a regional specificity, followed by targeting to a more local site by the Rab structural variations caused by the hypervariable

domains or unique prenylation groups [34, 61].

Regardless, it is clear from extensive reports on Rab localization and function that they demarcate faithfully distinct intracellular compartments, or even microdomains within a specific compartment. Because of this, Rabs are used as compartment-specific markers of the biosynthetic, endocytic, degradative, and recycling traffic pathways (See Figure 1.6) and their function within these pathways is used to characterize the intracellular transport of integral membrane proteins that range in function from receptors to ion channels.

In the following sections, I will introduce a specific family of the Rab GTPases that is involved intimately in the trafficking process of membrane recycling: the Rab11 family of GTPases. I will discuss the Rab11 family member localization to the intracellular recycling compartments in both non-polarized and polarized cell systems as well as what is known about their functional role in regulating cargo recycling through these pathways.

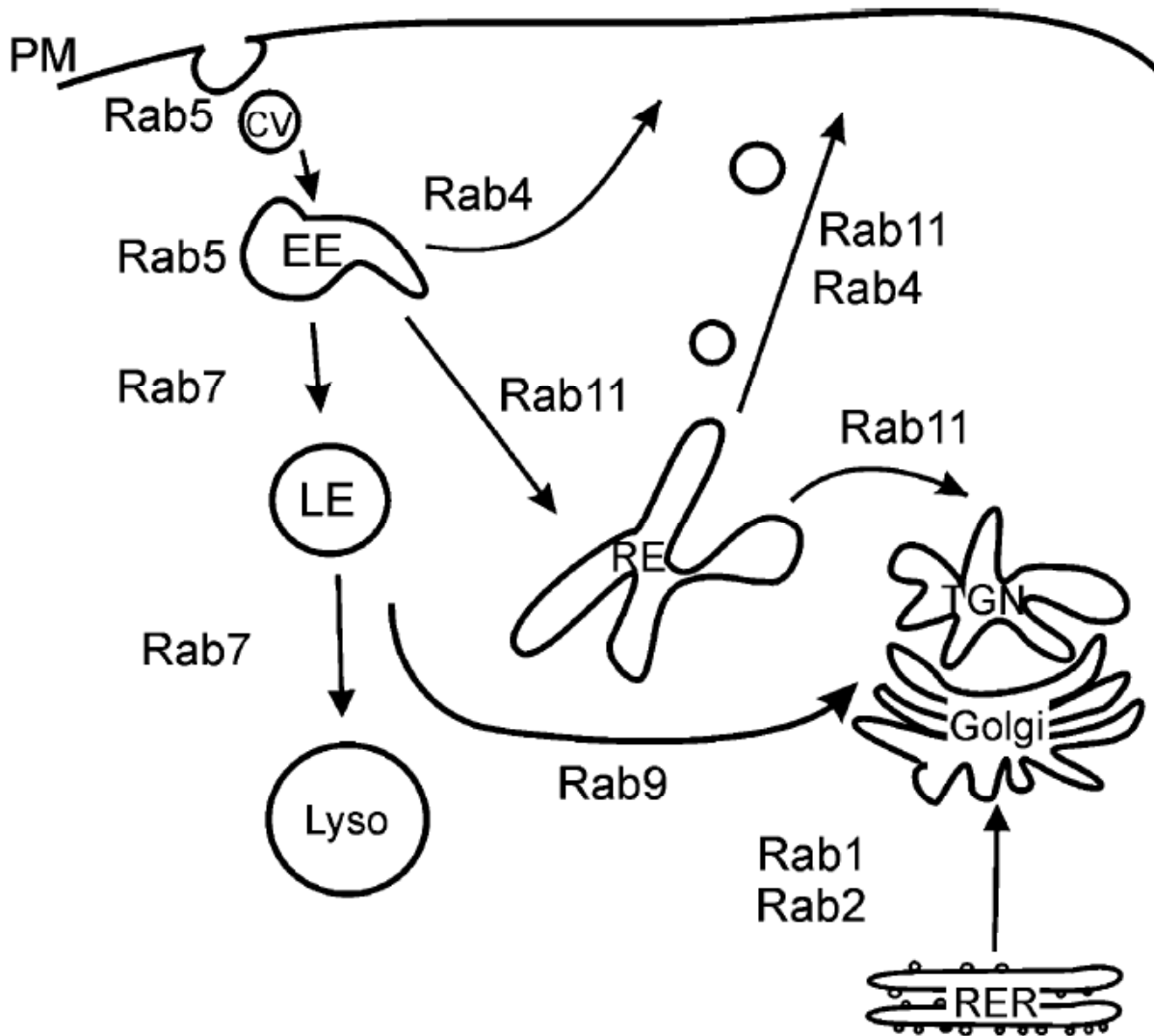


Figure 1.6: Rabs decipher membrane identity [62].

Rabs are localized to distinct subsets of membranes along the secretory and endocytic pathway. The schematic above illustrates generally the localization of some Rabs to their respective intracellular compartments. Rab5 localizes to the plasma membrane (PM) where it regulates the internalization of clathrin-coated vesicles (CV) and homotypic fusion of early endosomes (EE) containing cargo internalized from the extracellular space [63]. Rab4 regulates an early, immediate recycling pathway to the PM [64], while Rab11 is responsible for regulating recycling through the pericentriolar recycling endosomes (RE) [65]. Material targeted for degradation is sorted from early endosomes to Rab7-positive late endosomes (LE) followed by delivery to lysosomes (Lyso) [66], while Rab9 regulates traffic between the lysosomes and Golgi [67]. Rab1 and 2 play a role in biosynthetic traffic from the rough endoplasmic reticulum (RER) to the Golgi [68].

1.4.7 Rab11 Family of GTPases

The Rab11 subfamily of GTPases includes the three closely related, evolutionary conserved proteins: Rab11a, Rab11b, and Rab25. Rab11a is synthesized ubiquitously [69, 70]; Rab11b is enriched in brain, heart, and testis [70]; and Rab25 is found only in epithelial cells [71]. In general, the Rab11 family members, especially Rab11a, have been described as regulators of membrane recycling from the endocytic recycling compartment to the plasma membrane and to the *trans*-Golgi network [65, 72-74]. In polarized epithelial models, both Rab11a and Rab25 have been implicated in membrane recycling at the apical pole [75, 76]. Interestingly, while Rab11a and Rab11b share 89% amino acid homology, increasing evidence suggests that Rab11a and Rab11b may participate in unique recycling itineraries within the apical recycling pathway of polarized epithelial cells. In the following section, I will highlight what is known about Rab11a and Rab11b localization in non-polarized and polarized cell systems. In addition, I will introduce what has been reported regarding their roles in membrane recycling in these disparate eukaryotic cell types.

1.4.7.1 Rab11a and Rab11b Localization

Rab11a was initially characterized as a 24-kDa GTP-binding protein that was isolated and purified from bovine brain membranes [77]. Subsequently, the Rab11a gene was cloned from several different sources, including MDCK cells [78], mouse kidney [79], and rabbit gastric parietal cells [76]. Numerous biochemical, immunofluorescent, and electron microscopy techniques have been used to characterize the subcellular location of Rab11a in various cell systems. These studies often utilized the addition of extracellular ligands to stimulate internalization of their cognate, membrane-bound

receptor. After internalization and entry into early endosomes, proteins destined for return to the plasma membrane, such as the transferrin receptor (TfR), are sorted for recycling and enter subsequently into the recycling compartment.

In non-polarized fibroblasts, such as Chinese Hamster Ovary (CHO) and Baby Hamster Kidney (BHK) cells, a 30 minute internalization of fluorophore-labeled transferrin from the plasma membrane revealed that Rab11a antibodies identified a transferrin-containing recycling compartment [65, 80]. The Rab11a overlap with these transferrin-containing recycling endosomes revealed a pericentriolar-localized and tubulovesicular morphology for the recycling compartment. In addition, immunoisolation of TfR-containing vesicles that were purified from endosome-enriched subcellular CHO cell fractions after the addition of transferrin demonstrated biochemically that Rab11a localizes to a post early endosomal, tubulovesicular compartment bearing the recycling TfR [81]. Since these early reports of the colocalization of Rab11a with internalized proteins destined for recycling, numerous other recycling proteins have been localized to the Rab11a-positive recycling endosomes, confirming that Rab11a localizes to, and demarcates the recycling compartment in non-polarized cells. The characterization of the recycling endosomes as a unique, subcellular vesicular population positive for Rab11a in non-polarized cell systems was foundational for studies performed subsequently in the more complex polarized epithelial cell models.

A study of Rab11a localization in tissue, performed by Goldenring *et al.*, revealed prominent Rab11a immunostaining in the subapical region of a number of epithelial tissues including the surface mucous cells of the gastric mucosa, the intestinal enterocytes and colonocytes, and the kidney collecting duct cells [75]. Further work

demonstrated that Rab11a identified apical vesicle populations with a pericentriolar localization in these polarized cell types. In addition, Rab11a colocalized with a known recycling protein, the H⁺-K⁺-ATPase proton pump, on intracellular tubulovesicular membranes in gastric parietal cells, which suggested that it also associates with recycling endosomes in polarized cell types *in vivo* [76].

Studies performed on what has become the classic polarized epithelial cell system, Madin-Darby Canine Kidney (MDCK) cells [82, 83], were the first to describe an apical recycling compartment in a polarized cell model. Specifically, Apodaca, *et al.* demonstrated that dimeric immunoglobulin A (dIgA), internalized from the basolateral membrane of polarized MDCK cells, localized at an apical, microtubule-sensitive, and pericentriolar compartment. Furthermore, this dIgA-containing compartment could be labeled with antibodies to its receptor, the poly-Immunoglobulin Receptor (pIgR), which had been internalized simultaneously from the apical membrane [83]. Subsequently, work by Cassanova, *et al.*, revealed that Rab11a antibodies overlapped the internalized dIgA that had originated from either the apical or the basolateral membrane, suggesting that Rab11a could identify reliably the apical recycling compartment in polarized cells [84]. Thus, studies revealed that the apical recycling compartment could be identified by its intracellular, subapical localization; its dependence upon microtubule stability; and its accessibility to membrane-bound proteins that were internalized from either the apical or basolateral pole of the cell [83, 85]. Since the early work that was performed to identify and characterize the apical recycling compartment in polarized epithelial cells, it has become recognized widely that Rab11a localizes to and is the defining marker for what is now termed, the ‘apical recycling endosome’ (ARE), in polarized epithelial models [84, 86]. The ARE accepts and sorts the pIgR ligands, dIgA and dIgM, internalized from the apical or basolateral

membrane and recycles their receptors to the apical membrane. Thus, the ARE receives cargo undergoing transcytosis from the basolateral to apical plasma membrane in addition to cargo internalized apically that is targeted for recycling. Unlike non-polarized cell types, the Rab11a recycling compartment is devoid of transferrin (internalized from the basolateral membrane), which has been shown to recycle through the more distal common recycling endosome [86].

Rab11a was cloned three years prior to Rab11b; therefore, focus was placed on deciphering Rab11a localization and function and less is known about Rab11b to date. Rab11b was initially cloned from a mouse testis cDNA library in 1994 [70]. In non-polarized Vero (African green monkey kidney) cells, antibodies to Rab11b co-localized with internalized TfR, suggesting that Rab11b also labeled the endocytic recycling compartment [87]. In addition, internalized transferrin showed a partial overlap with compartments labeled with GFP-tagged Rab11b that was expressed in non-polarized, epithelial PtK1 cells [88]. Conversely, no colocalization of Rab11b with the TfR was detected in HeLa cells, suggesting either differences in the endocytic/recycling itinerary for TfR in this cell type or a different subcellular localization of Rab11b between these cell types [89]. In neuroendocrine PC12 cells, subcellular fractionation revealed that Rab11b cofractionated on sucrose gradients at the same buoyant density as Rab5a, Munc18, and synaptophysin I, which are markers for secretory vesicles, suggesting that Rab11b is present on these membranes. In the same report, Khvotchev *et al.*, further demonstrated that Rab11b was also found on mature synaptic vesicles that were purified from rat brain, suggesting a potential role for Rab11b in stimulated synaptic vesicle exocytosis [90].

In polarized cell models, endogenous Rab11b localizes to subapical vesicles in the pericentriolar region of MDCK and gastric parietal cells, similar to the subcellular localization of Rab11a. However, Rab11b antibodies revealed a unique staining pattern unlike that for Rab11a

and Rab11b failed to overlap morphologically or biochemically with the Rab11a-identified ARE compartment [89]. Specifically, endogenous Rab11b did not co-localize with H⁺-K⁺-ATPase in rabbit gastric parietal cells, nor did it co-immunoprecipitate with H⁺-K⁺-ATPase-containing vesicles [89]. In polarized MDCK cells, Rab11b failed to colocalize with IgA or transferrin that had been internalized from the apical or basolateral membranes, respectively. In addition, reagents that disrupt microtubule formation or stability had only minor effects on Rab11b distribution, suggesting that the Rab11b compartment in the apical region is not dependent upon microtubules like Rab11a. These observations suggest that Rab11b and Rab11a occupy unique compartments within the polarized epithelial MDCK cell model; however, the identity of the Rab11b compartment remains poorly defined as no other studies have characterized it in additional polarized cell models.

1.4.7.2 Rab11a and Rab11b function

After the initial documentation that demonstrated the Rab11a colocalization with internalized transferrin, several studies reported immediately a functional role for Rab11a in the return of membrane-bound proteins from the endocytic recycling compartment to the plasma membrane. Researchers quickly realized the utility of creating mutant Rab11 constructs that preferentially bound to one form of guanine nucleotide, thereby locking Rab11 in an inactive, GDP-bound (dominant negative) or active, GTP-bound (dominant active) state. Ullrich *et al.* found that a mutant of Rab11a, defective in GTP binding (Rab11aS25N), impaired recycling of internalized transferrin in CHO and BHK cells, apparently by inhibiting transport from sorting endosomes to the recycling endosome [65]. Hence, the identification of Rab11a as a reliable marker for the recycling compartment signaled its functional role in

regulating the recycling cargo with which its location overlapped.

Perhaps the earliest indication that Rab11a participates in polarized membrane recycling came from studies on rabbit gastric parietal cells, which demonstrated that Rab11a relocalized with H⁺-K⁺-ATPase-containing tubulovesicles to the plasma membrane upon histamine addition [91]. Within the next year, functional Rab11a was shown to be required for the fusion of these tubulovesicles with the apical, canalicular membrane upon agonist stimulation [92]. Later work revealed that Rab11a (and Rab25) also regulated the apical recycling of dIgA in polarized MDCK cells [93]. However, unlike non-polarized cell models, transferrin receptor recycling was unaffected by the mutant Rab11a proteins that altered dIgA recycling at the apical membrane. It is now well understood that Rab11a regulates the apical recycling and exocytic insertion of numerous membrane proteins through the ARE, including the polymeric immunoglobulin receptor (pIgR) in MDCK cells [93], the bile salt export pump (ABCB11) in polarized hepatic cells [94], and the H⁺-K⁺-ATPase in gastric parietal cells [92]. Furthermore, Swiatecka-Urban reported a role for Rab11a in the recycling of CFTR that was expressed exogenously in polarized airway cells [95].

The strongest evidence for Rab11b in protein recycling was reported by Schlierf *et al.*, who demonstrated that both the dominant negative and dominant active mutant forms of Rab11b inhibited the recycling of transferrin in Vero cells, without affecting its uptake from the plasma membrane [87]. Thus, it appeared originally as though Rab11b may play a redundant role in recycling cargo to the plasma membrane of non-polarized cell types, mimicking the action of Rab11a. In a study performed on PC12 cells, all members of the Rab11 family, Rab11a, Rab11b, and Rab25, were found to regulate calcium-induced exocytosis of hGH (human growth hormone) from the secretory pathway [90]. Interestingly, both GTP- and GDP-bound states of Rab11b inhibited exocytosis of secretory granules, but through different mechanisms. GDP-

locked Rab11b stimulated the constitutive secretion of hGH, thereby depleting intracellular hGH stores from secretory vesicles that were destined to fuse the plasma membrane. The GTP-bound Rab11b did not affect constitutive secretion, but impaired directly the Ca^{2+} -induced exocytosis, which resulted in an accumulation of intracellular hGH. However, in non-neuronal human epithelial kidney (HEK) cells, both forms of the mutant Rab11b inhibited the constitutive secretion of hGH, causing a significant intracellular accumulation. Hence, Rab11b regulates exocytosis differently between cell types, suggesting that the organization of the secretory pathway differs fundamentally between cells in which regulated and constitutive exocytosis reactions are performed in parallel compared to cells that only execute constitutive exocytosis. Most recently, Sugawara *et al*, reported that Rab11b regulates the protein kinase A (PKA)-stimulated secretion of insulin-containing granules from pancreatic β -cells [96]. These studies suggest that Rab11b may also participate in the regulated secretion of biosynthetic cargo upon agonist stimulation.

These studies suggest a role for Rab11b in the recycling of transferrin and in the regulated secretion from specialized secretory cell types, yet no other work has reported a role for Rab11b in recycling. In addition, while the localization of Rab11b to a unique subapical compartment was documented, no studies have demonstrated a role for Rab11b in polarized membrane trafficking.

In the following sections, I will briefly discuss cystic fibrosis, followed by an overview of the CFTR protein structure, function, biosynthesis, and polarized localization. Finally, I will discuss what is known about CFTR recycling in polarized epithelial cells and point out why the work contained within this dissertation is necessary to fill the large gaps in our current understanding of protein recycling at the apical membrane.

1.5 CYSTIC FIBROSIS

Cystic fibrosis (CF) is one of the most common, life-shortening genetic diseases in Caucasians, with 1 in every 2500 live births afflicted [97]. The most prevalent mutation in the cystic fibrosis gene, *CFTR*, is a deletion of a phenylalanine residue at position 508 ($\Delta F508$) [98]; however, more than 1000 mutations in *CFTR* have been documented that give rise to varying severities of the disease. The *CFTR* mutation, $\Delta F508$, prevents the correct folding of the protein it encodes, the Cystic Fibrosis Transmembrane conductance Regulator (CFTR), which causes its retention and subsequent degradation by the quality control mechanisms within the endoplasmic reticulum [99]. The resulting absence of CFTR channel activity and expression at the apical membranes of epithelial cells causes the clinical manifestations of CF [100], which include; elevated levels of sweat electrolytes, chronic infection and obstruction of the respiratory tract, exocrine pancreatic insufficiency, malabsorption in the gut, and intestinal obstruction [101].

1.6 CFTR

1.6.1 CFTR Structure

The CFTR, a 1480 amino acid integral membrane glycoprotein, contains cytosolic carboxyl- and amino-termini that flank its six transmembrane domains, which line the pore of this anion-selective channel [102] (See Figure 1.7). CFTR channel activity is modulated by the binding and hydrolysis of ATP on its two nucleotide binding domains, in addition to the PKA-mediated phosphorylation status of its regulatory domain [103, 104]. The post-translational addition and modification of two N-linked oligosaccharides on the fourth extracellular loop of CFTR occurs as it traverses the *trans* Golgi network; allowing researchers to determine the maturity of CFTR within the biosynthetic pathway based on its glycosylation status [105-107]. CFTR functions as a cAMP-regulated, protein kinase (PKA)-phosphorylated anion channel that is expressed at the apical membrane domain of epithelial cells lining the gastrointestinal tract, salivary and sweat glands, lungs, and the pancreas [108, 109]. CFTR that is resident within the apical plasma membrane of polarized epithelial cells mediates transepithelial chloride secretion and is required for maintaining the proper fluid composition at these anatomical sites. As will be discussed in further detail in Section 1.7.2, CFTR is the primary apical chloride conductance in intestinal epithelial cells where its localization and function at the apical membrane is required for normal intestinal physiology.

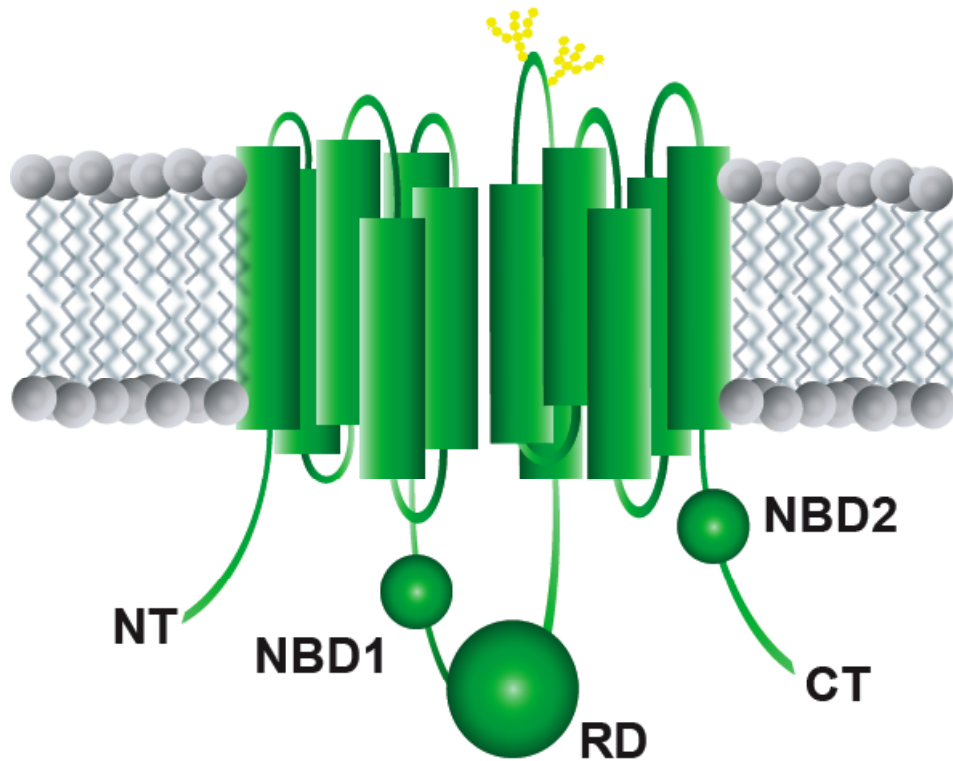


Figure1.7. Model depicting the proposed structure of CFTR.

The CFTR transmembrane domains (green cylinders) pass through lipid bilayer (grey lipids) twelve times. The intracellular structures of CFTR consist of an amino-terminal domain (NT); two nucleotide binding domains (NBD1 & 2) that bind and hydrolyze ATP; a large regulatory domain (RD) that is phosphorylated by PKA; and a carboxyl-terminal tail (CT). The fourth extracellular loop of CFTR has two N-linked glycosylation sites that are modified by the addition oligosaccharide moieties (yellow structures) as CFTR traverses the Golgi apparatus.

1.6.2 CFTR localization in native tissue and endogenous expression systems

Two years after the 1989 discovery of the CFTR gene [97, 98], immunocytochemical studies performed on human tissues using anti-sera raised against the CFTR regulatory domain revealed the tissue distribution of CFTR *in vivo* [110]. CFTR expression was found to be most abundant in the pancreas, kidney, sweat ducts, and the gut. Furthermore, CFTR staining localized to the apical plasma membrane domain and intracellular, subapical vesicles of epithelia lining these tissues. Additional experiments performed *in vivo* by Webster *et al.*, demonstrated that CFTR localized to the apical pole of striated duct epithelial cells in tissue sections of rat submandibular gland [111]. In addition, CFTR resided within the plasma membrane and subapical, Rab4-positive endosomal/recycling vesicles, as determined by electron microscopy.

The characterization of CFTR localization within the human epithelial colonic cell line, T84, revealed that CFTR was also present in the apical membrane domain within this *in vitro* polarized cell model [112]. Other studies confirmed these findings, showing that endogenous CFTR localized constitutively to the apical plasma membrane, or immediately juxtaposed to it, in polarized T84 cells and other human intestinal epithelial models [113, 114]. Taken together, these experiments suggested that the CFTR was not retained within the apical membrane, but was able to undergo endocytosis or exocytosis, possibly to regulate the cell surface densities of CFTR. Since these original reports, numerous studies on primary cell lines, tissues *in vivo*, and established epithelial cell lines, which all express endogenous levels of CFTR, have shown that CFTR localizes to the apical plasma membrane and within subapical vesicular compartments. However, the nature of these compartments that contain CFTR is not understood.

The biochemical isolation of CFTR from endosomal populations obtained from tissue and *in vitro* cell models that express CFTR endogenously, support the morphological localization of CFTR within endosomal membranes. Furthermore, by fusing these CFTR-containing endosomal populations with lipid-bilayers, electrophysiological studies demonstrated that CFTR within these compartments is functional [115-117]. These biochemical findings suggested that a

pool of CFTR-containing vesicles is able to be recruited to the membrane to mediate chloride secretion in response to increases in the intracellular concentrations of molecules that activate CFTR, such as cAMP.

Despite this wealth of morphological and biochemical data that demonstrates the presence of CFTR within the apical plasma membrane and subapical vesicle populations, the mechanisms that regulate the localization and trafficking of CFTR between these two cellular domains are largely unknown. In addition, it is still incompletely understood what contribution the cycling between the apical cell surface and intracellular compartments has in the physiology of the tissues that express CFTR (See Section 1.6.4) [118].

1.6.3 CFTR biosynthesis in polarized epithelial cells

The $\Delta F508$ mutation in CFTR results in a misfolded protein that is retained by the ER and degraded [99]. Hence, numerous studies have been performed to detail the biosynthesis of wild type and mutant CFTR molecules within heterologous expression systems that express CFTR exogenously, largely due to their relative ease of use. However, for reasons outlined in the goals of this dissertation (Section 1.8), the work performed within this dissertation was performed only within the polarized epithelial T84 cell model (see Section 1.7: Colonic Epithelial T84 Cells). Interestingly, work by Varga *et al.*, has shown that unlike heterologous overexpression systems, CFTR biosynthesis in endogenous expression systems is highly efficient [119]. Specifically, the conversion of the core glycosylated band B CFTR to the band C form as it traverses the *trans* Golgi network is nearly 100% efficient in polarized T84 cells and other cell models that express CFTR inherently [119]. This is in contrast to what has been demonstrated for CFTR biosynthesis in non-polarized expression systems that are transduced to overexpress CFTR, where biosynthetic conversion is approximately 30-40% efficient.

Furthermore, the majority of CFTR within polarized epithelial cell types has been shown to be that of the mature glycosylated, band C CFTR, which is extremely stable and has a half life

of more than 20 hours in T84 cells and other endogenous expression models [119, 120]. In fact, little of the immature band B CFTR is detected in cell types that express wild type CFTR endogenously [119]. Therefore, biochemically speaking, the majority of CFTR present within polarized epithelial cells is that of the mature, band C CFTR, which has traversed the biosynthetic compartment and is localized distal to the TGN.

Finally, as discussed in detail previously, the localization of CFTR within polarized epithelial cell types confirms that the mature CFTR is localized at the apical plasma membrane and within subapical compartments, with no CFTR at the basolateral or perinuclear regions [113, 114]. This suggests that very little CFTR is present within the ER at steady state within polarized phenotypes. Thus, when taken together: the efficient biosynthesis, long half-life, and apical localization of CFTR suggest that it must recycle. In the section below, I will summarize what is known about CFTR recycling in polarized epithelial models.

1.6.4 CFTR endocytosis and recycling in polarized epithelial cells

The efficient biosynthesis and long half-life of CFTR within cell systems that express it inherently suggest that CFTR must recycle efficiently in order to maintain an appropriate cellular expression level, which is required for its function at the apical membrane. Newly synthesized CFTR molecules that emerge from the biosynthetic pathway are delivered to the apical plasma membrane and early studies demonstrated that CFTR could be purified from clathrin-coated vesicles [117]. This suggested that CFTR within the apical membrane is not static, but instead is internalized by clathrin-mediated endocytosis. Later studies in heterologous expression systems revealed that CFTR undergoes rapid, clathrin-mediated endocytosis that is mediated by interactions with its cytoplasmic domain and clathrin adaptor proteins [117, 121]. Work done in polarized T84 cells confirmed the rapid and efficient internalization of CFTR within a polarized epithelial cell model [122]. Furthermore, by following the fate of the internalized CFTR molecules that were labeled at the cell surface, this study demonstrated their rapid recycling after

endocytosis. This was the first study within an *in vitro* polarized epithelial cell system to provide biochemical evidence for the constitutive recycling of CFTR, a process which maintains an appropriate number of channels resident within the cell surface and is therefore critical for mediating the apical chloride conductance in response to activation by CFTR agonists [118].

1.6.5 Constitutive recycling of CFTR in polarized epithelia

More recent studies in polarized bronchial epithelial cells, CFBE41o-, have also revealed the rapid and efficient constitutive turnover of CFTR at the apical membrane [95, 123]. CFTR recycling was shown to require the function and expression of Rab11a and the actin motor, Myosin Vb [95, 123]. This work, which represents the first and most thorough report to date on the constitutive CFTR recycling process, begins to elucidate the underlying molecular mechanisms that mediate this recycling within a physiologically pertinent cell system. Additionally, the following studies suggest that various membrane trafficking proteins, such as SNAREs and actin, are also important for CFTR turnover in polarized cell systems, yet do not examine CFTR recycling. For example, studies in intestinal epithelial Caco-2 cells, which express CFTR endogenously, demonstrated that overexpression of SNARE proteins, VAMP8, syntaxin8, syntaxin7, and vti1b, reduced the apical density of CFTR; however, CFTR recycling was not directly measured in this study [124]. In colonic epithelial HT-29Cl19A cells, the inhibition of N-WASP-mediated actin polymerization by wiskostatin, reduced the CFTR channel density at the apical membrane, suggesting that actin polymerization is necessary for the constitutive recycling of CFTR [125].

Thus, while these studies have begun to shed light on the underlying cellular mechanisms that are responsible for regulating apical CFTR recycling within a polarized epithelial model, this process is understood poorly, especially in polarized cell systems. This is due, in part, to technical difficulties that arise from attempting to study the endogenous trafficking of CFTR, which has a very low copy number in the epithelial systems that express it. Furthermore, the

lack of available antigenic sites on the small portions of the extracellular loops of CFTR, which would enable antibody detection and labeling of cell surface CFTR, have failed to produce useful antibodies for trafficking studies. Therefore, the mechanisms that mediate the constitutive turnover of CFTR in relevant systems remain largely unknown and were therefore a focus of this dissertation work.

1.6.6 Regulated recycling of CFTR

In addition to the constitutive recycling of CFTR after internalization from the apical membrane, there is evidence that the cellular distribution of CFTR between the subapical membrane-bound compartments and the apical cell surface is modulated in response to agonist stimulation and CFTR activation by cAMP. The most detailed examination of this was performed in rat duodenal villus epithelial cells, which showed an upregulation of the apical surface CFTR channel density upon activation of CFTR by the cAMP-agonist, vasoactive intestinal peptide (VIP) [126]. Additionally, VIP increases CFTR channel density at the apical membrane of Calu-3 cells through a protein kinase C-dependent mechanism [127]. Thus, these studies demonstrate that while CFTR is able to function as a regulated conductance pathway while it is resident within the apical membrane, intracellular increases in cAMP can modulate the distribution of CFTR between intracellular compartments and the apical plasma membrane. In addition, numerous other studies in non-polarized, heterologous expression systems have suggested that CFTR recycling is regulated by its activation state [118]. However, while both the activation of membrane-resident channels and insertion of CFTR from subapical pools occur, it is not known how these processes are linked mechanistically, and this process is almost completely unexplored in polarized epithelial systems. Furthermore, the underlying trafficking machinery that mediates these processes is unknown to date; however, it is likely that the trafficking proteins involved in the constitutive recycling of CFTR may play a role in its regulated recycling. Therefore, the focus of this dissertation work is to elucidate the trafficking

mechanisms that regulate the constitutive and regulated recycling of CFTR within a polarized epithelial cell system that expresses CFTR endogenously.

In the following section, I will introduce the model system used within this dissertation work. In addition, I will discuss why the human intestinal epithelial cell line, T84, is a physiologically relevant system for morphological and functional experimentation that is aimed at elucidating the recycling itineraries of apical CFTR.

1.7 COLONIC EPITHELIAL T84 CELLS

The human colonic epithelial cell line, T84, were derived from a colonic carcinoma and characterized originally by Dharmasathaphorn, *et al.*, in 1984 [128]. As discussed below, when grown in culture, this epithelial cell line closely resembles both the morphology and function of intact large intestine. This allows for the *in vitro* studies on the cell biological and electrophysiological mechanisms of the large intestine within a convenient, relatively malleable cell model that produces a continuous supply of uniform epithelial cells.

1.7.1 Morphology

Seeding T84 cells onto semipermeable transwell supports enables the formation of a polarized monolayer, with the basolateral surface adhering to the surface of the transwell filter and the apical microvilli facing the culturing media. Upon cell-cell contact, T84s begin to form junctional complexes such as tight junctions, adherens junctions, and desmosomes, which are necessary for the establishment of a differentiated and polarized phenotype. After culturing the cells for 7-10 days, T84s develop high levels of transepithelial resistance (TER) reaching 1000-2000 Ω cm², which indicates the formation of the tight junctions between adjacent cells. Transmission electron microscopic (TEM) examination of T84 cells has revealed that polarized

monolayers resemble the morphology of intact or isolated intestinal tissues, with the formation of a single layer of columnar, elongated cells (See Figure 1.8). In addition, polarized T84 cells show the presence of desmosomes and tight junctions between adjacent cells, with microvilli studing the apical membrane [128]. Thus, T84s resemble morphologically the structured polarity that is characteristic of differentiated epithelial cells.

1.7.2 Functional studies

In addition to their morphological similarities to intact tissue of the large intestine, confluent monolayers of T84 cells maintain transepithelial electrolyte transport in response to various hormones and neurotransmitters, as assessed by changes in short circuit current (I_{SC}). Specifically, T84 monolayers respond in a similar manner as isolated large intestinal tissue in Ussing Chamber experiments upon the addition of vasoactive intestinal peptide (VIP), carbachol, somatostatin and verapamil [128, 130]. Early studies also revealed that confluent T84 monolayers were a relevant cell model for the study of transepithelial Na^+ and Cl^- transport as they responded to the physiological cAMP agonist, VIP, in a manner similar to isolated intestine [130].

Additional Ussing chamber experiments revealed that the cAMP-sensitive Cl^- transport mechanism was localized to the apical membrane in polarized T84 cells; while the bumetanide-sensitive, Na^+ , K^+ , Cl^- cotransporter, which is necessary for increasing the intracellular Cl^- potential and required for apical Cl^- conductance, was localized to the basolateral membrane [131, 132]. Studies by Bell *et al.*, characterized the apical chloride conductance in T84s as being consistent with the characteristics of tissues affected by cystic fibrosis, making them a clinically relevant model for Cl^- conductance studies [133]. Shortly thereafter, indirect immunofluorescence experiments performed with CFTR-specific antibodies revealed its localization at the apical membrane in polarized T84 monolayers [112, 134].

Since the original characterizations of T84 cell morphology and ion transport capabilities, hundreds of functional studies have been performed on this epithelial cell model. It is now well

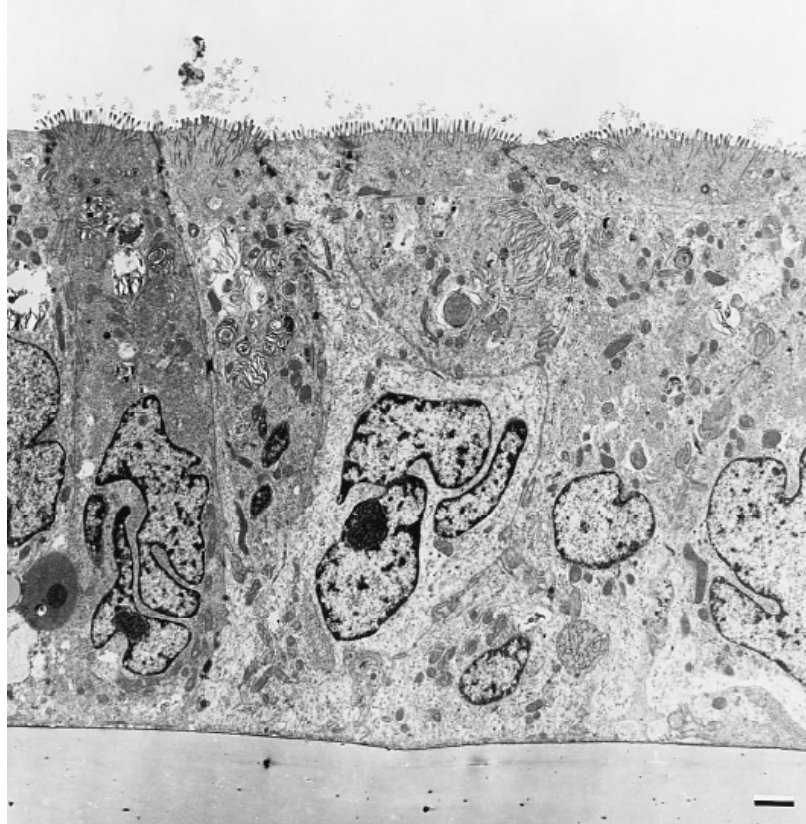


Figure 1.8 Transmission Electron Micrograph of a polarized T84 cell monolayer [129].

The morphological examination of T84 cells grown to confluence as a monolayer demonstrates a polarized phenotype with basolateral membranes facing the underlying semi-permeable support and adjacent cells. Note that the apical membrane, which is studded with microvilli, is exposed to the culturing media.

agreed upon that activation of the basolateral Na^+ , K^+ , Cl^- cotransporter, NKCC1, by cAMP-increasing agonists, such as forskolin, increases the intracellular chloride concentrations and potentiates Cl^- conductance through a primary apical membrane conductor, CFTR (See Figure 1.9) [135]. Thus, the T84 cell model is a physiologically relevant system for the morphological and functional examination of the underlying molecular mechanisms that support transepithelial transport mechanisms.

1.7.3 T84 cells as a model of intestinal physiology

The intestines perform the important physiological task of absorption and secretion of nutrients. The distal colon represents the final area for recapturing electrolytes and water prior to excretion, which requires a complex balance between the secretory and absorptive processes of the colonic epithelia [7]. In addition, fluid secretion by the large intestine is necessary for maintaining luminal fluidity and thereby is necessary for aiding in the passage of contents through the alimentary canal [135]. Recent reports have demonstrated that both the surface and crypt epithelial cells of the colon epithelia can perform the secretory and absorptive functions necessary for balancing the luminal fluidity homeostasis (See Figure 1.10). This process is accomplished by the passive transcellular movement of sodium and water, which are driven by the osmotic forces established by the active chloride secretion from polarized epithelial monolayers lining the lumen [135]. Thus, CFTR-mediated chloride secretion through the apical membrane of intestinal enterocytes represents a physiologically necessary process, the importance of which is most evident in alterations in CFTR function or localization that result in disease. For instance, the pathological consequences resulting from the dysregulation or absence of CFTR, as seen in secretory diarrhea or the intestinal obstruction seen in CF, respectively, underscore the critical role of CFTR in intestinal secretory mechanisms [136]. Therefore, as an *in vitro* model that mimics the intact human colon morphology and function, the

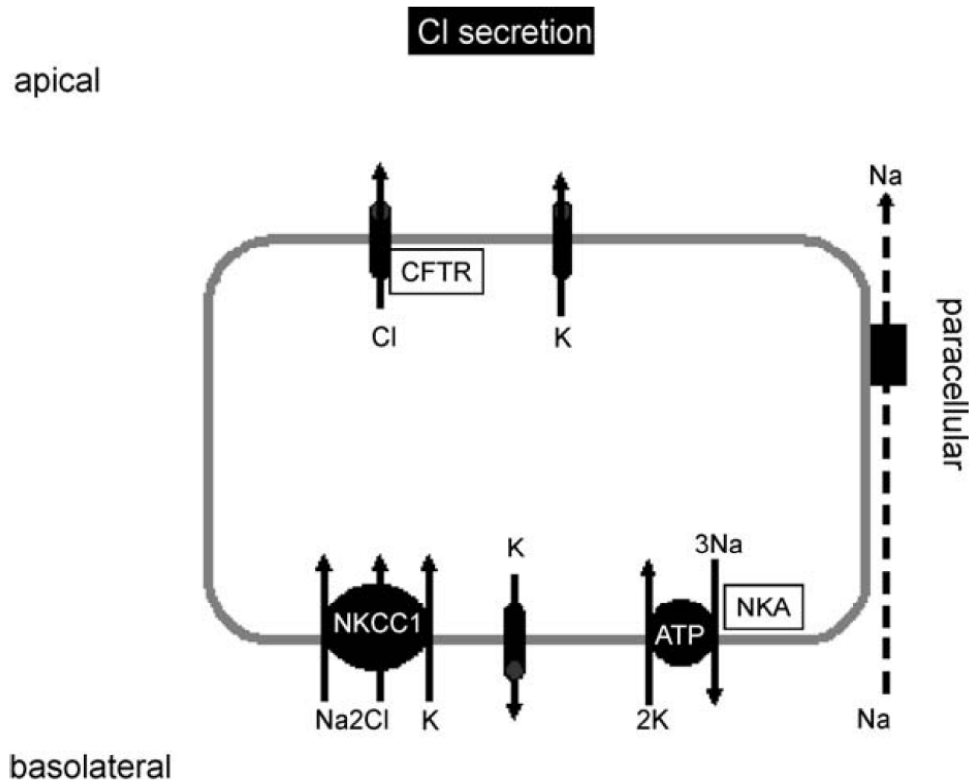


Figure 1.9 Schematic representation of Cl⁻ secretion in colonic epithelial cells [7].

The uptake of ions at the basolateral membrane of colonic epithelial cells by the Na⁺-2Cl⁻-K⁺ cotransporter type 1 (NKCC1) enables apical conductance of Cl⁻ through CFTR. NKCC1 and CFTR are both activated by PKA and other second messenger pathways. Functional basolateral K⁺ channels are required to maintain a hyperpolarizing membrane voltage and the driving force for Cl⁻ secretion and Na⁺ absorption. CFTR-mediated Cl⁻ secretion establishes the electrical and osmotic driving forces for the paracellular secondary sodium and water transport.

colonic epithelial cell line, T84, is a physiologically relevant system for studies focused on understanding CFTR apical membrane recycling pathways and their underlying molecular mechanisms.

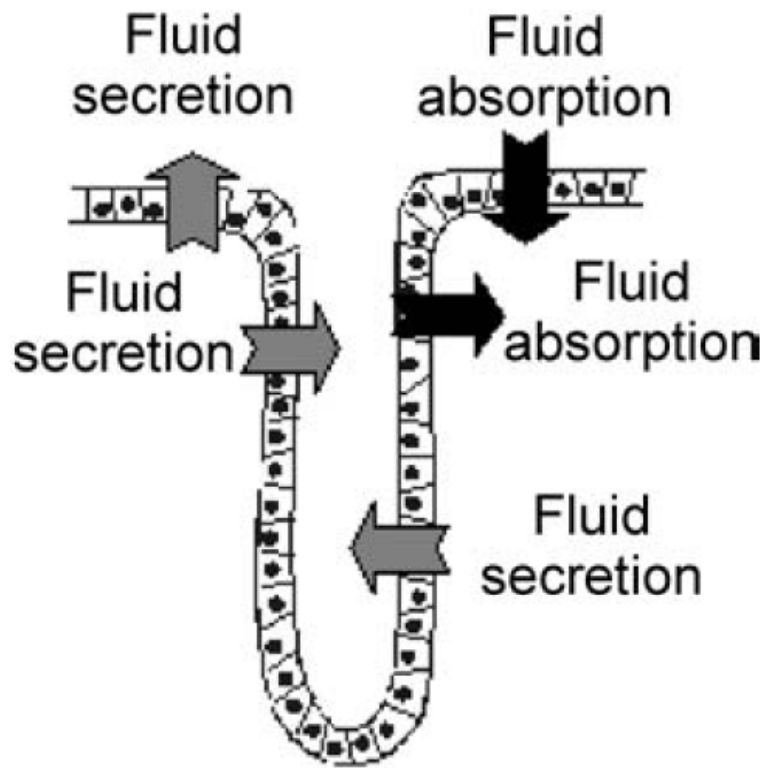


Figure 1.10 Schematic representation of Cl secretion in colonic epithelial cells [7].

The base of the crypt epithelia contains columnar cells with the greatest proliferative activity, while the surface cells have a lower tendency to proliferate and show the greatest differentiation. Crypt epithelial cells continuously migrate toward the surface, thereby replacing the cells that slough off. Both crypt and surface epithelial cells are involved in secretion and absorption of water and solutes, which must be balanced to maintain intraluminal fluid homeostasis.

1.8 GOALS OF THIS DISSERTATION

Recycling of membrane proteins is an important intracellular trafficking process that is required for regulating and maintaining the specific quantity of proteins at the cell surface, which is necessary for proper cell function. As I have summarized previously, the membrane recycling of CFTR within non-polarized, exogenously expressing cell lines has been studied and reported. While these studies provide proof-of-concept to support CFTR trafficking in non-polarized cells, the distinct apical and basolateral membrane domains of polarized epithelial cells, which are formed, established, and maintained by complex spatial and temporal regulation of membrane trafficking events in polarized cells cannot be recapitulated in non-polarized systems. The underlying recycling mechanisms responsible for CFTR traffic in a fully polarized, endogenous expression system have not been detailed thus far. Thus, my dissertation research seeks to better understand the apical trafficking itineraries of an endogenously-expressed membrane protein, CFTR, within a physiologically relevant, polarized epithelial system that allows for morphological, biochemical, cellular, and functional studies. The general goal of this project is to identify the molecular mechanisms that regulate apical CFTR recycling in polarized epithelia. The Rab family of small GTPases represent a solid starting point for studies aimed at better understanding the complexity of polarized protein trafficking as I have summarized above. While information on the Rab11a isoform has flooded the scientific arena with reports of its importance in regulating a myriad of proteins in non-polarized and polarized systems alike, the functions of the other members of the Rab11 family of GTPases has not been thoroughly examined. Therefore, my dissertation hypothesis is that recycling of cell surface internalized CFTR molecules from subapical pools back to the apical plasma membrane in polarized epithelia is regulated by Rab GTPases and that specific members of the Rab family of small GTPases regulate the apical membrane recycling of CFTR within a polarized epithelial cell system. In Chapter 2.1, I demonstrate the colocalization of endogenous CFTR with the Rab11 GTPases by revealing their subcellular distributions in fully polarized T84 cells and *in vivo* in rat jejunum.

Data showing the expression of endogenous CFTR within specifically isolated Rab11 endosomes from tissue and T84 cells confirms the localization of CFTR within the recycling compartment. In Chapter 2.2, I present evidence that functional Rab11b, but not Rab11a, is required for the correct function of endogenous CFTR using a live-cell imaging system. Furthermore, I demonstrate that the dominant active forms of both of the Rab11 isoforms influence the rates CFTR response to agonist. Short circuit measurements taken from across fully polarized T84 cell monolayers confirm that Rab11b function is necessary for conductance through CFTR at the apical membrane. In Chapter 2.3, I present biochemical data that details the trafficking process regulated by Rab11b expression and function and show that recycling through a Rab11b-mediated pathway regulates endogenous CFTR levels at the apical membrane. This work contributes information about an additional apical membrane protein recycling pathway to the field of cell biology that was uncharacterized previously in polarized epithelial cells. Furthermore, it demonstrates the importance of membrane trafficking processes for the normal physiological function of the large intestine and emphasizes the strengths of using relevant models that mirror closely the *in vivo* physiological processes to study CFTR trafficking and function. Finally, from a pathological perspective, regarding specifically the inability of the $\Delta F508$ CFTR to recycle, a detailed understanding of the wild type CFTR trafficking itinerary may be necessary for the development of therapies to treat cystic fibrosis.

2.0 RAB11B REGULATION OF APICAL CFTR RECYCLING IN POLARIZED INTESTINAL EPITHELIAL CELLS

*Reprinted from *Molecular Biology of the Cell*, (2009, Volume 20, April 15, pp. 2337-2350), with permission from the American Society for Cell Biology.

2.1 INTRODUCTION

Regulation of transport protein copy numbers at the apical and basolateral plasma membranes of polarized epithelial cells controls the vectorial movement of solutes and water and thereby establishes the physiological functions of secretory and absorptive epithelia [118, 137]. Intestinal epithelia regulate luminal fluidity by balancing solute absorption with regulated salt and water secretion; in the latter process, chloride transport establishes the electrical and osmotic driving forces for secondary sodium and water transport [136]. The Cystic Fibrosis Transmembrane conductance Regulator (CFTR), an apically localized cAMP/PKA-activated anion channel, is the primary chloride conductance at the apical membranes of intestinal epithelial cells [112, 138-140]. Its significance is reflected by the phenotype of CFTR null mice and pigs, which die of intestinal obstruction due to luminal dehydration [141, 142]. The pathological consequences resulting from the dysregulation or absence of CFTR, as seen in secretory diarrhea or the intestinal obstruction seen in cystic fibrosis, respectively, underscore the critical role of CFTR in intestinal secretory mechanisms.

CFTR-mediated chloride transport is regulated by cAMP/PKA activation of plasma membrane-localized channels as well as by acute modifications in the apical membrane density of CFTR channels in response to agonists [118]. The latter is accomplished by decreased internalization of CFTR channels from the plasma membrane and increased exocytic insertion of additional CFTR from intracellular pools. Morphological studies examining CFTR localization

in native tissue and polarized epithelial cells have noted both apical plasma membrane- and subapical, intracellular-localized CFTR populations [111, 114, 117, 143, 144]. However, few studies have investigated the identity of the CFTR-containing, subapical compartments that are responsible for acute modifications in apical membrane copy number in a polarized epithelia that expresses CFTR endogenously.

In the absence of agonist, CFTR channels in the apical membrane are not static. Rather, CFTR undergoes rapid, constitutive endocytosis [122] via clathrin coated vesicles [117, 119, 122] through interactions with the AP-2 adaptor complex [121] and in concert with the actin motor, myosin VI [145, 146]. With a half-life of more than 20 hours, the majority of internalized CFTR channels are not degraded, but rather undergo efficient recycling back to the apical plasma membrane [122]. Indeed, work by Swiatecka-Urban, *et. al.*, demonstrates that CFTR recycling in polarized CFBE41o- cells, a bronchial epithelial cell line transduced to express wild type CFTR exogenously, requires Myosin Vb. However, the mechanisms that regulate CFTR recycling and its importance in modulating apical membrane CFTR copy number remain poorly understood, particularly for native expression systems.

Members of the Rab family of small GTPases localize to specific subcellular compartments of eukaryotic cells where they regulate membrane trafficking processes; including budding, targeting, docking, and fusion of vesicles [30, 147]. GTP binding allows Rab proteins to engage effectors that mediate downstream trafficking events, while GTP hydrolysis by their intrinsic GTPase activity inactivates Rabs and halts vesicular traffic. The Rab11 subfamily of Rab GTPases, including Rab11a and Rab11b, has been implicated in membrane recycling in polarized epithelial models [75, 76]. Rab11a is expressed ubiquitously [69] while Rab11b is enriched in brain, heart and testis [70]. The Rab11a and Rab11b isoforms share 89% amino acid homology, with the least similarity found in their membrane binding, hypervariable C-termini [70].

Rab11a localizes to the pericentriolar, microtubule-associated Apical Recycling Endosome (ARE) in polarized epithelial cells [84, 86]. It regulates the apical recycling and exocytic insertion of numerous membrane proteins; including the polymeric immunoglobulin receptor (pIgR) in Madin-Darby canine kidney (MDCK) cells [84, 93], the bile salt export pump (ABCB11) in hepatic cells [94], and the H⁺-K⁺-ATPase in gastric parietal cells (Calhoun, 1998). In addition, a role for Rab11a has been implicated in the recycling of exogenously expressed CFTR in polarized airway cells ([95])

Less is known about Rab11b, which localizes to apical vesicles disparate from the Rab11a-labelled compartment in the pericentriolar region of polarized MDCK and gastric parietal cells [89]. In non-polarized cells, Rab11b controls transferrin receptor recycling [87] and Ca²⁺-induced exocytosis of human growth hormone [90]. However, there is no data supporting a role for Rab11b in apical recycling in polarized epithelial cells.

Here we examined the functions of Rab11a and Rab11b in regulating apical CFTR trafficking in a physiologically relevant system that expresses CFTR endogenously and recapitulates the salt secretion functions of the large intestinal epithelia. Our data suggest that while CFTR localizes to both Rab11a and Rab11b compartments, only Rab11b functions to regulate CFTR recycling to the apical plasma membrane.

2.2 RESULTS

2.2.1 Endogenous CFTR Localizes to Punctate Vesicles at the Apical Pole of Polarized T84 Cells

The colonic epithelial cell line, T84, forms polarized monolayers that are similar both morphologically and functionally to intact intestinal tissues and therefore serve as a relevant

model for studying the contribution of polarized protein trafficking to vectorial electrolyte transport [128, 132, 148]. T84 cells express CFTR endogenously [112, 144] and have been used extensively to characterize CFTR-mediated chloride secretion [133, 135]. We examined CFTR cellular localization in this system by performing confocal microscopy using indirect immunofluorescence. CFTR localized to punctate, vesicle-like structures at the apical pole of polarized T84 cells (Figure 1A-E) that were at and beneath the apical plasma membrane as determined by their juxtaposition with the tight junction marker, ZO-1. Analysis of confocal stacks in the XZ plane (Figure 1F & G) confirmed that CFTR localized to the apical membrane domain in this system. Our findings are in agreement with prior studies of the polarized localization of endogenous CFTR in epithelia, including T84 cells [112, 113, 149].

2.2.2 CFTR colocalizes with both Rab11a and Rab11b in polarized T84 cells

Several studies have suggested that CFTR found within the subapical vesicle population in native systems is localized to endocytic and recycling compartments that facilitate its apical membrane trafficking [111, 117, 143]. Indeed, efficient CFTR endocytosis and recycling have been demonstrated in T84 cells [122]; however, no studies have examined the localization of CFTR relative to known markers of membrane recycling compartments in this system. Given the role of Rab11 in regulating the recycling of membrane proteins [86, 93] we speculated that CFTR would be present within the Rab11 recycling compartment. To test this, we first examined the expression of the Rab11a and Rab11b isoforms in T84 cells. Figure 2A reveals the presence of both Rab11a and Rab11b transcripts (lanes 1 & 3) as detected by RT-PCR using isoform-specific primers on cDNA generated from polarized T84 cell mRNA. Western blotting of cell lysates using Rab11a- or Rab11b-specific antibodies identified single bands of the expected 25kDa molecular weight, confirming the expression of both isoforms in this system (Figure 2B).

We next examined whether CFTR colocalized with either Rab11a or Rab11b by immuno-

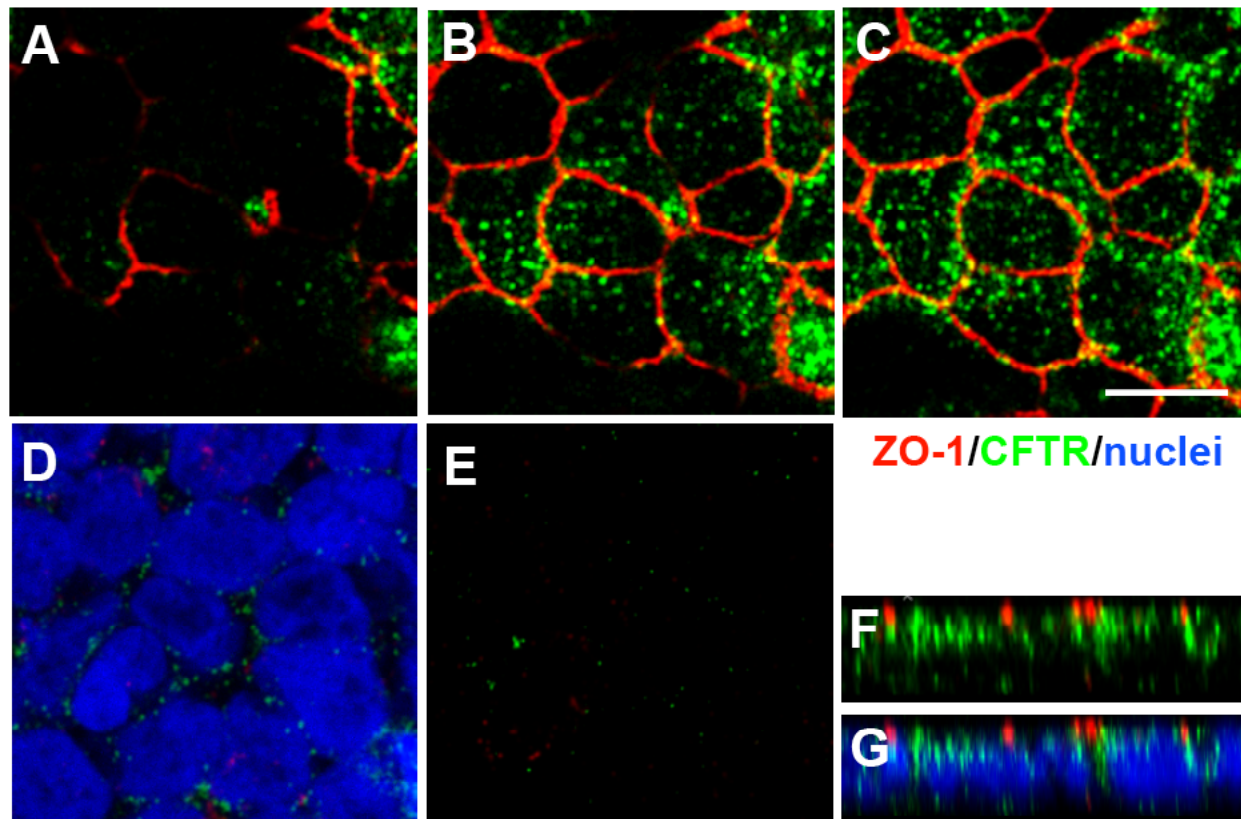


Figure 2.1: Localization of endogenous CFTR in polarized T84 cells.

(A-G) T84 cells were grown on Transwell supports for 7-10 days and then fixed and immunostained for ZO-1 (red), CFTR (green), and nuclei (blue) as described in MATERIALS AND METHODS. Confocal cross-sections were taken at 1 μ m (A), 2 μ m (B), 3 μ m (C), 6 μ m (D), and 12 μ m (E) from the first apically detectable fluorescence. The XZ section (F) demonstrates localization of endogenous CFTR (green) within apposition and sub-apical to the apical tight junction protein, ZO-1 (red). The identical XZ section is shown with nuclei (G). Scale bar = 5 μ m.

staining polarized T84 monolayers. Confocal microscopy revealed that Rab11a localized to the apical pole of T84 cells (Figure 2C, XZ) with a staining pattern that was more diffuse than the pericentriolar localization of Rab11a originally reported in MDCK cells [84]. CFTR staining overlapped significantly with that of Rab11a (Figure 2C, bottom panel & XZ), demonstrating that CFTR in T84 epithelia localizes to the apical recycling endosome (ARE) as defined by the presence of Rab11a in MDCK cells [86]. Next, we examined CFTR localization in relation to Rab11b, shown previously to localize to a different internal compartment than the Rab11a-identified ARE in MDCK cells [89]. Rab11b displayed a staining pattern at the apical pole of T84 cells similar to that reported previously for MDCK cells, and it also overlapped significantly with endogenous CFTR (Figure 2D, bottom panel & XZ). Finally, we also examined CFTR localization in relation to Rab21. Rab21 was identified and characterized in intestinal epithelial Caco-2 cells where it colocalizes with known markers of the early endocytic pathway at the apical membrane [150, 151]. Rab21 staining was more punctate than the staining observed for either Rab11a or Rab11b. We observed minor colocalization of CFTR with Rab21 as compared with Rab11a or Rab11b (Figure 2E), which suggests that CFTR is not localized primarily to this apical endocytic compartment under steady-state conditions. We conclude that endogenous CFTR localizes to both the Rab11a-identified ARE and Rab11b-positive compartments in polarized intestinal epithelial cells.

2.2.3 CFTR and Rab11 colocalize *in vivo*

Cryo-immunogold electron microscopy (EM) on rat intestine has demonstrated CFTR localization to the apical plasma membrane and within subapical vesicles of enterocytes lining the crypt [126, 143]. Early studies examining Rab11 localization in rabbit epithelial tissues, including the intestine, revealed prominent vesicular-like staining in the apical region [75]. To examine whether CFTR colocalized with Rab11 in native tissue, we co-stained isolated cryostat sections of rat jejunum with CFTR, Rab11, and actin antibodies and analyzed their localization

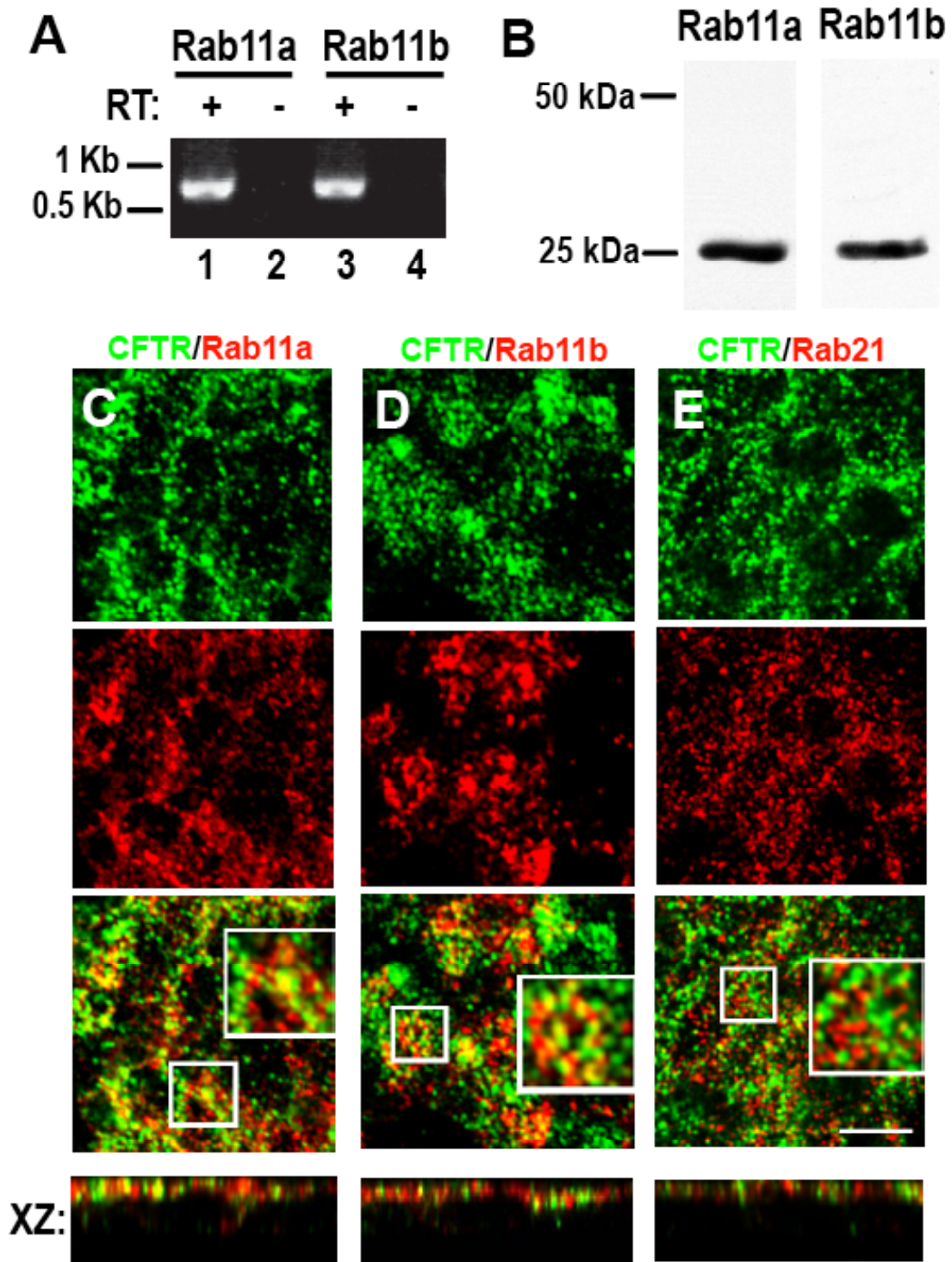


Figure 2.2: Rab11a and Rab11b are expressed in T84 cells and co-localize with CFTR.

(A-B) Expression of the Rab11 isoforms in T84 cells: (A) RT-PCR using Rab11a- or Rab11b-specific primers was performed using mRNA isolated from polarized T84 cells. Reactions without reverse transcriptase (RT) in lanes 2 & 4 confirm the absence of a genomic DNA contribution to the products from the mRNA samples. (B) Western blot analysis of T84 cell lysates with Rab11a- or Rab11b-specific antibodies shows the presence of each Rab11 isoform at the expected molecular weight of 25kDa. (C-E) Endogenous CFTR colocalizes with Rab11a and Rab11b at the apical pole in T84 cells. Confocal microscopic sections of polarized T84 cells stained for CFTR (green) and Rab11a (C), Rab11b (D), or Rab21 (E) (red). Both Rab11a and Rab11b colocalize with CFTR at the apical domain (yellow, bottom panel and XZ). Insets show enlarged regions within white boxes. Confocal sections shown were obtained at 3 μ m below the first detectable fluorescence at the apical surface (see Figure 1C). Scale bar = 5 μ m.

by confocal microscopy (Figure 3A-E). The Rab11 antibody used for this experiment recognizes both Rab11a and Rab11b (see MATERIALS & METHODS). We observed that CFTR colocalized with Rab11 and actin in native tissue at the apical region of enterocytes lining the crypt. We were unable to examine isoform-specific colocalization with CFTR *in vivo* due to the unavailability of isoform specific antibodies that recognize rat tissue. We conclude that CFTR is localized to apical, Rab11-positive recycling endosomes in rat intestine.

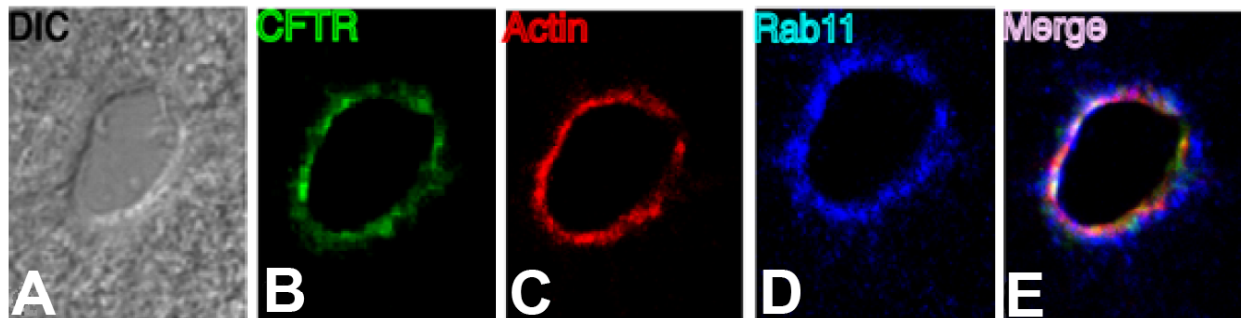


Figure 2.3: CFTR and Rab11 co-localize in rat intestinal crypts *in vivo*.

(A-E) Cryostat sections through rat jejunum at the level of the crypt are displayed. (A) Differential interference contrast (DIC) image showing histology of the section stained for CFTR (B), Actin (C), and Rab11 (D). Merge (E) demonstrates that CFTR colocalizes with Rab11 and actin at the apical pole of the crypt-lining enterocytes.

2.2.4 Immuno-magnetic isolation of Rab11-positive vesicles reveals the presence of CFTR

Studies examining the role of Rab GTPases in membrane trafficking have utilized immunoisolation of Rab-positive vesicles from endosome-enriched subcellular fractions [81, 152]. This biochemical technique allows for the isolation of intact, specific Rab-bearing compartments with subsequent identification of associated proteins. While our immunofluorescence data suggests that CFTR colocalizes with both Rab11a and Rab11b, it does not necessarily place CFTR within the Rab11 compartments. Therefore, to determine whether CFTR resides within the Rab11a- and Rab11b-labelled vesicular compartments and thereby support our morphological observations, we immunoisolated the Rab11 vesicles biochemically and tested for the presence of endogenous CFTR. T84 cells were homogenized and the homogenate was fractionated on a step-flotation sucrose gradient by ultracentrifugation. The 25/35% sucrose interface, which is enriched in Rab11-positive vesicles [81], was isolated and incubated with Rab11 isoform-specific antibodies. Antibody-bound endosomes were then immunoisolated with magnetic beads pre-coated with a secondary IgG and washed extensively. Bound vesicles were solubilized in Laemmli buffer, separated on SDS-PAGE, and immunoblotted for proteins of interest. Both Rab11a and Rab11b immunoisolations revealed an enrichment of endogenous CFTR within these vesicular compartments as compared to Rab21 or a non-specific IgG isolation (Figure 4A, top row). Immunoisolated samples were blotted for an ER-resident (Bip/GRP78) or a soluble (Actin) protein to confirm the purity and specificity of the immunoisolations (Figure 4A, rows 2 & 3). Further western blotting with a pan-Rab11 antibody that recognizes both Rab11a and Rab11b demonstrates that Rab11 endosomes were isolated successfully (Figure 4A, row 4).

Given the colocalization of CFTR with Rab11 in rat intestine (Figure 3), we investigated whether CFTR and Rab11 could be visualized within the same endosomes. Immuno-EM examination of vesicles isolated on sucrose gradients from rat jejunum enterocytes demonstrates the presence of CFTR-positive vesicles as shown in Figure 4B (left, 15nm gold particles).

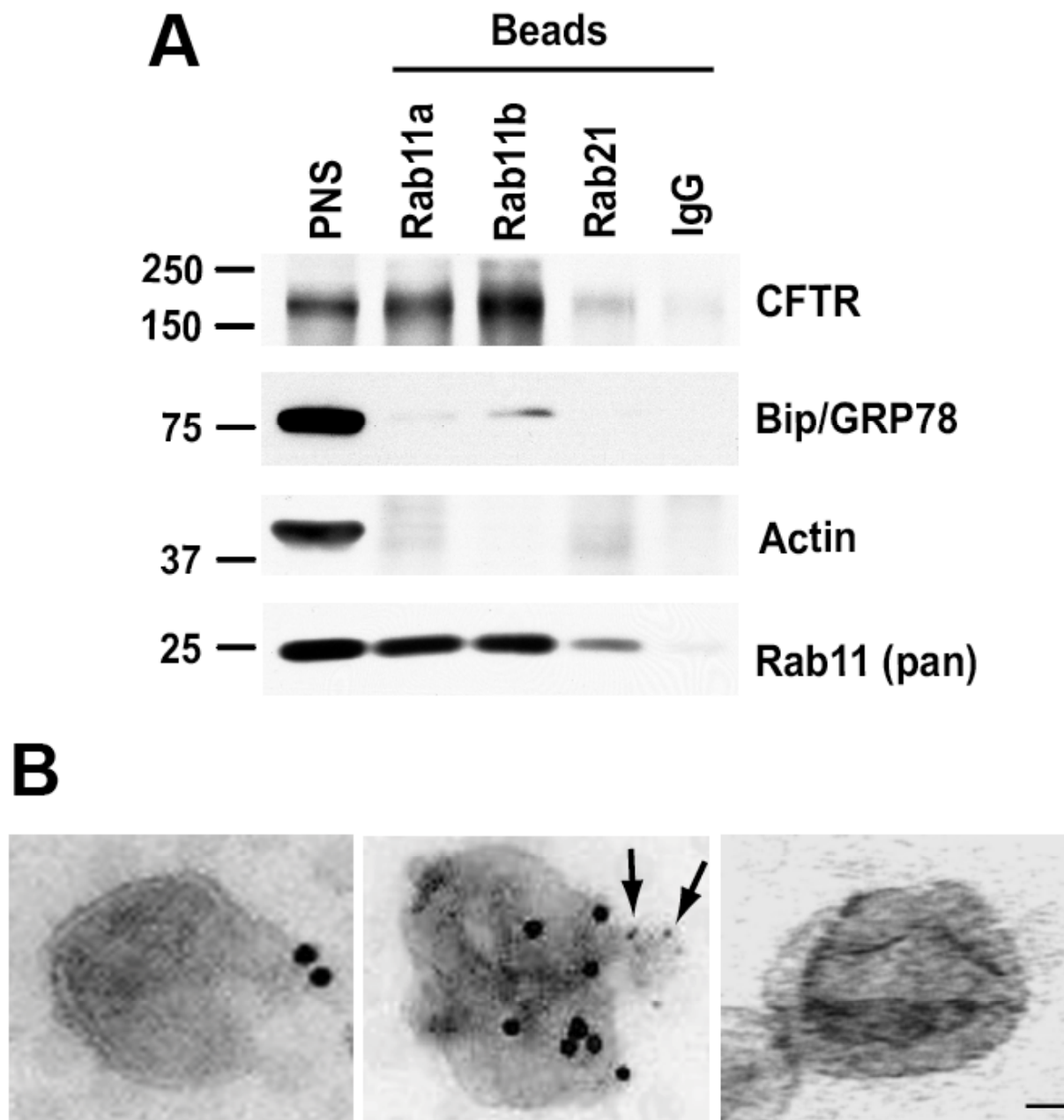


Figure 2.4: CFTR is present within Rab11 immuno-isolated vesicles.

(A) A T84 cell post-nuclear supernatant (PNS) was obtained following cell homogenization, loaded on a step-floatation sucrose gradient and centrifuged for 3 hours at 108,000xg. The 25/35% interface containing recycling and early endosomes was incubated with antibodies specific for Rab11a, Rab11b, Rab21, or a non-specific IgG. Rab-positive vesicles were isolated using magnetic Dynabeads pre-conjugated to an anti-rabbit secondary antibody. Beads were washed, bound vesicles were solubilized in sample buffer and separated on SDS-PAGE, and blotted for CFTR, Bip/GRP78 (ER), Actin, and Rab11 (pan antibody recognizes both isoforms). A representative blot of three independent experiments is shown. (B) Rat jejunum enterocytes were isolated and homogenized as described in MATERIALS and METHODS. The PNS was loaded on a step-floatation sucrose gradient and the 25/35% interface was isolated. Membranes

were deposited on an EM grid and micrographs obtained following immunogold labeling for CFTR (15nm) or CFTR and Rab11 (5nm, arrows). Endosomes incubated in the absence of the primary antibodies provide a negative control for the secondary immunogold labeling (right panel). Scale bar = 60nm.

Isolated vesicles co-stained for CFTR and Rab11 (5nm gold) revealed that both proteins could be localized to the same vesicle (Figure 4B, right). Thus, CFTR is present within Rab11-positive vesicles isolated from an endogenous-expression system and native tissue. These findings confirm our immunofluorescence observations.

2.2.5 Rab11b S25N selectively impairs CFTR function in SPQ halide efflux assays

To determine whether Rab11 was able to modulate CFTR function at the apical membrane, we performed SPQ halide efflux assays on T84 cells expressing Rab11 mutants. The iodide-sensitive, membrane impermeant fluorescent indicator, 6-methoxy-*N*-(3-sulfopropyl) quinolinium (SPQ), which is quenched in the presence of iodide, was introduced into coverslip-grown T84 cells by hypotonic shock in the presence of a NaI buffer [148]. After recovery, SPQ-loaded cells were mounted on a heated microscope stage in the continued presence of NaI buffer, and changes in CFTR-mediated SPQ fluorescence were monitored during perfusion at 37°C with NaNO₃ buffer (which does not quench SPQ fluorescence) containing the cAMP/PKA agonist, forskolin, or with vehicle as control. As shown in Figure 5A, perfusion of cells with nitrate buffer lacking forskolin results in a minor increase in fluorescence (blue triangles), due to iodide leakage from the cells under non-stimulated conditions. However, when T84 cells were perfused with nitrate buffer containing 10uM forskolin; cAMP/PKA-activation of CFTR yielded a robust increase in SPQ fluorescence, which results from the dequenching of SPQ as iodide exits the cells through CFTR in exchange for nitrate (red circles). The SPQ fluorescence was quenched rapidly upon reperfusion with iodide buffer, indicating re-entry of iodide through still-open CFTR channels.

To verify that the cAMP-evoked increase in SPQ fluorescence resulted from iodide efflux through CFTR channels, we performed SPQ experiments in the presence of the CFTR-specific inhibitors, GlyH101 and CFTR_{inh}172. While vehicle-treated cells responded robustly to agonist, similar to the data of Figure 5A, addition of the CFTR inhibitors reduced 90% of the SPQ

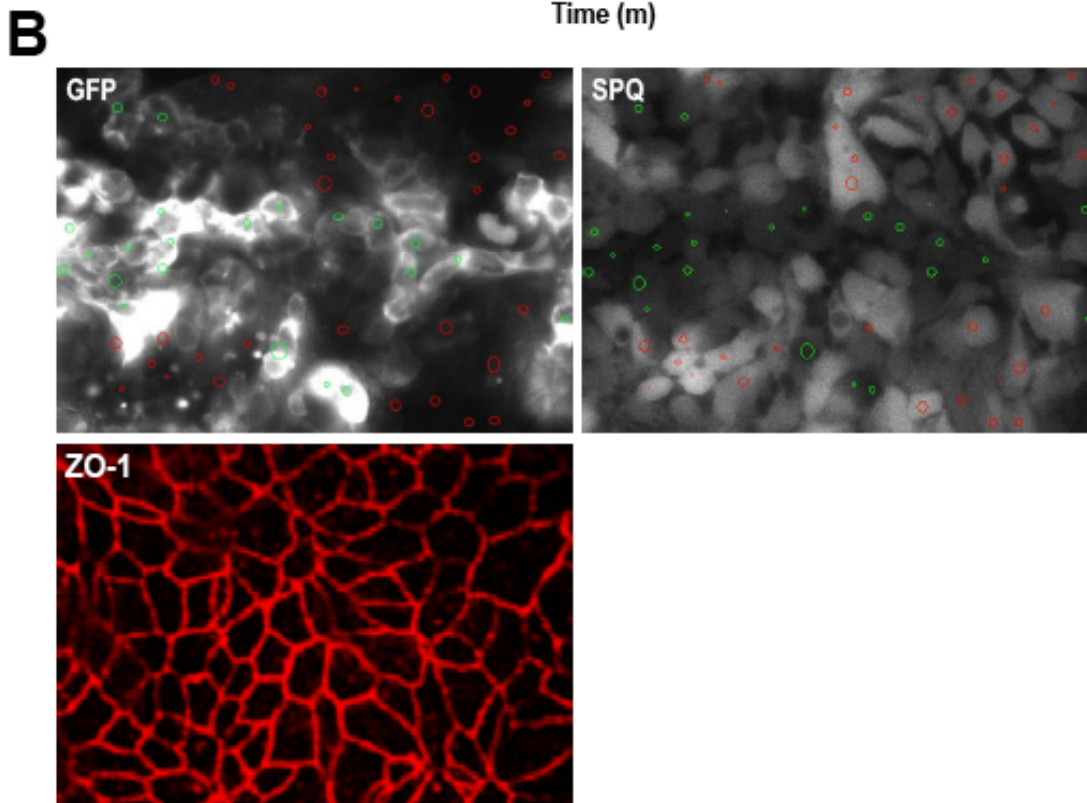
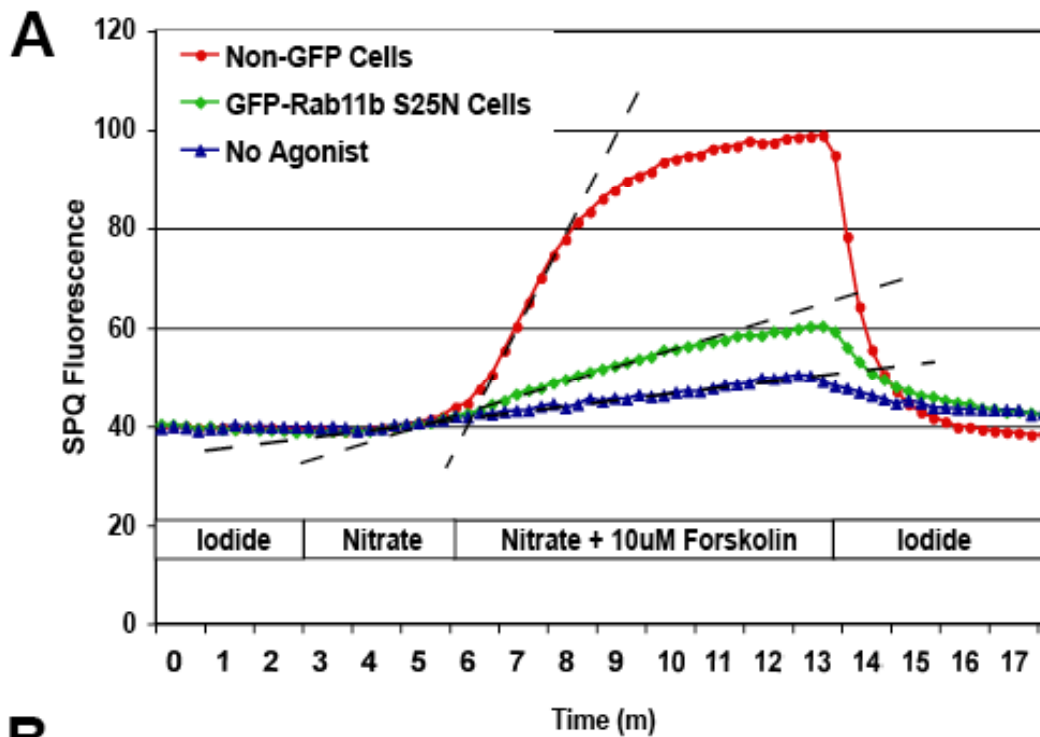


Figure 2.5: Dominant negative Rab11b impairs CFTR-mediated increases in halide permeability.

(A) Representative SPQ fluorescence traces showing increases in normalized fluorescence units for T84 cells perfused with nitrate buffer alone (blue triangles) or nitrate buffer with 10 μ M forskolin for T84 cells with (green diamonds) or without (red circles) GFP-Rab11b-S25N

expression. (B) Epifluorescent images of T84 cells expressing GFP-Rab11b-S25N collected at the 520nm (GFP) and the 460nm (SPQ) emission wavelengths for the same field of cells. The SPQ image depicts the image obtained at the peak fluorescence observed after perfusion for 6 minutes with nitrate buffer containing forskolin and shows that cells expressing the GFP-Rab11b-DN construct remain dim relative to those not expressing the GFP construct. Populations of cells expressing GFP-tagged Rabs were identified with green region of interest (ROI) circles while non-GFP cells were identified with red ROIs. Also shown is a field of T84 cells that were fixed and stained for ZO-1 after performing an SPQ experiment (ZO-1). Confocal sections reveal that ZO-1 localized to the tight junctions at the apical pole of T84 cells in the pattern characteristic of polarized cells.

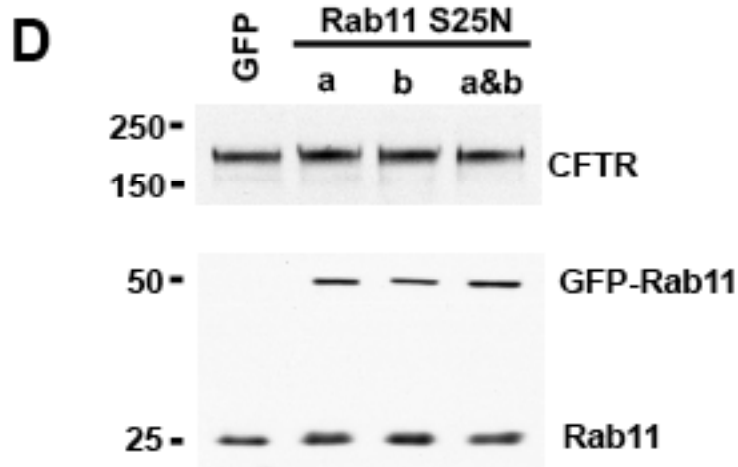
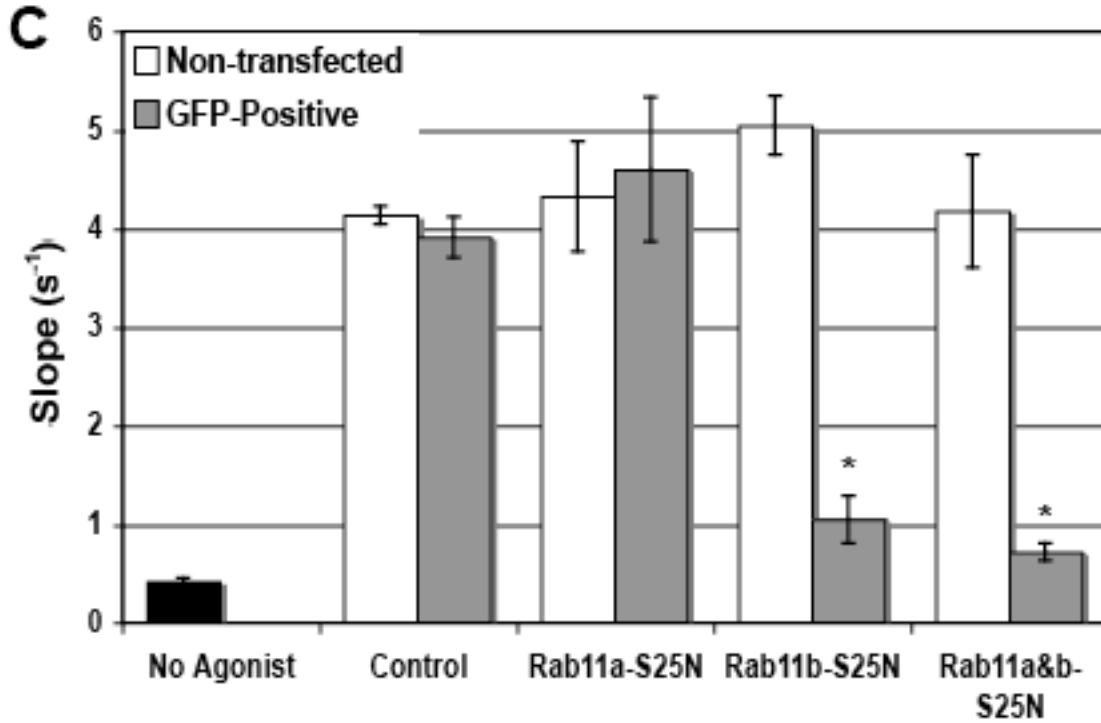
fluorescence increase (See Supplemental Figure 1A & B). These data confirm that SPQ fluorescence assays are a valuable technique for measuring cAMP/PKA regulated CFTR function in T84 cells.

To test for the role of the Rab11 isoforms in regulating CFTR function, T84 cells were electroporated with GFP-fused Rab11a and/or Rab11b dominant negative (S25N) constructs. Electroporation of T84 cells provides a technique for introducing constructs into these otherwise difficult-to-transfect epithelial cells with approximately 75% efficiency as estimated from the GFP fluorescence at 24 hours after electroporation (our unpublished observations, See MATERIALS & METHODS). Figure 5B shows epifluorescent images of T84 cells at the appropriate wavelength for GFP and SPQ detection for the same field of cells. Regions of interest (ROIs) were chosen for GFP-expressing cells (green circles) or for non-transfected cells, which did not express GFP (red circles). This approach allowed changes in SPQ fluorescence to be monitored in expressing and non-expressing populations within the same field of cells. After the SPQ determinations, T84 cells were fixed and stained for ZO-1 to examine whether cells grown on glass coverslips displayed a polarized phenotype. Figure 5B (ZO-1) shows that T84 cells grown for 3-5 days on glass were able to form tight junctions similar to cells grown on transwell filters (Figure 1C).

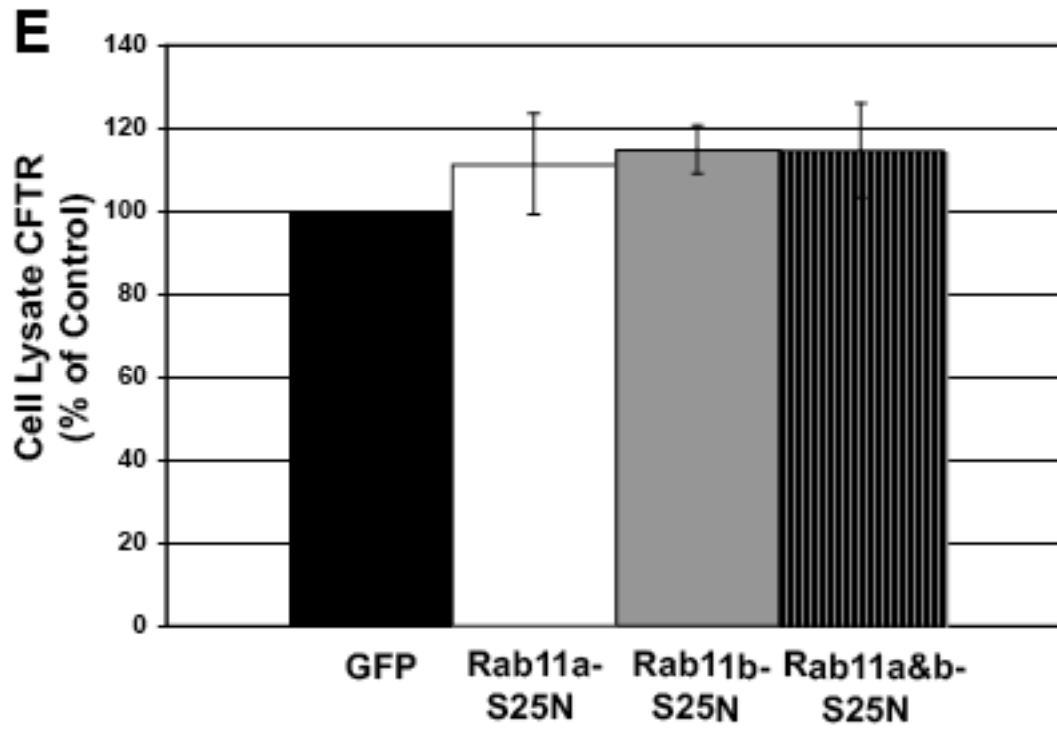
The S25N point mutation in Rab11a and Rab11b has been shown to increase its affinity for GDP, thereby locking the Rab GTPase in an inactive, non-membrane associated state [65, 87]. Figure 5A shows a representative SPQ tracing of GFP-Rab11b-S25N-expressing cells (green diamonds), while Figure 5B (SPQ) shows the corresponding SPQ image for the same field of cells at the peak of the response (6 minutes after forskolin addition). Note that GFP-Rab11b-S25N expressing cells (green ROIs) show a lower SPQ fluorescence peak signal compared to the neighboring non-GFP-Rab11b-S25N expressing cells (red ROIs), providing visualization of the signals depicted in Figure 5A. The summary figure (5C), provides the mean slope of the fluorescence increase (see dashed lines, Figure 5A) observed for cells under the three conditions examined: black bar, no agonist added; open bars, non-transfected (no GFP

expression detected); grey bars, cells expressing GFP. As shown in the first pair of bars, cAMP activation of CFTR-mediated halide efflux in GFP transfected cells did not differ when GFP-expressing and non-expressing cells were compared. The same was true in GFP-Rab11a-S25N transfected cell populations. However, cells expressing the GFP-Rab11b-S25N showed an ~80% inhibition of cAMP-stimulated CFTR activity compared to the non-expressing cells within the same field. Co-expression of dominant negative Rab11a and b did not cause any further significant decrease in cAMP stimulated CFTR activity over that observed for dominant negative Rab11b alone.

Due to the strong inhibition in CFTR function observed with overexpression of GFP-Rab11b-S25N, we lysed cells after SPQ assays and immuno-blotted to test for possible changes in CFTR protein expression. As shown in Figure 5D and quantitated in Figure 5E, CFTR levels remained unchanged in T84 cells overexpressing the Rab11b dominant negative as compared with GFP or Rab11a dominant negative cells. The expression of both of the GFP-fused Rab11 constructs (~50kDa) and the combined signal from each endogenous Rab11 isoform (~25kDa) are revealed by the pan-Rab11 antibody (Figure 5D, bottom panel). These findings show that the Rab11b dominant negative overexpression does not modulate total cellular levels of CFTR significantly, which suggests that its inhibition of CFTR function may reflect the regulation of membrane CFTR channel density by Rab11b. Overall, these results demonstrate that Rab11b regulates CFTR function in the plasma membrane of T84 cells and that functional Rab11b is required for CFTR-mediated halide efflux.



(C) Bars provide mean values for the maximal rate of fluorescence increase (see B, dashed lines, and MATERIALS & METHODS) for ROI populations from 4 different monolayers on coverslips (>200 cells total). Slopes were calculated for non-GFP-expressing (open bars) or GFP-expressing (grey bars) T84 cells within the same field. Data is mean \pm S.E.M. Statistically significant differences in GFP slopes compared to non-GFP slopes are denoted by * with $p < 0.01$. (D) T84 coverslips were scraped and lysed in lysis buffer immediately after SPQ experiments. Protein levels were quantitated; equal amounts of protein were loaded and separated by SDS-PAGE; and proteins were then transferred to PVDF for western blotting. The 50kDa band, as detected by the pan Rab11 antibody, represents the expression levels of the GFP-tagged Rab11 isoforms as compared with the combined (a + b) endogenous levels (25kDa).



(E) Quantitation of western blots reveals that CFTR protein levels are not altered significantly with overexpression of GFP-Rab11a- and/or b-S25N as compared to GFP (n=3, p>0.05).

2.2.6 Rab11b Q70L increases CFTR-mediated anion efflux

Studies examining the functional role of Rab GTPases in regulating membrane trafficking often also rely on the use of dominant active, GTP-locked mutants to further elucidate Rab trafficking mechanisms. We speculated that overexpression of the Rab11b dominant active mutant, Q70L, would produce increased CFTR activity in SPQ fluorescence assays, an effect opposite to that of the dominant negative mutant. As shown in Figure 6A (bottom panel), GFP-Rab11b-Q70L-expressing T84 cells showed an increase in the rate of SPQ dequenching (iodide efflux) in response to agonist, which was evident from the steeper slope of GFP-expressing cells (black diamonds) as compared to non-GFP cells (grey circles) within the same field. This difference was not observed for GFP-Rab11a-Q70L expressing cells relative to non-GFP cells (Figure 6A, top). The absence of an increase in the plateau of SPQ fluorescence with the Rab11b mutant is most likely due to saturation of dye fluorescence intensity, which is reached more rapidly in cells expressing the active form of Rab11b. To display the summary data, we calculated the rate constants by fitting the increases in SPQ fluorescence observed between the 6.5 to 11 minute time intervals to a single-exponential function. Figure 6B shows the mean rate constants for GFP-Rab11a- or b-Q70L expressing cells (GFP-positive) as compared to non-expressing cells (Non-transfected) for more than 200 cells from 4 different monolayers for each group. These data show that overexpression of the dominant active Rab11b increases the kinetics of the CFTR-mediated SPQ fluorescence response.

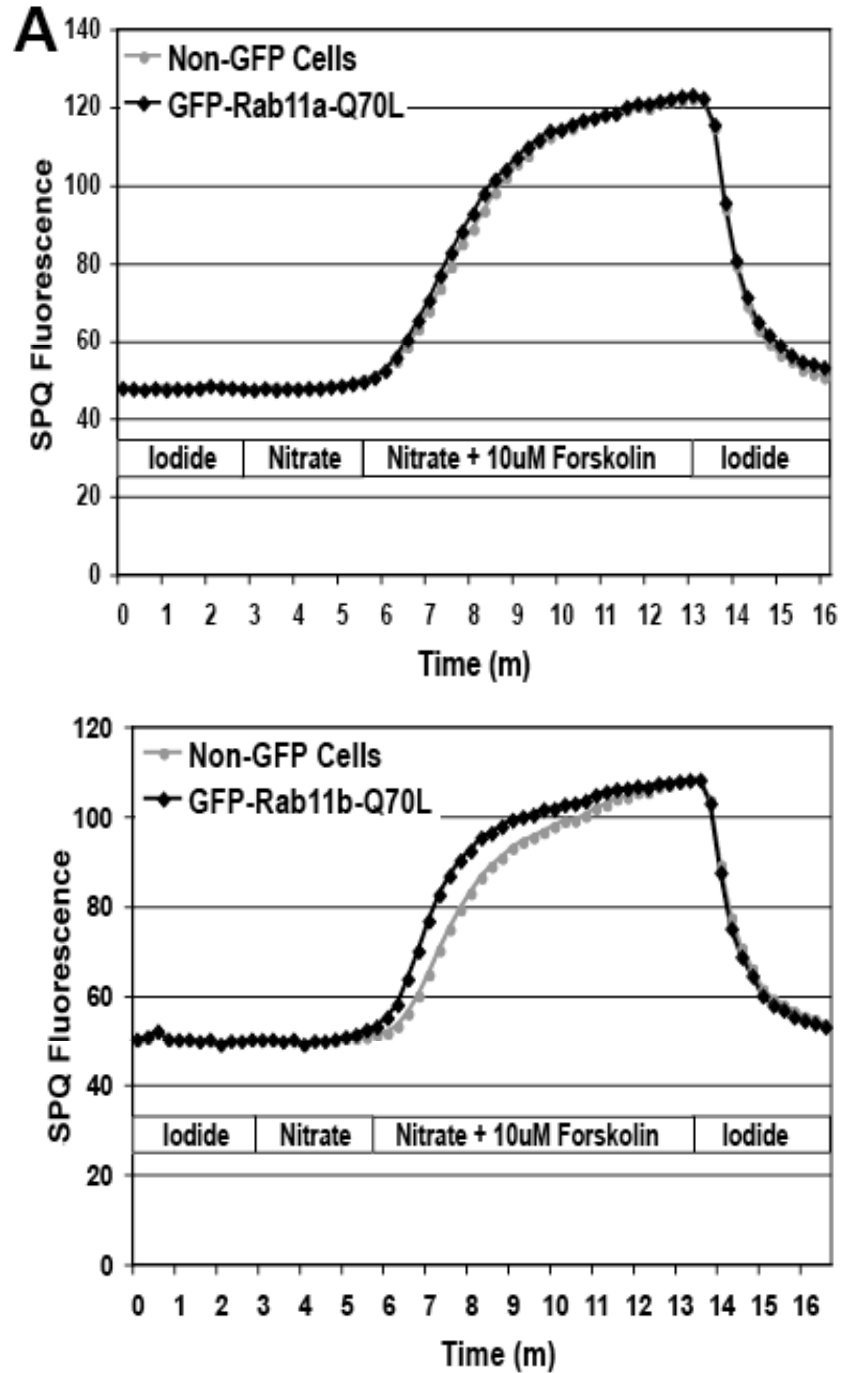
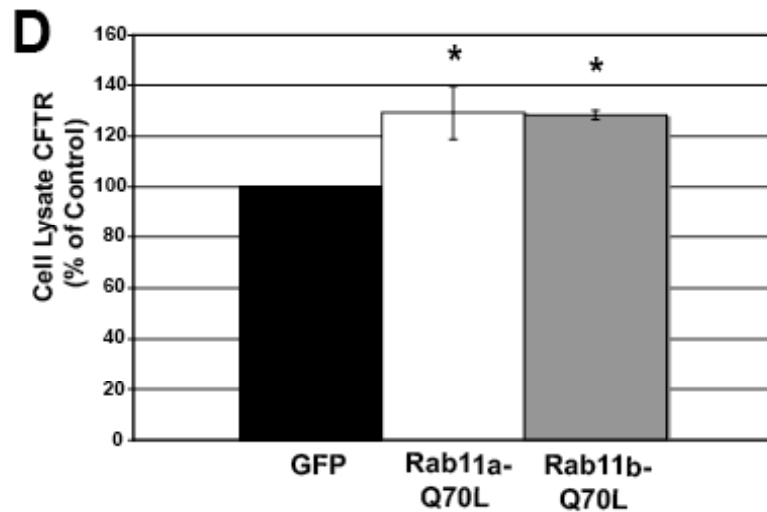
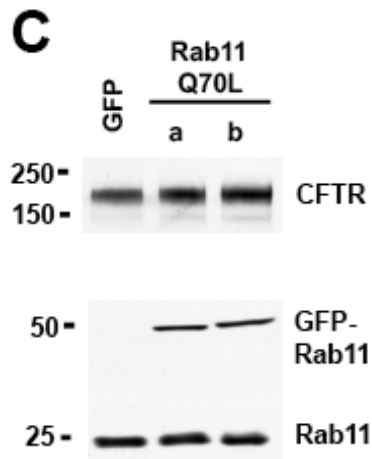
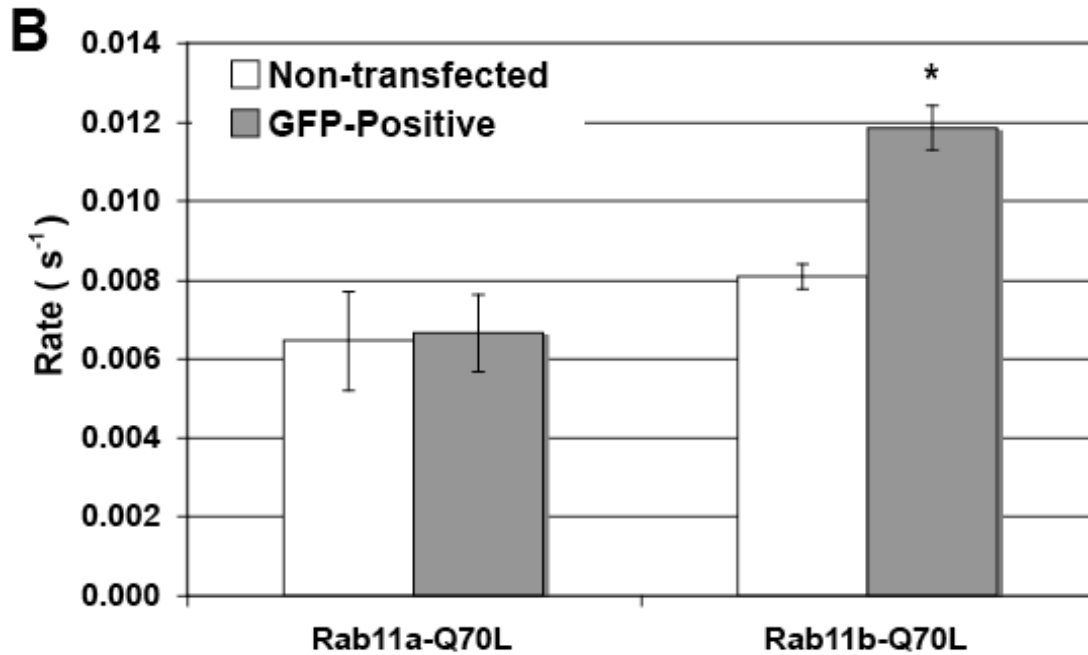


Figure 2.6: Dominant active Rab11b accelerates the CFTR-mediated halide permeability response to agonist.

(A) Representative SPQ fluorescence traces (mean of 40 cells) for GFP-Rab11a- (upper panel) or Rab11b-Q70L- (lower panel) expressing cells (black diamonds) as compared to non-GFP expressing cells (grey circles) within the same field, show an increased response rate for the GFP-Rab11b-Q70L expressing cells.



(B) Rate constants were calculated from the mean rates from 4 different monolayers (>200 cells) using a single-exponential function (See MATERIALS & METHODS) for the two populations. Data are mean \pm S.E.M. *Value is significantly different ($p < 0.01$) from non-GFP expressing cells. (C & D) Western blot analysis of lysates obtained from T84 cells used for SPQ experiments shows that total CFTR levels in GFP-Rab11a-Q70L and GFP-Rab11b-Q70L expressing cells increase by $29 \pm 10\%$ and $28 \pm 2\%$, respectively. Each * denotes a significantly different value relative to non-GFP expressing cells ($p < 0.005$).

To examine CFTR protein levels within dominant active-expressing cells, western blotting for CFTR was performed on lysates obtained from cells used for SPQ experiments. Unlike the dominant negative mutant, we detected a minor but significant increase in the steady-state CFTR protein levels in both of the dominant active Rab11a and Rab11b cell populations as compared to GFP transfected cells (Figure 6C & D). These results suggest that overexpression of the dominant active Rab11 isoforms influences endogenous CFTR expression levels; however, only overexpression of the Rab11b dominant active yielded an increase in the rate of SPQ dequenching in the halide efflux experiments.

2.2.7 Dominant negative Rab11b expression inhibits CFTR chloride secretion across polarized T84 monolayers

T84 cells seeded onto semi-permeable transwell supports form polarized monolayers that develop high levels of transepithelial resistance (TER), enabling them to generate vectorial chloride secretion similar to the native intestinal epithelia [128]. The asymmetric distribution of ion transporters and channels that mediate net transepithelial movement of ions have been thoroughly described in this system, and it is well accepted that CFTR provides the primary exit pathway for chloride secretion across the apical membrane in polarized T84 cell monolayers (reviewed in [135]). Therefore, this system serves as an ideal model for testing the contribution of apical CFTR traffic regulation to the secretory function of the epithelia. To examine whether Rab11b regulates CFTR function in a fully polarized cell system, short-circuit current (I_{sc}) measurements were performed in Ussing chambers using T84 epithelia transduced with adenoviruses that express GFP, GFP-Rab11a-S25N or GFP-Rab11b-S25N. Figure 7A shows representative I_{sc} tracings for GFP (black), GFP-Rab11a-S25N (light grey), or GFP-Rab11b-S25N (dark grey) expressing cells and reveals a robust inhibition of forskolin-activated, CFTR-conducted chloride current in the dominant negative Rab11b-transduced monolayer as compared to the GFP- or GFP-Rab11a-S25N-transduced monolayer. Addition of bumetanide to block the

basolateral $\text{Na}^+\text{-K}^+\text{-2Cl}^-$ (NKCC1) cotransporter inhibited the Isc by blocking chloride uptake across the basolateral membrane, which is required for chloride secretion. The summary figure (7B) shows the mean change in forskolin-induced short-circuit current across adenovirus-transduced T84 monolayers expressing GFP (black bar), GFP-Rab11a-S25N (light grey bar), or GFP-Rab11b-S25N (dark grey bar). In agreement with our SPQ data (Figure 5C), the dominant negative Rab11a construct failed to inhibit the forskolin-stimulated increase in Isc as compared to GFP expressing control monolayers. However, overexpression of the dominant negative Rab11b reduced CFTR-mediated chloride secretion by $\sim 70\%$, as compared to the control GFP expressing monolayers. The ability of the GFP-Rab11a-S25N virus to inhibit apical recycling through the ARE was verified as it was shown to block dIgA recycling in polarized MDCK cells (personal communication, Dr. A. Oztan; data not shown). Visual inspection of the transduced cell monolayers by epifluorescence microscopy prior to Ussing chamber experiments allowed an approximation of expression for the virally-delivered constructs. An epifluorescent image of a T84 monolayer expressing GFP-Rab11b-S25N is shown in Figure 7C, which demonstrates the high percentage of cells transduced. To examine whether the robust inhibition in CFTR-mediated current was a result of decreased total cell CFTR expression, we lysed cells from transwell supports after Ussing chamber experiments and performed western blots for CFTR and Rab11. As shown in Figure 7D and quantitated in 7E, endogenous CFTR protein levels in T84 monolayers remained unaltered with adenovirus-mediated overexpression of either dominant negative Rab11 isoform as compared to GFP expressing T84 cells. The pan Rab11 antibody was used to detect both GFP-fused Rab11 isoforms in addition to the endogenous Rab11 isoforms. These results demonstrate the selective requirement for the Rab11b isoform function in supporting regulated, CFTR-mediated transepithelial chloride secretion across polarized T84 cell monolayers.

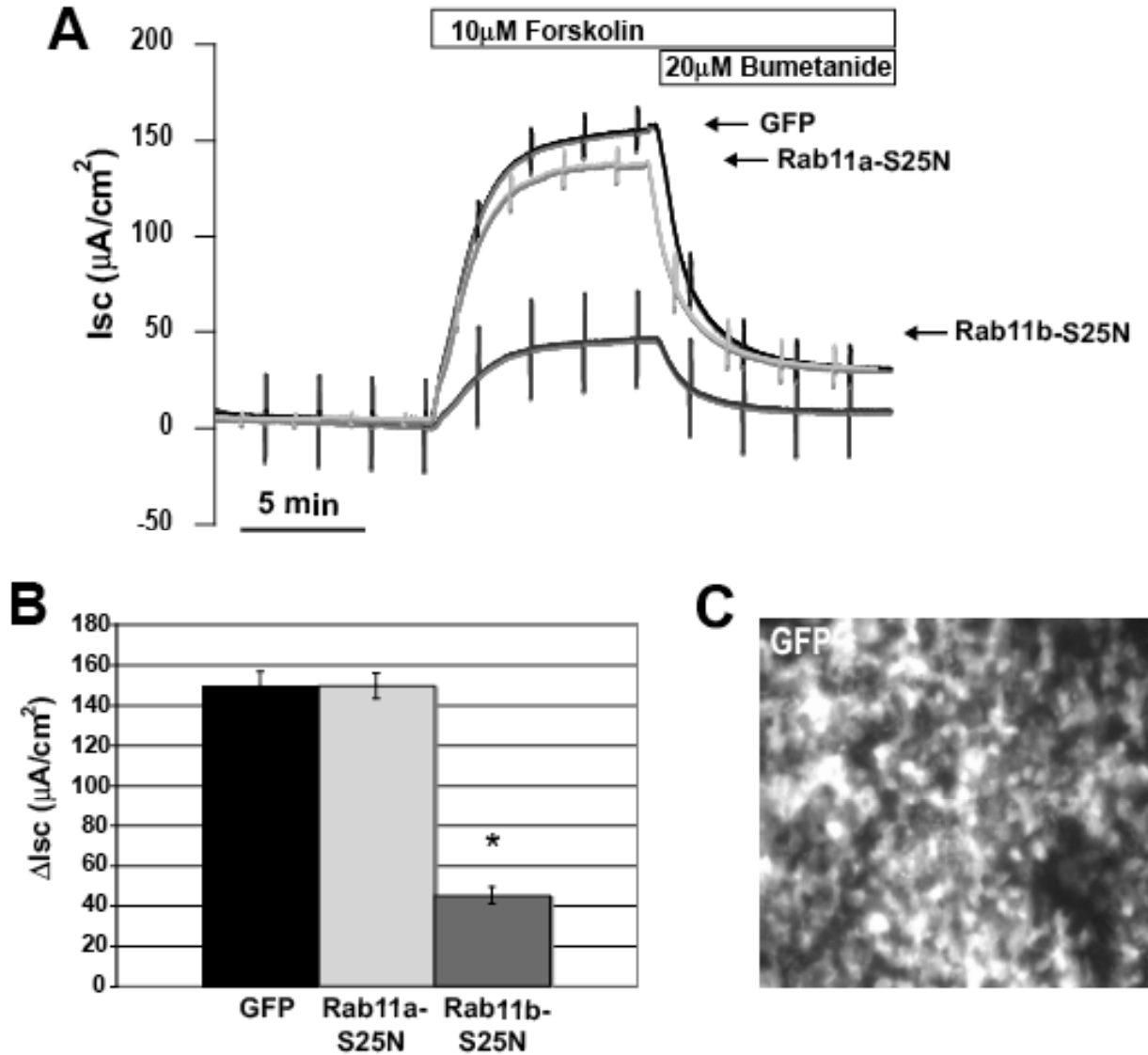
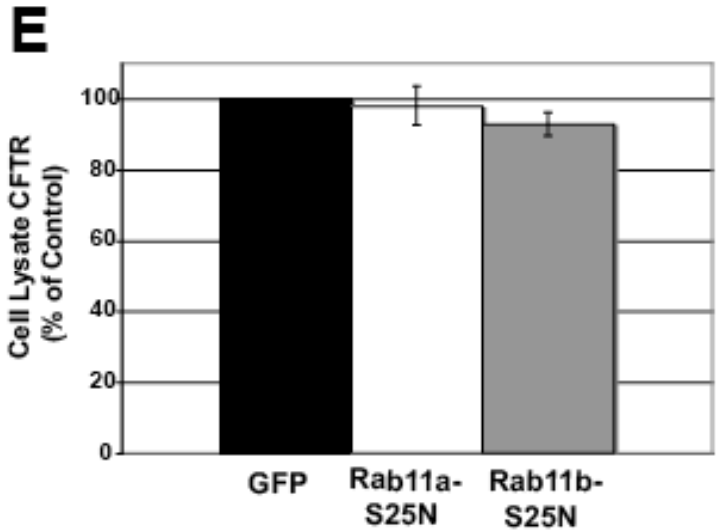
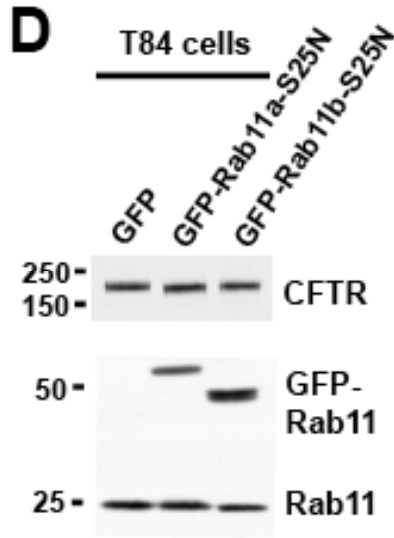


Figure 2.7: Dominant negative Rab11b expression inhibits short circuit current (Isc) in polarized T84 cell monolayers.

(A) Representative Isc traces recorded from T84 monolayers transduced with GFP (black), GFP-Rab11b-S25N (light grey), or GFP-Rab11a-S25N (dark grey) show that only dominant negative Rab11b strongly inhibits forskolin-activated CFTR chloride currents. (B) Bars provide mean (\pm S.E.M) changes in CFTR-mediated Isc for GFP (black), GFP-Rab11a-S25N (light grey), or GFP-Rab11b-S25N (dark grey) expressing T84 cell monolayers (n=6). * denotes $p < 0.0003$. (C) Image depicts fluorescent capture of T84 cell monolayer prior to current measurements demonstrating robust expression of GFP-Rab11b-S25N. Similar micrographs were evidenced for GFP and GFP-Rab11a-S25N cells (not shown).



(D) Western blot of T84 lysates obtained after short circuit current measurements on GFP, GFP-Rab11a- & b-S25N. GFP-tagged Rab11 mutants detected at the expected 50kDa molecular weight with a pan-Rab11 antibody reveals similar expression of each dominant negative Rab11 isoform. (E) Quantitation of whole cell lysate protein levels reveal that total cellular CFTR levels (\pm S.E.M.) in GFP-Rab11a & b-S25N cells remain unchanged relative to GFP control (n=4, p>0.1).

2.2.8 Dominant negative Rab11b expression decreases CFTR protein expression at the apical membranes of polarized T84 monolayers

To determine whether the reduction in transepithelial chloride transport across T84 epithelia reflects Rab11b modulation of CFTR density at the apical membrane, we used cell surface biotinylation to examine the levels of endogenous CFTR present at the apical surface of polarized T84 monolayers transduced to express GFP, GFP-Rab11a-S25N, or GFP-Rab11b-S25N. Epifluorescent inspection of GFP expression in monolayers 24 hours after adenoviral transduction revealed similar expression efficiency as evidenced in monolayers used for the short circuit current measurements (Figure 7C; data not shown). In addition, measurements taken 24 hours after transduction showed recovery of the TER of T84 monolayers to approximately 75% of that recorded prior to tight junction disruption and viral transduction (data not shown, see MATERIALS & METHODS). As shown in Figure 8A, biotinylation of the apical membrane followed by streptavidin-mediated precipitation and CFTR immunoblotting revealed a significant decrease in apical membrane CFTR protein levels in GFP-Rab11b-S25N cells as compared to GFP- or GFP-Rab11a-S25N-expressing T84 cells (top panel). Quantitation showed a $49 \pm 13\%$ decrease in the apical membrane CFTR as compared to GFP or GFP-Rab11a-S25N cells (Figure 8B). Western blot analysis of the input used for biotin pull down showed that total CFTR levels were unaltered (Figure 8A, second row), which is in agreement with the total cellular CFTR levels measured in cells used for short circuit current measurements (Figure 7D & 7E). These results show that Rab11b, not Rab11a, regulates CFTR channel density at the apical membranes of polarized T84 intestinal epithelial cells under cAMP/PKA stimulation conditions. The magnitude of this reduction in apical CFTR suggests that it is responsible primarily for the inhibition of the short circuit currents elicited by the expression of the dominant negative Rab11b.

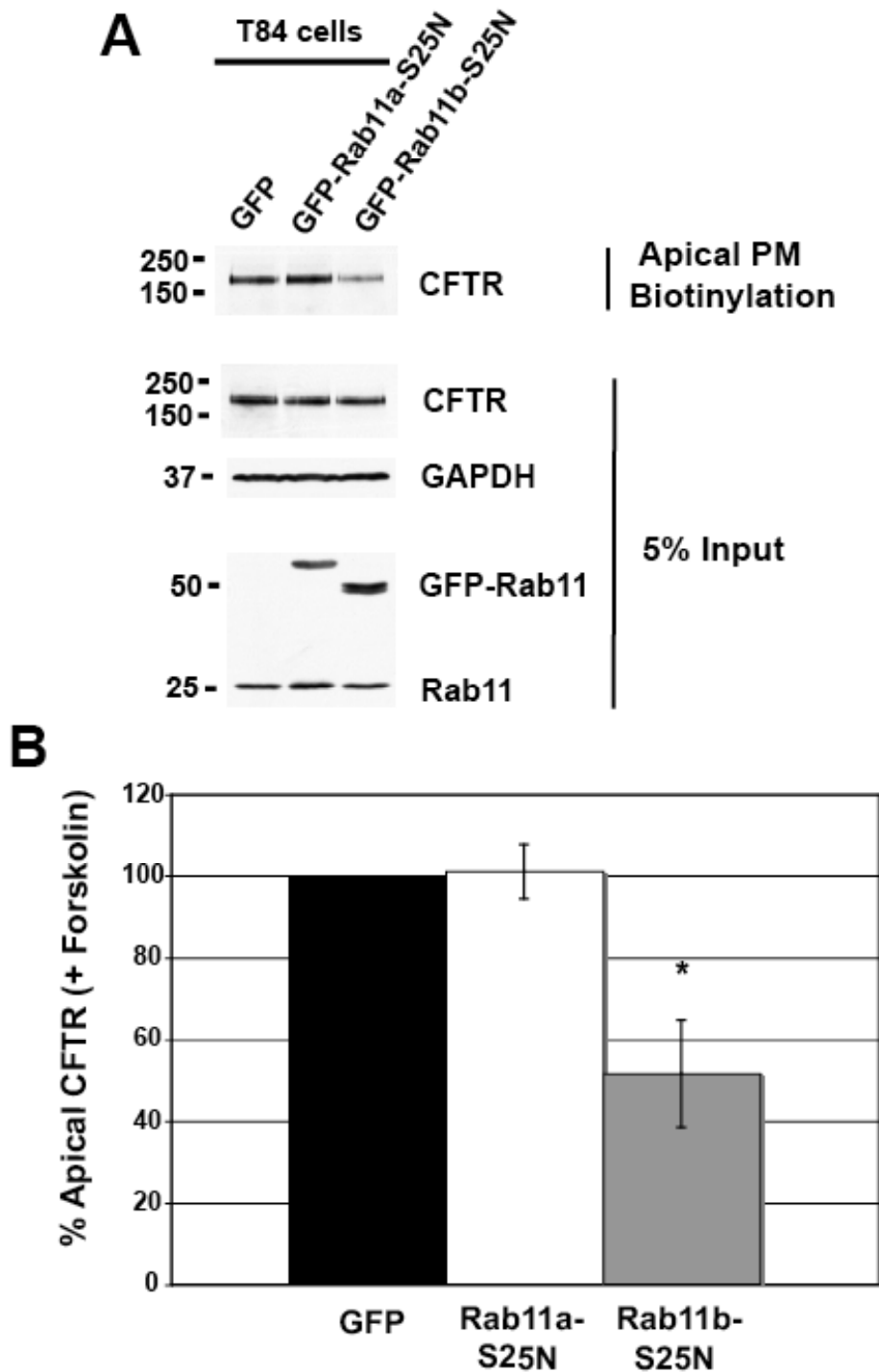


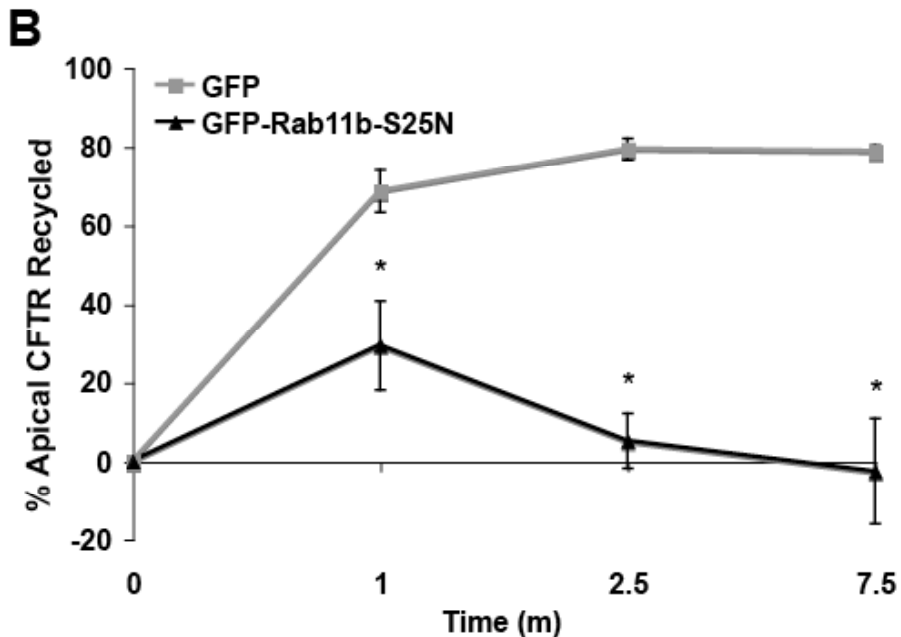
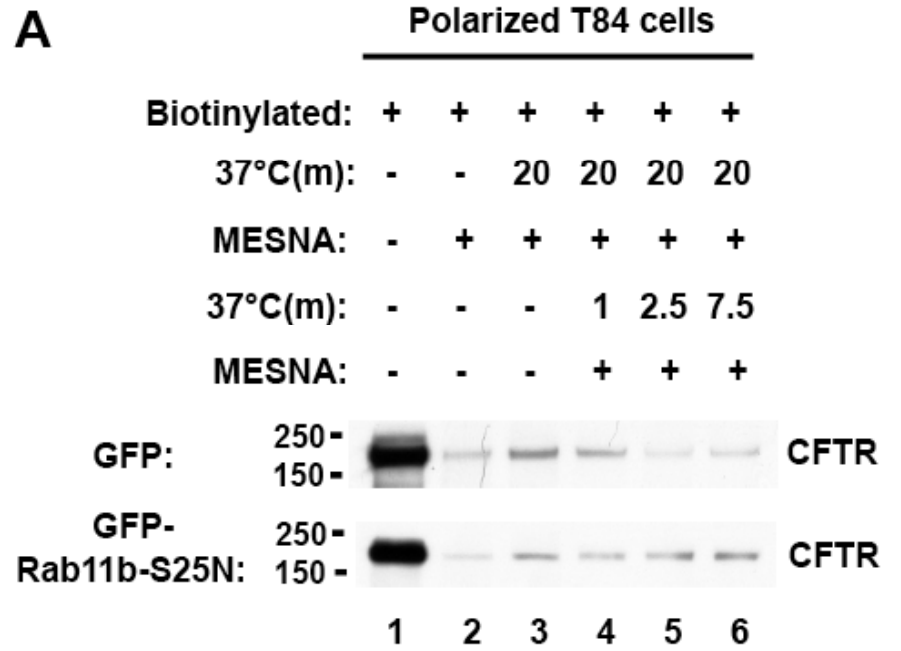
Figure 2.8: Dominant negative Rab11b overexpression decreases apical membrane CFTR in polarized T84 cells.

(A) Representative CFTR western blot following apical membrane biotinylation and streptavidin pull down shows decreased cell surface CFTR in GFP-Rab11b-S25N expressing cells relative to the GFP control or GFP-Rab11a-S25N expressing monolayers. To mirror the apical CFTR density measurements with the functional analysis reported in Figure 7,

biotinylation was performed after a 10 minute stimulation of the epithelia with 10 μ M forskolin. Western blotting of 5% of the precipitate (input) reveals that total CFTR levels remain unchanged (see Figure 7E); GAPDH was used as loading control. Immunoblotting with pan-Rab11 antibody demonstrates the expression of endogenous Rab11 and both dominant negative GFP-fused Rab11 isoforms. (B) Quantitation of apical membrane CFTR from biotinylation of polarized T84 cells transduced with GFP, GFP-Rab11a- or b-S25N (n=3), showing that the Rab11b dominant negative construct decreases the mean levels of apical membrane CFTR by 48 \pm 13%, relative to the GFP control. * denotes p<0.05.

2.2.9 Dominant negative Rab11b inhibits apical recycling of CFTR in polarized intestinal epithelial cells

Given the efficient apical recycling of endogenous CFTR in polarized epithelial cells and the well described role for Rab11a in membrane recycling, we speculated that Rab11b may also function as a regulator of apical membrane recycling. Therefore, the apical recycling of endogenous CFTR in polarized T84 monolayers transduced to express either GFP or GFP-Rab11b-S25N was examined using a biotin protection assay as described in MATERIALS & METHODS. As shown in Figure 9A (see figure legend) and quantitated in Figure 9B, endogenous CFTR recycled rapidly in GFP-transduced control cells (grey squares), with ~68% of the biotin-labeled, internalized CFTR returning to the apical surface after 1 minute in the presence of forskolin. However, only 5% of apical CFTR recycled at 2.5 minutes in GFP-Rab11b-S25N expressing cells (black triangles), compared with ~80% recycling in control, GFP-expressing cells. Together, the results from dominant negative construct expression show that CFTR requires the selective function of Rab11b to maintain proper CFTR channel density at the apical membrane and that this is accomplished by its efficient and rapid recycling through a Rab11b-regulated pathway.



Figure

2.9:

Dominant negative Rab11b inhibits the apical recycling of endogenous CFTR in polarized T84 cells.

(A) Representative CFTR blots obtained from biotin protection assays utilized to measure CFTR recycling in polarized T84 cells transduced with GFP (top row, exposure time = 30 seconds) or GFP-Rab11b-S25N (bottom row, exposure time = 45 seconds) (see MATERIALS & METHODS). Lane 1 depicts the total apical membrane CFTR that was biotinylated at 4°C while lane 2 demonstrates that the MESNA stripping buffer removes biotin from the apical monolayer surface efficiently (at 4°C) by reduction of the disulfide bond in the cleavable biotin reagent. The amount of cell surface biotinylated CFTR internalized during 20 minutes at 37°C is shown in lane 3, while lanes 4, 5, and 6 represent the internalized CFTR that remains in the cells at 1, 2.5, and 7.5 minutes, respectively, that is, the difference between lanes 3 and 4, 5, or 6 represents

recycled CFTR. Note that the biotinylated CFTR in GFP expressing cells is protected from the MESNA reducing agent after internalization (lane 3), but becomes sensitive again after recycling to the cell surface as indicated by the progressive decrease in band intensity seen in lanes 4, 5, & 6 (top row). T84 monolayers overexpressing dominant negative Rab11b accumulate MESNA-resistant biotinylated CFTR, indicating its failure to recycle (bottom row, lanes 4, 5, and 6). (B) Quantitation of apical CFTR recycling for GFP (grey squares) and GFP-Rab11b-S25N (black triangles) expressing T84 monolayers (GFP-Rab11b-S25N, n=3; GFP, n=5). * denotes a significantly different value for GFP-Rab11b-S25N recycling as compared to CFTR recycling in GFP control monolayers (1 min = $p < 0.05$, 2.5 min = $p < 0.001$, 7.5 min = $p < 0.005$). CFTR recycling values obtained at 1, 2.5, or 7.5 minutes for GFP-Rab11b-S25N expressing monolayers are not significantly different from one another, $p > 0.1$.

2.2.10 shRNA-mediated knockdown of Rab11b inhibits CFTR-mediated increases in SPQ fluorescence in T84 cells

Work done to examine the effector protein binding properties for each of the Rab11 isoforms suggested that they may share common downstream effectors due to their high level of similarity [153]. To confirm that our results obtained with the dominant negative Rab11b overexpression were not a result of impairing indirectly the function of Rab11a, and to determine whether Rab11b protein expression is required for recycling of endogenous CFTR, we performed SPQ fluorescence assays on T84 cells depleted of either Rab11 isoform using shRNA-mediated knockdown. Figure 10A shows the results of SPQ fluorescence experiments performed on T84 cells expressing GFP-tagged shRNA constructs for a scrambled, non-specific sequence or specific for Rab11a or Rab11b. Data from non-transfected, control cells (open bars) within the same field as the GFP-positive, shRNA knockdown cells (grey bars) is provided as the slope of the increase in SPQ fluorescence dequenching. Neither scrambled nor Rab11a shRNA expressing knockdown cell populations (GFP-positive) differed significantly from non-transfected cells when the slopes of the SPQ fluorescence increase in response to forskolin were compared. However, cells with reduced Rab11b expression showed a $53 \pm 14\%$ reduction in agonist-evoked halide efflux, again demonstrating isoform specificity in the Rab11 effect on CFTR function. Western blotting with Rab11a or Rab11b-specific antibodies of T84 lysates collected after SPQ experiments confirmed significant knockdown of Rab11a or Rab11b (Figure 10B). In addition, steady-state levels of CFTR were reduced differentially by knockdown of Rab11a or Rab11b: $17 \pm 7\%$ or $63 \pm 10\%$, respectively. These isoform-specific knockdown results support our previous conclusions, drawn from the mutant Rab11b experiments, and suggest that expression of Rab11b, but not Rab11a, is required to control the CFTR density at the membranes of T84 cells.

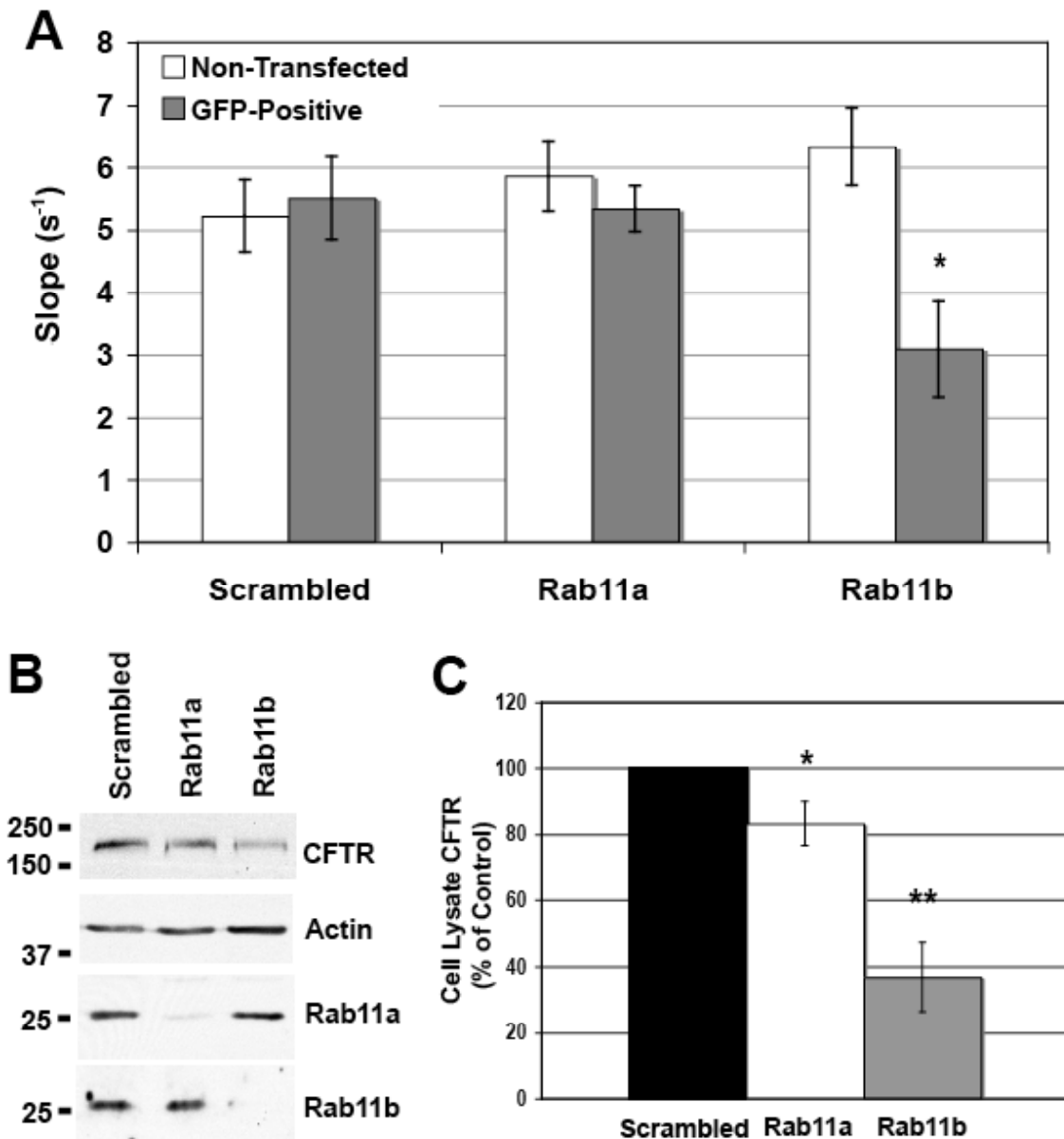


Figure 2.10: shRNA knockdown of Rab11b inhibits CFTR-mediated halide efflux from T84 cells.

(A) Mean values for the maximal slope of the SPQ fluorescence increase (halide efflux) for ROI populations of T84 monolayers, as follows: non-transfected, non-GFP-expressing (open bars) or GFP-expressing (grey bars) cells imaged within the same field (see MATERIALS & METHODS and Figure 5 Legend). Mean data were derived from 3 monolayers each; >100 cells total; mean \pm S.E.M. Statistically significant difference ($p=0.01$) in SPQ response is denoted by *. (B) T84 coverslips were scraped and solubilized in lysis buffer immediately after SPQ experiments. Protein levels were quantitated and equal amounts of protein were loaded and separated by SDS-PAGE. Knockdown of the individual Rab11 isoforms was confirmed using isoform-specific

Rab11a or Rab11b antibodies, as shown. (C) Quantitation of the total cellular CFTR in Rab11 isoform knockdown cells. Knockdown of either Rab11a or Rab11b decreases the endogenous CFTR protein expression by $17 \pm 7\%$ or $63 \pm 10\%$, respectively. * Denotes p-value < 0.05 , ** denotes $p < 0.005$, (n=4).

2.3 DISCUSSION

CFTR is a dynamic protein within the apical membrane of epithelial cells, where it undergoes rapid and efficient endocytic internalization and recycling back to the cell surface [118, 154]. Extensive data from our own work and numerous other investigators has demonstrated the importance of CFTR recycling in the maintenance of apical membrane CFTR (reviewed in [118]). CFTR internalization and recycling rates influence both plasma membrane copy number and the channel's functional half-life directly, and therefore, these processes directly impact CFTR-mediated anion secretion. Herein, we tested the hypothesis that a member of the Rab family of small GTPases functions to maintain appropriate CFTR density at the apical membrane in polarized epithelial cells by facilitating its efficient recycling.

We demonstrate that Rab11b, a member of the Rab11 family of GTPases, regulates the intracellular recycling of CFTR in polarized T84 epithelial cells. Our immunofluorescent staining for CFTR revealed punctate structures localized at and beneath the TJ marker, ZO-1, suggesting endogenous CFTR localization at the plasma membrane and within subcellular compartments. These findings agree with the biochemical data obtained from studies performed previously in T84 cells [122]. In addition, we show that a portion of this CFTR co-localized with both Rab11a- and Rab11b-labeled vesicles at the apical pole of T84 epithelial cells. The localization of CFTR to Rab11 positive compartments was confirmed by the immunoisolation of both Rab11a- and Rab11b-containing vesicles from T84 cells and immuno-EM on Rab11 vesicles isolated from rat jejunal enterocytes, which demonstrates the presence of endogenous CFTR within these subcellular compartments, not only in cell culture but also *in vivo*.

Despite the observation that CFTR co-localized with both Rab11a and Rab11b, our results from halide efflux measurements and transepithelial chloride secretion across polarized T84 monolayers show that only Rab11b is involved in maintaining functional CFTR at the apical plasma membrane. Diminished CFTR function produced by overexpression of the dominant negative Rab11b could not be explained by alterations in CFTR biosynthesis or degradation, as

whole cell CFTR protein levels remained unchanged. However, the strong inhibition of CFTR function observed suggested that CFTR was depleted from the apical membrane; therefore, we employed biochemical assays to examine endogenous CFTR channel localization and recycling. Our biotinylation experiments revealed that CFTR channel density within the apical plasma membrane is modulated through a Rab11b-dependent recycling pathway. Additionally, in knockdown experiments, only cells depleted of Rab11b, not Rab11a, exhibited a reduced CFTR-mediated SPQ fluorescence response upon agonist addition, demonstrating the physiological significance of Rab11b expression for apical CFTR function. These knockdown results suggest that the effects of the dominant negative Rab11b overexpression on CFTR recycling are not due to perturbations of other pathways, such as an indirect effect on Rab11a function.

Interestingly, knockdown of Rab11b also resulted in a significant decrease in CFTR protein expression. A similar effect was reported for the C-type lectin, Langerin, in HeLa and M10-22E cells, as either overexpression of the dominant negative Rab11a, or its depletion, resulted in decreased Langerin protein expression [155]. Further investigation revealed that Rab11a expression and function were required for the formation of Birbeck Granules, a specialized subdomain of the recycling compartment that facilitates Langerin recycling in Langerhans cells. In the absence of Rab11a expression or function, Langerin was targeted for lysosomal degradation. Likewise, Rab11b expression may be required for the establishment or stability of a recycling compartment within T84 cells that recruits CFTR molecules that are destined for apical recycling, similar to that reported for Langerin. If so, it will be interesting to determine whether the lack of Rab11b expression targets endocytosed CFTR to the degradative, rather than the recycling, pathway.

However, unlike the Langerin studies, overexpression of the GDP-locked Rab11b mutant in T84 cells did not affect endogenous CFTR expression levels significantly. This may be due to the retention of recycling capability by natively expressed Rab11b, providing a pathway to which CFTR may be recruited but not recycled. This outcome could prevent its appropriate localization and function at the apical membrane without resulting in altered whole cell

expression levels. Conversely, CFTR may be shuttled to the unperturbed Rab11a compartment, rather than to a degradative pathway. Further work is required to elucidate the disparities observed between the knockdown and dominant negative effects on CFTR protein expression reported herein.

2.3.1 Rab11 Isoform Comparisons

Rab11b has not received the attention given its near relative, Rab11a, particularly in regard to protein recycling. Early studies had implicated a role for Rab11b, similar to that ascribed to Rab11a, since it regulated transferrin receptor recycling in non-polarized 293 cells [87]. In polarized cell models (e.g. MDCK cells), Rab11b localized to a subapical vesicular compartment, distinct from that for Rab11a or the known apical recycling cargoes, H⁺-K⁺-ATPase and pIgR. These findings suggested that Rab11b was localized to a compartment that is different from the Rab11a-identified ARE [89]. Furthermore, Rab11b staining did not overlap with staining for internalized transferrin receptor, which localizes to the subapical common recycling endosomes in polarized MDCK cells, confirming also that it did not associate with this perinuclear recycling compartment [86, 89]. These data suggest the existence of two separate apical Rab11 recycling compartments within polarized epithelial cells. Our results establish the requirement for Rab11b expression and function in CFTR recycling in a polarized epithelial system, demonstrating that this process is independent of Rab11a. From these studies, however, we are unable to address further whether Rab11a and Rab11b form distinct recycling compartments, or whether they demarcate functionally distinct subdomains of the same interconnected recycling network, as described previously for Rab4, Rab5, and Rab11 [80]. Identification of additional cargoes that utilize these isoform-specific apical recycling pathways should further elucidate potential interplay in cargo handling between the Rab11a and Rab11b recycling compartments.

It was surprising that manipulation of the Rab11a isoform, which shares 89% amino acid sequence homology with Rab11b, failed to affect the apical membrane recycling of CFTR. The crystal structures of Rab11a and Rab11b show significant differences, including the presence of 11a as a dimer in the crystal structure, whereas 11b crystallized as a monomer. In addition, there were differences in subdomain orientations and helical region exposure that were interpreted to suggest different GTP hydrolysis rates in these isoforms [156]. These factors may lead to differences in downstream effector binding that account for functional disparities, as revealed by our data. Consistent with this concept, one study examined Rab11 isoform associations with the Rab11 family of interacting proteins (FIPs) and attempted to differentiate between Rab11a and Rab11b isoforms [153]. While they suggest that the FIPs could not differentiate between Rab11a or Rab11b in their active, GTP-bound conformations, not all members of the FIP family were examined in those studies, and it is also possible that other, as-of-yet unidentified Rab11 interacting proteins could mediate specific Rab11a or Rab11b downstream functions.

2.3.2 Cell type-dependent recycling pathways

It is well appreciated that trafficking pathways inherent to non-polarized cells do not mirror the pathways of more complex polarized epithelial systems [157]. Recent studies have examined CFTR trafficking itineraries in non-polarized heterologous expression systems and have noted co-localization with and regulation by specific trafficking regulators, including Rab GTPases [158] and SNARE proteins [159]. Although such studies provide proof-of-concept for a functional role of Rab GTPases in CFTR trafficking, they do not necessarily elucidate the trafficking components that are operative in the polarized epithelia where CFTR functions. Examples of disparities between data obtained from epithelial and non-epithelial systems include functions of protein trafficking and biogenesis mechanisms [113, 118, 119, 154].

Indeed, it is possible that the cellular context could affect the manner in which CFTR is handled, even within different types of epithelial cells. For example, a study by Swiatecka-

Urban, *et al.* (2005) examined apical membrane CFTR trafficking in human bronchial epithelial cells (CFBE41o-) that were transduced with lentivirus to express WT or Δ F508 CFTR [160]. The use of dominant negative or dominant active Rab11a constructs suggested that Rab11a regulated the cell surface density of CFTR in these polarized airway cells. Rab11b expression and function were not addressed in that work. Nevertheless, in relation to the present work, those studies suggested that CFTR recycling is regulated by Rab11a, and this comparison suggests that Rab isoform regulation may be cell type-specific, differing even when epithelia from different tissues are compared. Interestingly, while no significant Rab11a effect on CFTR function or localization at the apical membrane was detected in our intestinal cell studies, overexpression of the dominant active Rab11a or Rab11a knockdown both affected CFTR expression levels. These alterations in the steady state protein levels of endogenous CFTR verify detection of CFTR within the ARE, as shown by our immunofluorescence and immunoisolation data. Therefore, additional work will be required to determine the significance of the Rab11a-localized CFTR within this epithelial cell model. These comparative observations highlight the complexity of Rab11 recycling compartments and suggest that further studies of these systems may also reveal differences in Rab isoform effector proteins.

Some evidence [118, 161] is consistent with the concept that cAMP/PKA agonists redistribute CFTR from intracellular compartments to the apical membranes, and that this regulated trafficking of CFTR occurs in intestinal, but not airway, cells. Thus, it is possible that Rab11b mediates an agonist-sensitive, regulated recycling pathway, which is supported by this work. Our results demonstrating Rab11b dependence in intestinal epithelial cells utilized forskolin stimulation of cAMP levels to examine CFTR function, localization, and recycling. From this, it is tempting to speculate that CFTR localized to the Rab11a compartment in polarized T84 cells may be trafficked in an agonist independent, constitutive manner. If this is true, then stimulation of the Rab11b pathway by cAMP/PKA may have masked a role for Rab11a in constitutive CFTR trafficking. The implication that these isoforms may participate in

specialized recycling itineraries, possibly even varying between epithelial cell types, necessitates additional work.

Finally, additional studies have shown that the transit of CFTR out of the recycling compartment is regulated by Rab11 interactions with the class V family of myosin motors. For instance, further evidence from CFBE airway cells shows a role for Rab11a interactions with myosin Vb in CFTR recycling, including data from siRNA-mediated knockdown of myosin Vb [123]. It will be interesting to determine whether myosin Vb, or another motor isoform, facilitates Rab11b-mediated recycling, as myosin Vb appears also to bind Rab11b [162]. Future work should focus on elucidating the functional differences between these two highly similar, yet functionally distinct, Rab11 isoforms. In summary, our results show that Rab11b, not Rab11a, regulates CFTR recycling at the apical membranes of polarized intestinal epithelial cells, revealing a novel role for Rab11b in apical recycling.

3.0 CONCLUSIONS

Our understanding of the intricate intracellular movement of lipids and proteins among the myriad of specific subcellular organelles continues to deepen with the advancement of specialized techniques for their detection. In response, the ability to examine these pathways in increasingly more complex models is now feasible and in doing so, it has become apparent that trafficking networks in simple systems form a foundation for understanding such cellular processes in models that recapitulate precisely the *in vivo* properties of the normal tissue physiology. However, detailed elucidations of the divergences between specialized cell systems resembling the normal tissue and those of a more basic nature are now necessary, especially as we begin to realize the amazing specificity and intricacy inherent to normal tissue physiology.

In light of this, the overall goal of my work was to provide mechanistic insights in to the recycling pathways at the apical pole of polarized epithelial monolayers using a variety of pertinent biochemical and functional techniques to dissect such pathways within a relevant cell culture and tissue model. In this dissertation, I focused on examining the intracellular localization and trafficking of an endogenous anion channel, the CFTR, within a physiologically relevant, polarized intestinal cell model system and *in vivo* on rat intestinal tissue. The results of this effort have provided insight in to a previously unrecognized apical recycling itinerary that requires the function and expression of a particular member of the Rab11 subfamily, Rab11b.

Future work will be required to elucidate the precise mechanisms that regulate the constitutive and stimulated recruitment of CFTR to the apical plasma membrane and to determine how Rab11b functions to mediate the agonist-sensitive response, which is necessary

for the normal physiology of the intestine. Furthermore, given the apparent lack of efficient recycling by the mutant $\Delta F508$ CFTR upon rescue from the ERAD pathway [163], further exploration of the divergences between wild type and mutant CFTR recycling in polarized systems will likely be required for future therapeutic strategies aimed at treating cystic fibrosis. Therefore, the relevance of this recycling pathway to those within other polarized cell systems needs to be explored, as discussed below. Finally, this work highlights the complexity of apical membrane recycling processes in polarized epithelial phenotypes and stresses the necessity of further exploration of these specialized cell systems.

3.1 CFTR TRAFFIC IN POLARIZED EPITHELIAL CELLS

Despite the numerous reports detailing the vectorial ion transport systems that function within polarized T84 monolayers, only one study was performed previously that described the trafficking of endogenous CFTR within this intestinal cell model [122]. Herein, I report differences in both internalization and recycling rates for CFTR compared to that initial report. Specifically, in the study by Prince *et al.*, nearly 100% of plasma membrane CFTR was endocytosed after 2.5 minutes [122], while my work on polarized T84 cells demonstrates a significantly slower rate of internalization, with a maximum of approximately 24% of CFTR internalized in 20 minutes (See Figure A.3). In addition, a minor disparity in CFTR recycling rates reported for T84 cells also exists. Prince *et al.*, showed that 90% of cell surface labeled and internalized CFTR recycles in 1 minute, which is in contrast to what is reported in this work

where approximately 70% of CFTR recycles in 1 minute, with a maximum recycling efficiency of 80% after 7.5 minutes (Figure 2.9).

In support of my observations, results obtained from fully polarized CFBE41o- cells, a bronchial epithelial cell line, also show a slower rate of CFTR internalization, with approximately 15% of cell surface CFTR internalized in 10 minutes [123]. In addition, polarized CFBE41o- cells recycle apical CFTR slower than that reported originally for T84 cells, which strongly agrees with the rates I have reported here, with 60% of internalized CFTR recycling to the apical membrane in 5 minutes [123].

It is unlikely that slight variations in culturing techniques or cell passage number could have contributed to these significant differences in CFTR trafficking. For instance, the same culturing media and conditions, described originally by Dharmasathaphorn [128] and utilized in the Prince studies [164], were used in this work. In addition, early passage (passage 32) T84 cells were utilized for my studies, likely to be of similar passage to those used in the Prince work. Importantly, the studies on CFTR trafficking reported here were performed on T84 cells that were grown for 7-10 days on semi-permeable transwell supports, while the Prince studies used cells cultured on plastic for their experiments. In addition, the transepithelial resistance, which typically reaches 1000-2000 Ω cm² after 7 days [128], was observed starting at 5 days post-plating and only monolayers that reached this high TER were used for my experiments.

Therefore, the disparities in CFTR internalization and recycling rates may be indicative of variations in the differentiation state of the apical membrane protein trafficking pathways, which are sensitive to the polarization state of the monolayer as a whole. It is well understood that the biosynthetic and trafficking processes of nonepithelial cell types do not mirror the pathways of more complex polarized epithelial systems [118, 157]. My observations suggest

that the intracellular trafficking processes are also influenced by the polarization state of epithelial cell systems.

The formation of the apical junctional complexes in epithelial cell systems is initiated by cell-cell contacts. These junctions subsequently mediate the organization of the intracellular actin cytoskeleton (for review, see [165]) and signal for the maturation of the epithelial monolayer, which is characterized by the establishment of the polarized localization of proteins and lipids at their appropriate intracellular location [166]. Numerous studies have linked CFTR to the actin terminal web at the apical membrane [167, 168] and its maturity and arrangement could conceivably alter trafficking rates of CFTR. For instance, CFTR tethering to the actin cytoskeleton at the plasma membrane stabilizes CFTR and retards its mobility [169], while blocking actin polymerization accelerates CFTR internalization rates by approximately two-fold [125, 170]. In addition, the C-terminal CFTR PDZ-binding motifs bind to the Ezrin-radixin-moesin (ERM) proteins, connecting CFTR to filamentous actin through EBP50 (CFTR #282). Disrupting the C-terminal coupling of CFTR to the actin cytoskeleton destabilizes CFTR in the plasma membrane [171]. In light of these data, it is feasible that immature actin polymerization states in incompletely polarized T84 cells may yield more mobile CFTR and allow for its more efficient internalization. It will be interesting to determine how the rates of CFTR internalization and recycling vary based on the polarization state of T84 cell monolayers. Biotinylation-based trafficking measurements, similar to those performed here, could be performed in parallel on T84 monolayers at different stages of polarization by monitoring the development of the TER and actin labeling. In light of these observations, I suggest that the results presented in this work represent more closely the *in vivo* rates of CFTR turnover.

3.2 LOCALIZATION OF ENDOGENOUS CFTR

The identity of the apical compartments to which CFTR localizes in polarized epithelial cell types that express it inherently have not been explored thoroughly. Indirect immunofluorescence labeling followed by confocal microscopy to locate staining within the polarized phenotype demonstrates that endogenous CFTR localizes to both the Rab11a ARE and an apical Rab11b-positive compartment in polarized T84 cells (Figure 2.2). This work is the first to demonstrate an apical cargo molecule that is present within the Rab11b-identified vesicle population. Lapierre *et al.*, demonstrated that the well-characterized markers for the ARE, including the H⁺-K⁺-ATPase and the pIgR, did not reside within this compartment [89], thus the identity of any protein transferred through the Rab11b compartment in polarized epithelial cells has been unknown until now.

Interestingly, CFTR localizes to both Rab11 compartments, unlike data reported for the aforementioned cargo molecules. Whether this localization represents CFTR within distinct Rab11a or Rab11b compartments, or a potential overlap of Rab11a with Rab11b compartments, cannot be addressed by the immunofluorescence data presented herein. Unfortunately, limitations in available antibodies prevented the localization of Rab11a and Rab11b in relation to one-another within the T84 intestinal cell model. Despite this, my dissertation work provides the first evidence for a cargo molecule present within both Rab11 populations, the significance of which I will discuss in detail below.

I confirmed my initial visual observations by isolating Rab11 vesicles biochemically and western blotting for endogenous CFTR. The data I present in Figure 2.4 agrees with, but also enhances my immunofluorescence conclusions by suggesting an enrichment of CFTR within the

Rab11b compartment compared to the Rab11a compartment. Different efficiencies of antibody binding or endosome availability in the vesicle isolation technique could theoretically account for this disparity; however, immunoblotting with a pan-Rab11 antibody demonstrates a similar level of total Rab11 pulldown in both the Rab11a and Rab11b lanes. Furthermore, this observed enrichment of CFTR within the Rab11b compartment is substantiated when considering the strong influence of Rab11b function on CFTR traffic and function that is presented in Figures 2.5 - 2.10. In addition, failure to detect CFTR within the Rab21 compartment, which is in agreement with the immunofluorescence results, further supports the specificity of this approach. My development of the immunoisolation technique to specifically capture Rab11a- or Rab11b-containing vesicles would allow for the identification of additional cargo molecules by western blotting or mass spectrometry-mediated protein identification. Furthermore, the identification and characterization of the protein effectors that mediate the downstream actions for each isoform's specific itinerary would help elucidate the divergences in these functionally unique pathways. Therefore, future studies using this technique would aid in the characterization of the Rab11a and Rab11b compartments, enabling a direct comparison of cargo and trafficking machinery localized to each domain.

Interestingly, immunoisolation of Rab11a vesicles using a Rab11a-specific antibody resulted in the immunoprecipitation of Rab11b as well, and vice versa, as I have presented in Figure A.4. This is in contrast to data obtained from MDCK and parietal cells, where Rab11a and Rab11b failed to overlap biochemically [89]. Several interesting possibilities exist that may explain this. Rab11a and Rab11b may occupy distinct domains of the same tubulovesicular recycling compartment. For example, it has been demonstrated that different Rabs are capable of localizing to distinct subdomains of the same interconnected compartment [80], likely by the

unique Rab11 hypervariable carboxyl termini or specific domain targeting by interactions between their GDIs and distinct domain-localized GDFs [37]. Thus, it is feasible that the immunoisolation of intact Rab11a vesicles yields Rab11b protein contained within the same lipid bilayer, yet at a spatially distinct realm from that of Rab11a (See Figure 3.1). This “Domain Model” would allow for Rab11b to be detected in Rab11a isolations and vice versa.

Alternatively, given the remarkable sequence homology between Rab11a and b, they could potentially form heterodimers. Crystallography studies have revealed that the Rabs that are capable of homodimerization *in vitro*, including Rab9 [172] and Rab11a [173], do so through interactions between their Switch I and Switch II regions. Interestingly, the crystal structures of Rab11a and Rab11b reveal insignificant differences between their Switch I regions and only very minor Switch II differences [156]. Thus, it is theoretically possible that Rab11a and Rab11b dimerize and that this interaction is detected by the immunoisolation of one isoform, which allows for the detection of the other (see Dimerization Model in Figure 3.1). Conversely, if Rab11a and Rab11b do not dimerize directly, they may be linked indirectly through interactions with their effectors that are capable of dimerizing. For instance, members of the Rab11-FIP family of effectors have been shown to homo- and hetero-dimerize [174]. Therefore, these effectors may functionally link Rab11a and Rab11b and regulate trafficking processes by the cross-handling of cargo.

The potential spatial overlap of Rab11a and Rab11b that I have suggested here requires further investigation. Immuno-gold labeling of recycling vesicles isolated from polarized T84s with gold-conjugated primary antibodies for each isoform followed EM examination would be a strong approach to determine whether both isoforms could be localized to a single compartment. Additionally, immunoisolation of Rab11a-specific endosomes in the presence of detergent to

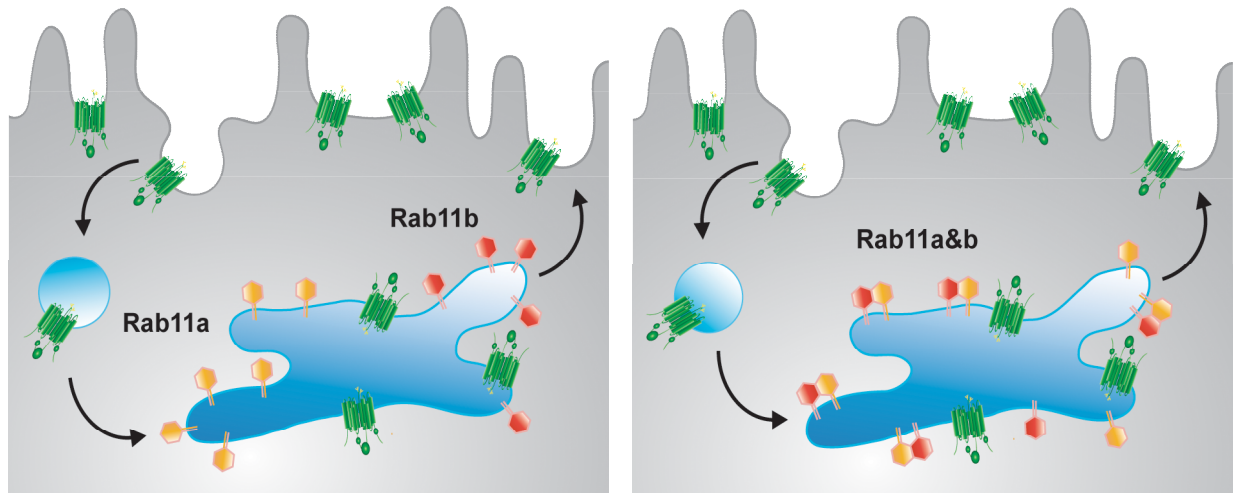


Figure 3.1 Two potential interrelationships for Rab11a and Rab11b.

The left panel depicts a “Domain Model” where Rab11a (🟠) and Rab11b (🔴) occupy discrete locations within the same interconnected recycling compartment. The model on the right represents the “Dimerization Model” for Rab11a and Rab11b relationships. Both of these models potentially explain the overlap between Rab11a and Rab11b that was detected biochemically in the immunoprecipitation technique (Figure A.4).

solubilize the lipid membranes would determine whether the Rab11b co-immunoprecipitation is dependent upon intact vesicles. Conversely, to determine whether the Rab11s form heterodimers, an immunoprecipitation from cell lysates using one Rab11 isoform-specific antibody, followed by blotting the precipitated proteins for the other isoform would determine whether they interact, provided that each antibody was highly specific for its isoform and that detergent solubilization was sufficient. In addition, crystallizing Rab11a and Rab11b together, *in vitro*, would determine whether they are able to form heterodimers. These studies would shed light on the potential interrelated nature of the Rab11 isoforms and would be beneficial for understanding their complex functions in cell recycling itineraries.

3.3 ROLE OF RAB11A IN CFTR TRAFFIC

Despite the lack of a significant alteration in CFTR function by Rab11a knock down or overexpression of its dominant negative mutant, both immunofluorescence and immunoisolation of Rab11a AREs show that endogenous CFTR localizes to this compartment in polarized T84 cells. In addition, subtle changes in CFTR protein expression levels were produced by Rab11a knockdown (~20% decrease) and overexpression of the dominant active mutant (~30% increase) compared to GFP controls. Thus, the morphological and biochemical evidence that reports CFTR residency within this compartment is likely to be accurate. Therefore, what role does Rab11a have in CFTR traffic?

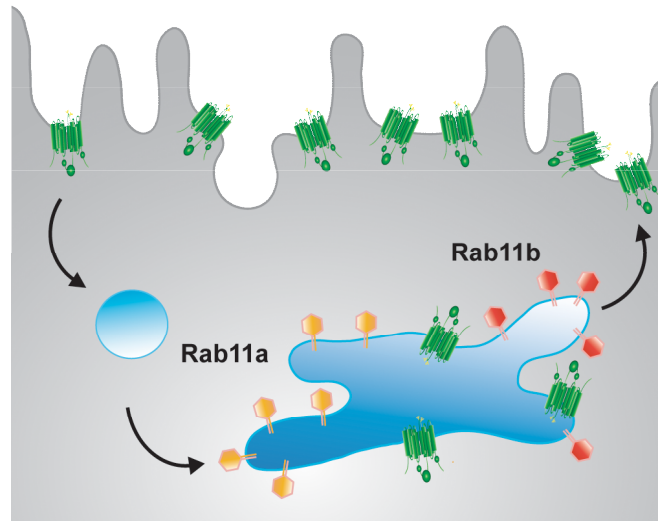
Additional experiments that I have performed suggest that Rab11a may regulate the steady state apical membrane CFTR density in polarized T84 cells, potentially through a

constitutive recycling pathway. As shown in Figure A.5A (Lane 2), GFP-Rab11a-S25N overexpression for 24 hours in polarized T84 cells reduces significantly the apical surface CFTR density to the level of that detected for GFP-Rab11b-S25N-expressing cells (Lane 3, approximately 45%, compared to GFP control, see Figure A.5B), but only in the absence of forskolin stimulation. This observation is extremely important in light of the failure to see an effect on CFTR traffic or function in the cell surface labeling assays (Figure 2.8) and Ussing chamber measurements of CFTR-mediated short circuit current (Figure 2.7), respectively. Despite the Rab11a-S25N adenovirus positive control that was performed in MDCK cells (discussed in RESULTS 2.2.7), the ability of the Rab11a dominant negative adenovirus to modulate the plasma membrane CFTR levels in polarized T84 monolayers, in the absence of forskolin, indicates its specific inhibition of Rab11a function. In support of my observation, overexpression of the dominant negative Rab11a mutant in polarized bronchial epithelial CFBE41o- cells also decreases the steady state apical membrane levels of CFTR by 40% in the absence of cAMP/PKA stimulation [95]. Importantly, the alterations in CFTR localization reported in that study were observed by using a cell surface biotinylation technique, similar to that used here. Taken together, these biochemical data suggest that Rab11a function is necessary for the establishment or regulation of an apical plasma membrane-localized CFTR population in the absence of agonist.

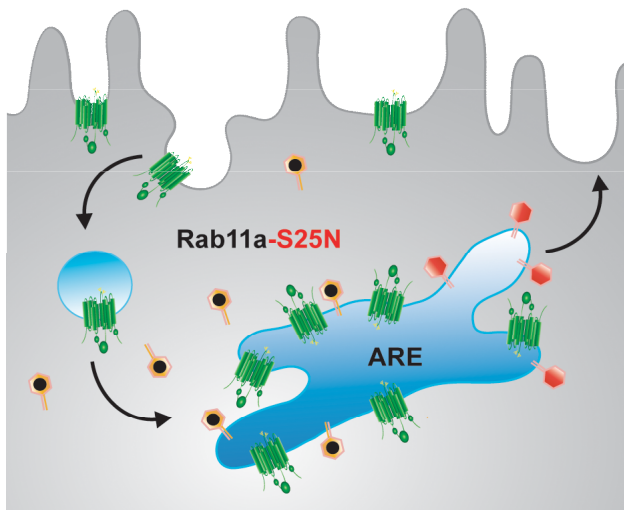
Interestingly, the addition of forskolin for ten minutes at 37°C prior to cell surface labeling restores the apical CFTR density in GFP-Rab11a-S25N cells (Lane 5) to that of the control GFP monolayer (Lane 4). This suggests that recycling or insertion of CFTR is able to proceed from an intracellular pool upon cAMP/PKA stimulation, but in the absence of Rab11a function. It should be noted that this biochemical finding is masked in functional assays; the

CFTR anion response in GFP-Rab11a-S25N-expressing T84 monolayers demonstrates an equivalent change in short circuit current as control, GFP-expressing monolayers (shown in Figure 2.7A&B). Because CFTR function can only be measured with cAMP/PKA stimulation, the functional assessment of the altered CFTR density at the apical membrane in Rab11a-S25N-expressing monolayers cannot be determined under basal, non-stimulated conditions. This observation explains the consistent failure to detect an effect of the dominant negative Rab11a in the SPQ (Figure 2.5C) or Ussing chamber assays (Figure 2.7A&C), which both require forskolin activation to measure CFTR function. Stimulation of CFTR insertion, mostly likely through the unperturbed Rab11b compartment, would mediate the full functional response by cAMP/PKA and thereby mask a role for Rab11a in constitutive CFTR trafficking (See Figure 3.2). Therefore, functional measurements of CFTR inhibition by alterations in Rab11a function are not feasible.

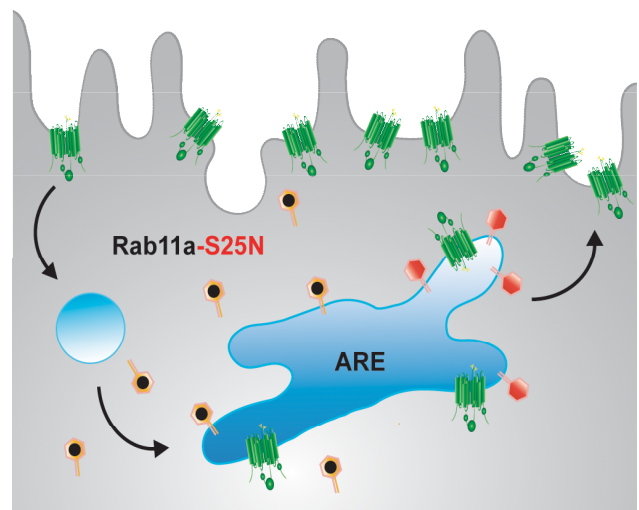
If the above theory is true, altering the constitutive turnover of CFTR through Rab11a knock down or its dominant active expression would explain the observed alterations in the steady state CFTR expression levels. Specifically, increased activity by the Rab11a-Q70L mutant could encourage constitutive CFTR recycling, possibly by diverting a percentage of internalized CFTR from a selective degradation pathway, which would result in eventual increases in the steady state expression as is reported in Figure 2.6C&D. Conversely, the lack of Rab11a expression potentially causes the collapse of a constitutive recycling pathway or compartment, resulting in a diminished CFTR pool as evidenced in Figure 2.10B&C. Finally, it is interesting that the relative amount of endogenous CFTR immunoprecipitated as a component of the Rab11a compartment (Figure 2.4A), when taken in relation to that detected within the Rab11b vesicles, correlates well with the ~20% decrease in CFTR expression observed upon



GFP Control



-Forskolin



+Forskolin

Figure 3.2 A potential role for Rab11a in recycling of CFTR.

The bottom left panel depicts a significantly decreased apical membrane CFTR density in the absence of cAMP/PKA activation when compared to GFP control cell (Top), which is due theoretically to an inhibited constitutive recycling pathway by the Rab11a-S25N mutant (●). On the right, the addition of forskolin initiates the recruitment of CFTR from intracellular pools, possibly through a functioning Rab11b-regulated pathway (⬆), resulting in a full CFTR anion response in functional assays despite the overexpression of the Rab11a-S25N.

Rab11a knock down (Figure 2.10C).

Dissecting the exact role of Rab11a in apical CFTR traffic within intestinal epithelia will require additional experiments. Constitutive CFTR recycling rates (in the absence of forskolin) could be measured in polarized monolayers expressing the dominant negative Rab11a and using the biotin protection assay that I developed in this dissertation work. A more precise approach would be to create adenoviruses carrying appropriate sequences to knock down Rab11a expression transiently, enabling the functional and biochemical elucidation of the proposed constitutive recycling pathway. Furthermore, additional experiments in other epithelial cell types that express CFTR (eg., CFBE41o-) would help determine whether the constitutive versus regulated recycling for Rab11a or Rab11b, respectively, is unique to intestinal cells or is inherent to other polarized cell types.

3.4 REGULATION OF STIMULATED AND CONSTITUTIVE CFTR TRAFFIC BY RAB11B

Of particular interest is the differential change in CFTR expression levels that were observed when the dominant negative Rab11b was overexpressed compared to the Rab11b knock down. While the GTP-binding mutant of Rab11b did not alter the CFTR expression levels significantly in the SPQ, Ussing chamber, or cell surface biotinylation experiments, Rab11b knockdown clearly decreased the steady state CFTR protein level (Figure 2.7C compared to Figure 2.10C). Given the robust inhibition of CFTR function and trafficking by the dominant negative Rab11b, one might expect that the dominant negative Rab11b overexpression would result in an

accumulation of CFTR, possibly by trapping CFTR within the Rab11b recycling compartment, or even upstream in an early endocytic compartment. This accumulation would be most evident in the western blots performed on lysates from SPQ experiments, as these cells overexpressed the GFP-Rab11b-S25N for 3-5 days prior to the SPQ fluorescence assays, rather than in the Ussing or biotinylation assay lysates that required only 24 hours of mutant Rab11b expression for an observable phenotype. However, no such accumulation of endogenous CFTR was detected in GFP-Rab11b-S25N-expressing cells and attempts to examine morphologically the changes in CFTR distribution in polarized T84 cells overexpressing the mutant Rab11b failed to reveal any reportable alteration in CFTR localization. It is possible that the Rab11b pathway is intimately associated with the endosomal quality control machinery which theoretically could prevent the accumulation of CFTR within the recycling compartment or at an upstream location by resulting in its selective degradation by targeting excess CFTR to lysosomes [163]. Additional experiments using lysosomal inhibitors will be necessary to determine whether CFTR is selectively degraded more robustly in GFP-Rab11b-S25N expressing cells compared to GFP control cells.

Similar experiments are necessary to determine if the CFTR depletion observed in Rab11b knockdown cells results in its degradation, which would explain the observed 65% decrease in steady state CFTR expression levels compared to GFP control that was reported in Figure 2.10C. It is possible that Rab11b expression is required for the formation of a discreet intracellular recycling compartment to which CFTR is trafficked after its endocytosis from the apical plasma membrane. Lack of Rab11b expression could cause the ablation of this recycling compartment, possibly resulting in the continuous degradation of internalized CFTR, and therefore result in the decrease in endogenous CFTR expression levels reported here.

As shown in Figures 2.7 and 2.10, both the dominant negative overexpression of Rab11b and the knock down of its expression with a Rab11b-specific shRNA inhibited CFTR function at the apical membrane, most likely due to a decrease in apical CFTR density due to defective recycling (supported by data in Figures 2.8 and 2.9). Importantly, all of these measurements were recorded with cAMP/PKA stimulation of CFTR by forskolin addition. The additional data presented in Figure A.4 (Lane 3) demonstrates that the Rab11b dominant negative also reduces the steady state levels of surface CFTR in the absence of forskolin, with a 45% decrease in apical membrane CFTR density when compared to the GFP control monolayers. This suggests that Rab11b function is also required for maintaining the steady state CFTR density at the apical plasma membrane, even in the presence of functional Rab11a (discussed further in RAB11A AND RAB11B).

This finding is particularly interesting when reflecting on the results obtained in the SPQ fluorescence efflux assays performed on T84 cells overexpressing the GFP-Rab11b-Q70L mutant. As reported in Figure 2.6B, the dominant active Rab11b caused an accelerated CFTR-mediated anion efflux response upon forskolin addition. Prior to the additional experiments reported in Figure A.5, this immediate, accelerated increase in the CFTR-mediated fluorescence intensity would be explained by a theoretical increase in the rate of CFTR insertion due to increased Rab11b activity. However, in light of the data presented in Figure A.5, the accelerated CFTR response, compared to Rab11a-Q70L-expressing cells, is better explained by a higher steady state cell surface CFTR density, due to the increased or more efficient constitutive recycling by the Rab11b-Q70L, which would cause higher levels of CFTR to be available for the immediate forskolin response. Furthermore, the 65% decrease in CFTR expression upon Rab11b knockdown (Figure 2.10C) also supports the role that Rab11b plays in the constitutive turnover

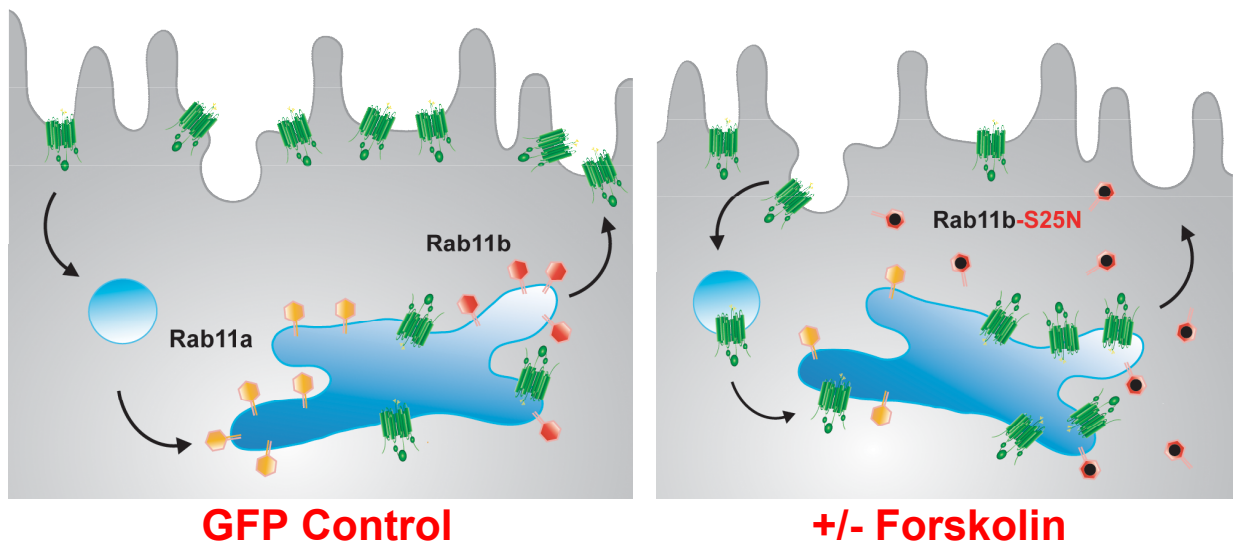


Figure 3.3: The roles of Rab11b in CFTR recycling at the apical plasma membrane.

The model above (Right) depicts a significantly decreased apical membrane CFTR density in the absence of cAMP/PKA activation compared with the GFP control (Left), which is due theoretically to an inhibited constitutive recycling pathway by the Rab11b-S25N (●). Functional Rab11a (●) is unable to regulate the apical plasma membranes in the absence of Rab11b function. Furthermore, the addition of forskolin fails to initiate the recruitment of CFTR from intracellular pools, despite wild type Rab11a function. Thus, Rab11b regulates the steady state and agonist-stimulated CFTR density in the apical membrane of polarized T84 cells, which is required for proper anion conductance in response to agonist.

of CFTR. The lack of Rab11b expression, which would prevent a percentage of CFTR from recycling constitutively, could result in its lysosomal degradation and decrease the steady state CFTR expression levels. Thus, these findings support the previously unidentified function of Rab11b that is necessary for the regulation of the constitutive turnover of CFTR. In summary, functional Rab11b is required for both the maintenance of the steady state levels of CFTR at the apical cell surface (see Figure 3.3), as well as for the acute, agonist-stimulated modifications in CFTR channel numbers that are required for physiological levels of anion secretion.

Dissecting the unique roles of Rab11b in both the constitutive and regulated recycling of apical CFTR within intestinal epithelia will require additional experiments. It will be interesting to determine if Rab11b constitutively recycles CFTR at a rate equal to that of Rab11a. It will be important to measure the recycling of CFTR without the use of forskolin stimulation in cells overexpressing the dominant negative Rab11b as well as cells in which Rab11b expression has been ablated. Finally, additional experiments are required to determine whether the Rab11b-controlled constitutive and regulated recycling pathways are inherent to other polarized cell types.

3.5 RAB11A AND RAB11B

Interestingly, the data presented here disagrees with work performed by LaPierre *et al.*, who showed that overexpression of the Rab11b wild type isoform in MDCK cells displaced Rab11a from membranes [89]. This suggested that trafficking studies using overexpression of either the wild type or mutant Rab11b cannot be interpreted reliably due to inadvertent effects on Rab11a

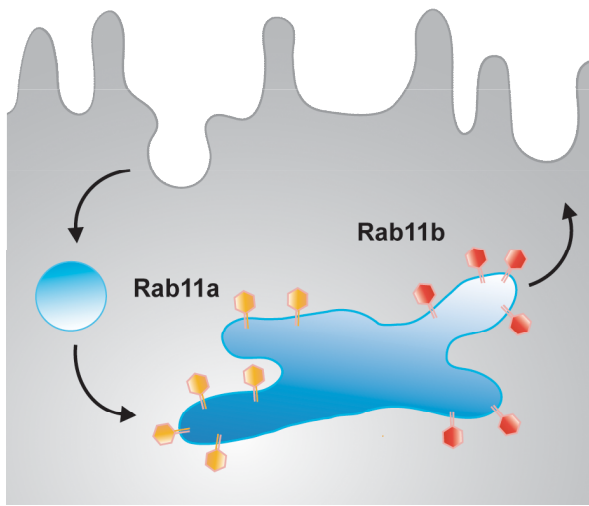
function. To the contrary, only the Rab11b knockdown, not the Rab11a knockdown, inhibited CFTR-mediated iodide efflux in SPQ assays, similar to what was shown for the dominant negative Rab11b. Therefore, the effect on CFTR produced by the mutant Rab11b is specific for Rab11b. Furthermore, it appears as though Rab11a and Rab11b may execute unique roles in the recycling of CFTR (discussed in the two previous sections) and this was dissected using overexpression of the Rab11 dominant negatives in polarized monolayers. The differential effects on CFTR localization to the apical plasma membrane, which was dependent upon changes in intracellular cAMP/PKA levels, strongly argues for specific functions for the Rab11a and Rab11b isoforms. Therefore, this eliminates the argument that one Rab11 dominant negative may cause silent defects in the function of the other, at least in regard to CFTR traffic and function.

Another study suggested that Rab11a and Rab11b may serve redundant roles at the apical pole, potentially through shared downstream effectors [89, 153]. However, this is counterintuitive given the distinct localizations of Rab11a and Rab11b and their failure to colocalize with the same cargo molecules, at least within MDCK and gastric parietal cells [89]. In addition, the disparate roles of Rab11a and Rab11b function, which I have discussed above, argue against a reiterative role for the two isoforms. Clearly, the unique function that Rab11a and Rab11b perform in both the stimulated and regulated trafficking of CFTR in polarized T84 cells suggests that while the Rab11 isoforms may overlap in this cell type, they do perform distinct roles.

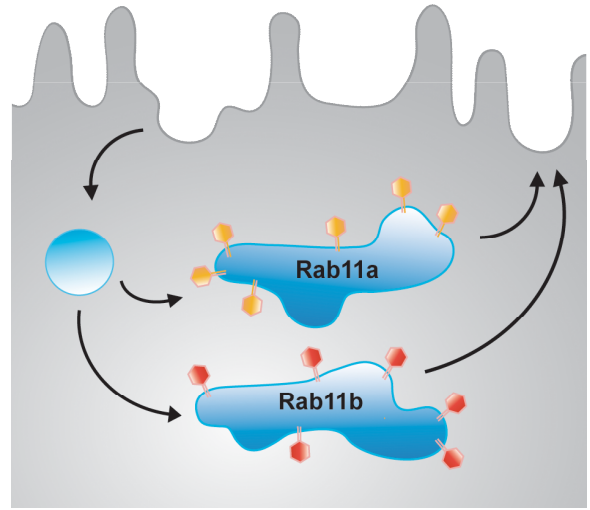
With the additional data that is presented in Figures A.4 & A.5, it is possible to speculate on the nature of the interrelationship between the Rab11a and Rab11b recycling itineraries. Two possibilities, which I have modeled in Figure 3.4, are presented here. In the “Series Model”,

Rab11b acts distally of Rab11a, in a series of recycling compartments that are interconnected and contain both Rab11a and Rab11b within distinct domains. In addition, this model is based upon one primary recycling pool of CFTR. For simplicity, I have used this model throughout this conclusion section. In the Series Model, traffic of CFTR through the Rab11a portion of the recycling compartment is sensitive to Rab11a function only for its constitutive flow through the compartment. In addition, constitutive CFTR recycling to the apical membrane must traverse the Rab11b domain prior to delivery to the apical membrane and after traversing the Rab11a domain. If this model is accurate, aberrant Rab11a function would prevent the constitutive shuttling of CFTR to the Rab11b domain, thereby reducing the steady state CFTR density at the membrane. With the addition of agonist, functional Rab11b could recruit CFTR molecules to the apical plasma membrane that were present within the same compartment lacking functional Rab11a. For instance, the accumulation of CFTR molecules within the non-functional Rab11a domain that are unable to recycle constitutively would not necessarily prevent Rab11b from recognizing the CFTR as cargo needing to be trafficked to the apical membrane. In fact, if there is an accumulation of CFTR at steady state with GFP-Rab11a-S25N overexpression, then this could enhance the interaction of Rab11b with CFTR, enabling the efficient recycling of CFTR through functional Rab11b.

In the Rab11b portion of the Series Model, functional Rab11b is required for both the constitutive flow of CFTR that originates from the Rab11a domain as well as the active, cAMP/PKA stimulated traffic to the apical membrane. Thus, Rab11b function is necessary for maintaining the steady state CFTR density at the apical plasma membrane, even in the presence of functional Rab11a, as this model depicts that Rab11b acts downstream of Rab11a to mediate the distal traffic of CFTR out of the recycling compartment. Therefore, a lack of Rab11b



Series Model



Parallel Model

Figure 3.4: Two potential interrelationships of the Rab11a and Rab11b recycling itineraries.

The model above on the left depicts the Series Model while the one on the right is that of the Parallel Model. See the text for detailed descriptions.

function would prevent the constitutive traffic from the Rab11a compartment to the cell surface, as well as the regulated, cAMP/PKA-sensitive trafficking step.

The strongest evidence in support of the Series Model comes from the biochemical overlap detected for the Rab11a and Rab11b immunisolated vesicles, which suggests that these compartments are interconnected (shown in Figure A.4). In addition, the robust reduction in the apical membrane CFTR density measured upon GFP-Rab11b-S25N overexpression, which was unchanged by the addition of forskolin (unlike the GFP-Rab11a-S25N monolayers), suggests that Rab11b acts downstream of Rab11a. All data presented in Figures 2.7-2.10 are in agreement this model, as Rab11b function is required for the cAMP/PKA stimulated function and traffic of CFTR.

An additional model, the “Parallel Model” (depicted in Figure 3.4) is also feasible based on the data presented in this dissertation. In the Parallel Model, two pools of recycling CFTR exist, which are not interconnected. In the Rab11a-regulated pool, CFTR recycling is handled in a constitutive manner that maintains an appropriate density of molecules at the apical membrane and are necessary for the immediate response to agonist. Inhibition of Rab11a function prevents the constitutive recycling of CFTR through this compartment, resulting in the reduction of CFTR at the apical surface under steady state conditions. Upon agonist addition, CFTR is recruited to the apical membrane through an unknown mechanism that is responsive to cAMP/PKA. The second pool of CFTR recycles through a Rab11b-regulated pathway and its function is required for maintaining the steady state density of a second pool of CFTR at the apical membrane. Furthermore, lack of Rab11b function or expression prevents traffic of CFTR to the cell surface in the presence of agonist. Thus, two unconnected pools of CFTR recycle through two parallel,

Rab11-regulated pathways to mediate the constitutive and regulated CFTR apical plasma membrane densities.

To support this model, the GFP-Rab11a- & b-S25N-induced reduction of the apical CFTR biotinylation signal reported in Figure A.4 (Lanes 2 and 3) must represent an inhibition of two different CFTR populations from recycling to the cell surface. When Rab11a function is perturbed (Lane 2), pool A is depleted from the membrane; and when Rab11b function is perturbed (Lane 3), pool B is depleted. However, upon agonist stimulation, the Rab11a pool of CFTR proceeds to the apical membrane in the absence of proper Rab11a function (Lane 5), yet Rab11b function is necessary for the stimulated traffic of CFTR from the Rab11b pool to the plasma membrane (Lane 6). The only data presented in this dissertation that suggests that the Parallel Model may not be theoretically correct is Figure A.4, the biochemical immunoisolation of the Rab11 compartments. Two possibilities exist that may explain how the immunoisolation data does not conflict this Parallel Model. It could be argued that if the Dimerization Model (discussed earlier) is correct, then the Parallel Model is also feasible, as the Rab11a and Rab11b overlap may be detected by a direct or indirect protein-protein interaction. Second, the immunoisolation method may allow for the mixing of the compartments and thus the detection of the Rab11 isoform overlap.

The models that I have presented above require much additional work to elucidate the actual itineraries of the Rab11 isoform-dependent recycling. It would be interesting to see the affect of overexpressing both Rab11 dominant negatives simultaneously to determine if CFTR expression at the membrane is reduced to a greater extent than that detected in the presence of an individual mutant Rab11. If so, this would argue in favor of the Parallel Model. Specifically, perturbing the traffic of the parallel Rab11a and Rab11b routes simultaneously would reduce the

apical CFTR levels to a greater extent than inhibiting them both when Rab11b acts distal to Rab11a, as discussed for the Series Model. If they act in series, inhibiting the function of both would be unlikely to cause a greater reduction in the apical CFTR levels as Rab11b would be the limiting factor for the amount of CFTR at the cell surface in this experiment. Additional experiments utilizing a lentivirus or adenovirus for the delivery of shRNAs to selectively ablate each or both isoform's expression would also be enlightening. In addition, it will be interesting to see what mechanism mediates the Rab11a-insensitive stimulated CFTR insertion. It is possible that Rab11b functions to traffic CFTR to the apical surface in the absence of Rab11a function (as discussed above for the Series Model). To test this, knocking down Rab11b in cells expressing the Rab11aS25N mutant would be a strong approach. If Rab11b is required for the stimulated insertion of CFTR in the absence of Rab11a function, decreasing its expression should prevent the insertion of CFTR back to control levels.

Examining whether these compartments overlap with one another is another direct approach to determine which model is correct. Using the biochemical immunoisolation technique performed within this work, it would be interesting to see if detergent solubilization of vesicles during the magnetic bead isolation would prevent detection of the isoform overlap and thereby argue for the presence of unique Rab11a and b domains within the same tubulovesicular compartment. In addition, immuno-EM examination of the Rab11 recycling vesicles using isoform specific antibodies would readily determine whether the isoforms demarcate disparate domains within the same compartment. If the Rab11a and Rab11b GTPases are not localized to the same recycling endosomes, then it is unlikely that the Domain Model is correct. Conversely, if there is a strong overlap in Rab11a and Rab11b signal, then I would speculate that the Series Model is the most accurate model. As the techniques to study intracellular trafficking via live

cell imaging continue to advance, it will be interesting to see if the interplay between Rab11a and Rab11b can be visualized in polarized cell models. Live cell imaging could be the most enlightening technique to address this question. Finally, it will be interesting to determine whether these pathways are similar in other polarized cell models; what additional cargo traverse these unique recycling pathways; and what upstream and downstream mechanisms regulate them.

3.6 RECYCLING MECHANISMS

The sections above have generated many questions that will require additional experiments and techniques to address. In the brief sections below, I will overview several areas of future research that need to be addressed due the work presented here.

3.6.1 Rab11 Trafficking

One of the most obvious questions to that needs to be addressed is: “What do Rab11a and Rab11b do?” Given the complex nature of the Rab GTPases and their role in all aspects of the trafficking itinerary that I have outlined in the INTRODUCTION, it is difficult to pinpoint what step or steps Rab11a and Rab11b mediate. For instance, they may control the budding of cargo-containing vesicles from the recycling endosomes. One piece of evidence supporting this view comes from CCD cells, an epithelial kidney cortical collecting duct cell line. Polarized CCD cells expressing the dominant negative Rab11b show a dramatic inhibition in the forskolin-

stimulated membrane insertion event in concert with significantly engorged intracellular vesicles (personal communication, Mike Butterworth). From these results, one might speculate that the Rab11b is required for the budding of vesicles containing cargo from the recycling compartment and inhibiting its function results in the accumulation of cargo and membrane. Whether Rab11a acts in a similar fashion also needs to be addressed.

Rab11a interacts with the plus-end-directed, actin-based mechanoenzyme, Myosin Vb, and this interaction is required for CFTR recycling to the apical cell surface in polarized CFBE41o- cells [123]. Thus, Rab11a and Rab11b are likely to function in recruiting cytoskeletal motors in their active, GTP-bound form, which are necessary for trafficking CFTR-containing vesicles to the apical membrane by linking these vesicles to the actin cytoskeleton. It is unknown whether Rab11b utilizes Myosin Vb, similar to Rab11a, to traffic vesicles on actin tracks. However, yeast two hybrid studies have revealed that Rab11b is capable of binding to Myosin Vb [175], making this a potentially interesting route of investigation.

It is also likely that Rab11a and Rab11b have an important role in specifying the identity or subcompartmentalization of the recycling vesicles. It is unknown whether the hypervariable carboxyl termini of the Rab11 isoforms are necessary for targeting each to a specific lipid-bound compartment, although this has been suggested for other Rabs [58]. One potentially interesting experiment would be to interchange the hypervariable carboxyl termini with one another and examine whether the functions of Rab11a and Rab11b are switched. In summary, while the specific mechanistic procedures that are performed by the Rab11 isoforms cannot be determined from this work, it is certain that these Rabs perform a myriad of crucial steps that are required for proper membrane trafficking.

3.6.2 Agonist-dependent recycling by Rab11s and their effectors

Given the cAMP/PKA-mediated alterations in CFTR traffic that are regulated by Rab11b, further investigation will be required to determine what mechanisms transduce the phosphorylation signaling event into trafficking events. No studies have examined the phosphorylation capability of Rab11b; however, it is known that Rab11a is unable to be phosphorylated [176] making it unlikely that Rab11b is able to be modified in this way. Instead, regulation of downstream, cAMP/PKA-sensitive trafficking steps may be conferred at the level of the effectors. For instance, the Rab11-specific effector, Rip11, differentially associates with Rab11a-containing membranes in polarized MDCK cells based on its threonine phosphorylation status [177]. More importantly, recent work in the insulin-secreting MIN6 cell line has demonstrated that Rip11 is phosphorylated by PKA on a serine residue and that its binding to Rab11b is required for the cAMP-potentiated insulin secretion by forskolin-mediated increases in cAMP/PKA [96]. My work demonstrates the requirement for functional Rab11b in the apical recycling of CFTR upon forskolin-stimulated cAMP/PKA activation so it will be interesting to see if Rip11 or other Rab11b effectors are responsible for mediating the forskolin-induced exocytic recycling of CFTR in polarized epithelia. Additional work will be required to determine if Rip11, or other Rab11b-specific effectors, are required for the Rab11b-mediated stimulated recycling of CFTR shown here. The identification of these effectors will require the screening of Rab11 effectors for their expression and function within a polarized epithelial models, which will be aided by the use of RNA-mediated interference to determine which effectors are important for the agonist-sensitive, Rab11b-specific trafficking steps.

3.6.3 Rab-cargo interactions and recycling motifs

Another necessary area of research in polarized epithelial cell recycling mechanisms that requires future investigation is determining how cargo molecules are selected for recycling. Interestingly, some evidence suggests that Rabs are capable of binding directly to the cargo that they traffic [178, 179]. For instance, it has been shown that Rab3b is able to bind directly to the pIgR, which is necessary for its transcytosis in polarized MDCK cells [180]. More relevantly, recycling of the human prostacyclin receptor in HEK293 and endothelial EA.hy 926 cells has been shown to be regulated through a direct interaction with Rab11a [181]. In addition, the presence of a recycling motif within the epithelial Ca²⁺ channels, TRPV5 and TRPV6, mediates a direct interaction with Rab11a, which is necessary for the recycling of these channels to the apical plasma membrane in mouse kidney epithelial cells [182]. While no direct Rab11b-cargo interactions have been documented, it is likely that Rab11b may also bind to cargo directly given its high degree of homology with Rab11a. It will be interesting to see if other cargo interact directly with Rab11a or Rab11b and whether CFTR is one of these cargos. Experiments performed using GST chimeras containing intracellular domains of the CFTR protein failed to reveal an specific isolation of Rab11 in GST pulldown experiments that I performed in this dissertation work (data not shown). It may be that the Rab11-CFTR interaction is weak, transient, or sensitive to the cAMP/PKA phosphorylation status of CFTR or Rab11 effectors, making it difficult to detect. In addition, it will need to be determined what additional recycling motifs exist and whether CFTR contains any of these Rab11a- or b-binding domains. Their identification would allow for the subsequent mutagenesis analysis of such motifs to identify alterations in the Rab11-mediated recycling of CFTR. Finally, additional work will be required to

determine how Rab11a and Rab11b differentiate between the specific cargos that they selectively traffic.

In conclusion, the work presented and discussed within this dissertation has provided a broad foundation for future lines of investigation. The questions outlined above represent a starting point for these efforts. Finally, as we continue to develop highly sensitive techniques to aid in the elucidation of the complex intracellular recycling itineraries within the epithelial cell model, so will the rate of discovery increase and deepen our understanding of the intricacies of polarized cells and their functions in tissue physiology.

3.7 IMPORTANCE FROM A CF PERSPECTIVE

Finally, this work focused on elucidating the trafficking of the wild type CFTR within relevant polarized epithelial cell systems. It should be noted that understanding the recycling itineraries of wild type CFTR, in addition to the molecular requirements that regulate its recycling within polarized systems, is likely to be necessary for future therapeutic interventions. As mentioned previously, the rescue of the mutant $\Delta F508$ CFTR from the ERAD pathway by chemical chaperones does not result in wild type densities of CFTR at the cell surface as studies have shown that $\Delta F508$ CFTR fails to recycle efficiently, at least in non-polarized BHK cells [163]. Therefore, a detailed understanding of the mechanisms that control wild type CFTR recycling are necessary for future studies that will be aimed at determining how to increase mutant CFTR recycling, and therefore have clinical importance in the therapeutic treatment of cystic fibrosis.

4.0 MATERIALS AND METHODS

4.1 Cell culture, electroporation, and adenoviral transduction

T84 cells (ATCC, Manassas, VA) were grown in DMEM/F12 (Invitrogen, Carlsbad, CA) supplemented with 5% FBS (Hyclone, Logan, UT) and maintained at 37°C in a humidified atmosphere of 5% CO₂. Cells were passaged weekly when they neared confluency. Cells were seeded onto 6.5mm transwell filters (Costar, Acton, MA) for immunofluorescence and Ussing chamber experiments, or onto 24mm transwell filters for cell surface biotinylation and apical recycling assays. Seeded cells were fed the next day and then every-other-day thereafter and grown for 5-10 days until they developed a transepithelial resistance (TER) of >2000 Ω cm².

For SPQ assays, electroporation of T84 cells was performed with Amaxa's Nucleofector II according to the manufacturer's instructions (Amaxa, Gaithersburg, MD). Briefly, electroporations were performed with 2ug (for GFP-fused Rab11a or Rab11b constructs) or 20ug (for GFP-tagged shRNA constructs) DNA per 2x10⁶ cells in Solution T and with Nucleofector II program, W017. Electroporated cells were seeded onto Poly-L-lysine (Sigma-Aldrich, St. Louis, MO) coated 25mm glass coverslips (Fisher Scientific, Pittsburgh, PA) in a 1:1 solution of Opti-MEM (Invitrogen) to DMEM/F12 T84 media. The Opti-MEM/DMEM-F12 was replaced with normal T84 media at 16 hours post-electroporation and cells were then fed every-other-day and used for SPQ fluorescence experiments 3-5 days later (for GFP-fused Rab11a or Rab11b constructs) or 5-7 days later (for GFP-tagged shRNA constructs). Visual inspection of the GFP-expressing cells relative to non-expressing cells revealed an electroporation efficiency of

approximately 75% at 24 hours post-electroporation. Loss of GFP expression was observed as early as 48 hours post-electroporation.

Adenoviral transductions of T84 cells were performed as described previously [183]. Briefly, 5-7 day-old filter-grown T84 monolayers were washed 4 times with 37°C PBS lacking CaCl₂ and MgCl₂ (PBS -CM) to disrupt the tight junctions. The filters were removed from the plates, placed in a 10cm² dish on drops of PBS -CM (20uL basolateral; 40uL apical for 6.5mm filters or 100uL basolateral; 300uL apical for 24mm filters) containing recombinant adenovirus at an MOI of 100. Filters were maintained at 37°C in a humidified atmosphere of 5% CO₂ for 1 hour in the presence of adenovirus. 10ml of media was then added to the 10cm² dish (basolateral compartment) and cells were allowed to recover until the next day when normal media was added to the apical and basolateral sides. The monolayers were used when the TER had recovered fully, within 48 hours of infection for Ussing chamber experiments, or 24 hours post-infection for apical plasma membrane biotinylation and recycling assays.

4.2 Antibodies

All antibodies were used at 1:1000 for IF and western blotting unless otherwise stated. Mouse monoclonal antibodies for immunofluorescence (IF) detection of CFTR were obtained from Millipore (M3A7, Billerica, MA) or purified from the mouse hybridoma clone 24-1 (ATCC) via ammonium sulfate precipitation and each was used at 1:500. The CFTR monoclonal 596 antibody (Cystic Fibrosis Folding Consortium) was used at 1:5000 for blotting of CFTR. The CFTR antibody used to stain rat tissue was produced and described previously [184]. The rabbit polyclonal Rab11a antibody was obtained from Invitrogen and used at 1:500 for western

blotting. The rabbit polyclonal Rab11b antibody used for IF (1:500) was kindly provided by Dr. J. Goldenring (Vanderbilt University, TN) and was described previously [89]. The rabbit polyclonal Rab11b antibody from Cell Signaling (Danvers, MA) was used for western blotting. The rabbit polyclonal zona occludin-1 (ZO-1) antibody was obtained from Invitrogen. The Rab21 polyclonal antibody (1:500 for IF) was kindly provided by Dr. Jack A. M. Fransen (University of Nijmegen, The Netherlands) and was described previously [151]. The polyclonal Rab11a (Invitrogen), Rab11b (Cell Signaling), and Rab21 antibodies were used for immunoisolations. Mouse monoclonal pan-Rab11 and Bip/GRP78 antibodies were from BD Transduction Labs (San Jose, CA). Goat Anti-Mouse-FITC and Goat Anti-Rabbit-Cy3 were obtained from Jackson ImmunoResearch Laboratories, Inc. (West Grove, PA) and used to label primary antibodies in IF experiments.

4.3 DNA constructs, RT-PCR, and Rab11a- & b-S25N Adenoviruses

GFP-tagged Rab11a S25N and Q70L constructs were obtained from Dr. M. Zerial (Max Planck Institute, Dresden, Germany). For RT-PCR analysis, T84 cell cDNA was generated with reverse transcriptase and oligo dT primers from mRNA isolated from polarized cells using the Purelink Micro-to-Midi RNA isolation kit from Invitrogen. The full length human Rab11a and Rab11b transcripts were amplified from T84 cDNA using the following primers: (Rab11a Forward – ATG GGC ACC CGC GAC GAC; Rab11a Reverse – TTA GAT GTT CTG ACA GCA CTG CAC C) and (Rab11b Forward - GGG GAC CCG GGA CGA CGA GTA C; Rab11b Reverse - CAC AGG TTC TGG CAG CAC TGC AGC). Amplicons were separated on an agarose gel containing ethidium bromide to examine the presence of the Rab11 isoform transcripts.

Amplified human Rab11a and Rab11b were TOPO-cloned into the pCR2.1 vector (Invitrogen) and then sequenced using M13 primers (Invitrogen). Results were verified by BLAST search and Rab11b was subcloned into pEGFP-C1 (Invitrogen) using NheI and XhoI sites (New England Biolabs, Ipswich, MA). The S25N and Q70L point mutations were introduced into the wild type GFP-Rab11b construct using the Quik-Change Site-directed Mutagenesis kit (Qiagen (Valencia, CA)) following the manufacturer's instructions. The following primers were used: (S25N forward primer – GGC GTG GGC AAG AAC AAC CTG CTG TCG; Q70L forward primer – GAC ACC GCT GGC CTG GAG CGC TAC CGC). All constructs were sequenced prior to use.

Recombinant adenovirus expressing GFP-tagged Rab11a-S25N (pAdTet-GFP-Rab11aS25N) was kindly provided by Dr. Asli Oztan (University of Pittsburgh, PA). Recombinant adenovirus expressing GFP-Rab11b-S25N was created using the ViraPower Adenoviral Expression System from Invitrogen as per the manufacturer's instructions. Briefly, GFP-tagged Rab11b-S25N was amplified using the following primers (forward- CAC CTT GGT ACC GGT CGC CAC CAT GGT GAG CAA GGG; reverse- TTG CGG CCG CGC TGA TTA TGA TCA GTT ATC TAG ATC CGG); TOPO cloned into the Gateway pENTR/D-TOPO vector; then recombined into the pAd/CMV/V5-DEST vector using LR Recombinase. 293A cells were transfected with pAd/CMV/V5-DEST-GFP-Rab11b-S25N using Lipofectamine 2000 (Invitrogen). High-titer adenovirus stocks were purified from 293A crude cell homogenates using the Vivapure AdenoPACK 100 kit (Sartorius, Edgewood, NY) by following the manufacturer's instructions.

SureSilencing shRNA plasmids containing GFP-tagged shRNAs for Rab11a- or Rab11b-specific knock down were obtained from SABiosciences (Frederick, MD).

4.4 Immunoisolation of Rab11-positive endosomes

An endosome-enriched fraction containing vesicles positive for markers of the early and recycling endosomal populations was obtained using a modified protocol [81] from that described originally [152]. Briefly, T84 cells were washed twice with PBS at 4°C and scraped in 300µL homogenization buffer (3 mM imidazole, pH 7.4, 250 mM sucrose, 0.5 mM EDTA, and Complete EDTA-free Protease Inhibitor cocktail (Roche Diagnostics, Indianapolis, IN)). Cells were homogenized by 20 strokes of a tight fitting Dounce homogenizer and then centrifuged for 10 minutes at 3,000 rpm in a table-top centrifuge. The resulting post-nuclear supernatant (PNS) was adjusted to 40.6% sucrose using 62% sucrose. The diluted PNS was placed in 12-ml capacity Polyclear centrifuge tubes (Sorvall, Newtown, CT) and overlaid with 6 ml of 35% sucrose and 4 ml of 25% sucrose, then centrifuged in a TH-641 rotor at 108,000 x g for 3 h at 4° C. The endosome-enriched fraction at the 25%/35% sucrose interface was collected (1 ml, approximately), diluted 3-fold with PBS and spun at 108,000 x g for 30 minutes at 4° C. Pelleted endosomes were resuspended in 1 mL of 0.1% BSA/PBS per variable. Rabbit anti-Rab11a, anti-Rab11b, anti-Rab21, or a non-specific rabbit IgG were added and incubated with the isolated endosomes overnight at 4° C with rotation. In addition, 50µL sheep anti-rabbit magnetic Dynabeads (Invitrogen) (per variable) were washed with 1% BSA/PBS three times and incubated with 1 ml 1% BSA/PBS overnight at 4° C. The following day the beads were recovered with a magnet and resuspended in 50µL of 1% BSA/PBS per variable. 50µL of the blocked and washed beads were then added and incubated with each of the antibody-endosome fractions for 6 hours at 4° C with rotation. The bead-antibody-endosome complexes were

collected with a magnet, washed twice with 1% BSA/PBS, once with 0.1% BSA/PBS, and then once with PBS. Laemmli sample buffer was added to the immunisolated endosomes and samples were resolved by 10% SDS PAGE, transferred to PVDF, and then blotted for proteins of interest.

4.5 Immunofluorescence labeling

All steps were performed at 4°C unless stated otherwise. Polarized, filter-grown T84 cells were rinsed twice with PBS containing 0.1mM CaCl₂ and 1mM MgCl₂ (PBS+CM) and 5mM DTT and then incubated with gentle shaking for 10 minutes in the second wash. Cells were then rinsed gently with PBS+CM six times to remove surface-accumulated mucus. Cells were fixed with 5% paraformaldehyde in PBS+CM for 30 minutes and then permeabilized with 0.1% Triton X-100 in PBS+CM for 10 minutes. Cells were labeled in blocking buffer consisting of 10% goat serum; 10% dry non-fat milk; 10mg/mL BSA; and 0.05% Triton X-100 in PBS+CM overnight at 4°C with gentle shaking. Unbound primary antibody was removed by four washes with PBS+CM. Primary antibodies were labeled with corresponding fluorescence-conjugated secondary antibodies in blocking buffer for 2 hours. Cells were washed again, then mounted on coverslips and used for confocal microscopy.

Cryostat sectioning and indirect immunofluorescence performed on rat jejunum was performed as described previously [145].

Rat jejunum enterocytes were isolated as described previously [185]. An endosome-enriched fraction used for immuno-gold EM was obtained from homogenized rat enterocytes as described above for T84 cells. Endosomes from the 25%/35% sucrose interface were washed in

0.1M phosphate buffer, pH 7.4, fixed in 2% paraformaldehyde for 1 hour and endosomes were immunolabeled to detect CFTR (15nm gold) and Rab11 (5nm gold) as described previously [143].

4.6 SPQ fluorescence assays

SPQ halide efflux assays were performed on electroporated T84 cells as described previously [148, 186, 187]. Briefly, the iodide-sensitive fluorescent indicator, 6-methoxy-*N*-(3-sulfopropyl) quinolinium, (SPQ) (Molecular Probes, Eugene, OR) was introduced into T84 cells in a hypotonic solution of iodide buffer (in mM: 130 NaI, 4 KNO₃, 1 Ca(NO₃)₂, 1 Mg(NO₃)₂, 10 glucose and 20 HEPES, pH 7.4) diluted 1:1 with water and containing a final concentration of 10mM SPQ. Cells were loaded for 20 minutes at 37°C in a humidified chamber with 5% CO₂. The SPQ-loaded cells were then mounted on a Nikon Diaphot 300 inverted microscope with a 37°C heated stage and perfused with iodide buffer while regions of interest (ROIs) were chosen for GFP and non-GFP expressing cells using the Simple PCI Version 5.1 software (Compix Inc., Imaging Systems, Cranberry Township, PA). The GFP signal intensity varied from cell-to-cell; therefore, three cell populations were chosen (based on GFP expression levels as estimated by visual inspection of the cells) for SPQ fluorescence data collection (see Supplemental Figure 2). Changes in CFTR-mediated SPQ fluorescence were monitored at the 445nm wavelength in response to excitation at 340nm during perfusion at 37°C in nitrate buffer (NaI replaced with 130mM NaNO₃) for 3 minutes without forskolin and then for 8 minutes with 10μM forskolin added. The slopes or single-exponential rates were calculated using SigmaPlot Version 7.1 for each mean fluorescence trace generated from the >50 cells examined per population per coverslip.

4.7 Ussing Chamber Experiments

T84 cells cultured on transwell filters were mounted in modified Costar Ussing chambers, and the cultures were short circuited continuously with an automatic voltage clamp to record the transepithelial short circuit current (I_{sc}) as described previously [188]. The bathing Ringer's solution was composed of (in mM) 120 NaCl, 25 NaHCO₃, 3.3 KH₂PO₄, 0.8 K₂HPO₄, 1.2 MgCl₂, 1.2 CaCl₂, and 10 glucose. The chambers were continuously gassed with a mixture of 95% O₂, 5% CO₂ at 37 °C, which maintained the pH at 7.4. Stocks of forskolin (10mM in 100% ethanol) and bumetanide (20mM in DMSO) were both used at 1:1000 dilution into the bath.

4.8 Cell Surface Biotinylation & Apical Recycling Assays

Cell surface biotinylation and apical recycling assays were performed as described previously [189]. Briefly, biotinylation of polarized T84 monolayers for the quantitation of apical cell surface CFTR protein levels was performed with the EZ-Link Sulfo-NHS-LC-LC-Biotin (Pierce, Rockford, IL), while biotin protection assays to measure recycling required the use of the disulfide-cleaveable, EZ-Link Sulfo-NHS-SS-Biotin (Pierce). Experiments were performed in a cold room on ice with all solutions at 4°C unless otherwise stated. To biotinylate apical membrane proteins, adenovirus-transduced, polarized T84 monolayers were rinsed once with PBS +CM, and then incubated with PBS+CM containing 5mM DTT (Sigma) for two, 10-minute periods with gentle rocking to remove the accumulated surface mucus. After three, 10-minute PBS+CM washes to remove all excess PBS+CM/DTT, PBS+CM containing 10% FBS was added to the basolateral surface. The apical surface was biotinylated with 1mg/mL EZ-Link Sulfo-NHS-LC-LC-Biotin (or EZ-Link Sulfo-NHS-SS-Biotin for recycling assays) in Borate buffer (85mM NaCl, 4mM KCl, 15mM Na₂B₄O₇, pH 9) for 30 minutes with gentle agitation.

Excess biotin was removed with two, 10-minute washes in PBS+CM/10%FBS followed by two washes in PBS+CM.

For cell surface CFTR quantitation, cells were lysed in 700 μ L Biotinylation Lysis Buffer (BLB) (0.4% Deoxycholate, 1% NP40, 50mM EGTA, 10mM Tris-Cl, pH 7.4, and Complete EDTA-free Protease Inhibitor cocktail (Roche Diagnostics)). Total protein levels were determined and normalized samples were incubated overnight with 150 μ L UltraLink Immobilized NeutrAvidin Protein Plus (Pierce). Precipitated proteins were washed three times with BLB, solubilized with Laemmli sample buffer, separated on a 10% SDS-PAGE and blotted for CFTR.

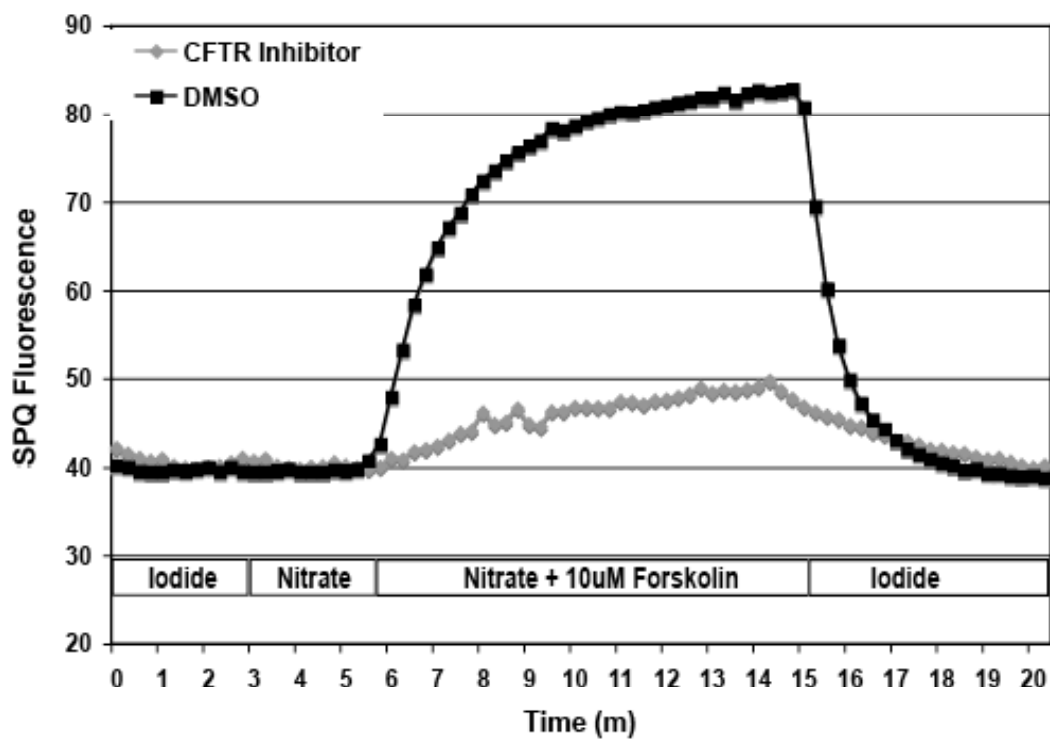
For apical recycling assays, the biotinylated membrane proteins were internalized during a 20-minute incubation in T84 media at 37°C (two filters were kept at 4°C for the cell surface labeling and stripping controls). Proteins remaining at the cell surface after 20 minutes at 37°C were stripped of biotin with four, 15-minute washes in MESNA stripping buffer (50mM MESNA, 150mM NaCl, 1mM EDTA, 0.2% BSA, 20mM Tris, pH 8.6). To detect the recycling of internalized, biotinylated proteins, three filters were quickly warmed to 37°C with T84 media containing 10 μ M forskolin for 1, 2.5, or 7.5 minutes and then immediately cooled to 4°C. Biotinylated proteins that recycled to the cell surface were then stripped of biotin with four, 15-minute MESNA washes followed by cell lysis and processing as described above.

4.9 Statistical analysis

Statistical significance was determined using Student's t-test. A p-value less than 0.05 was considered significant.

5.0 APPENDIX

A



B

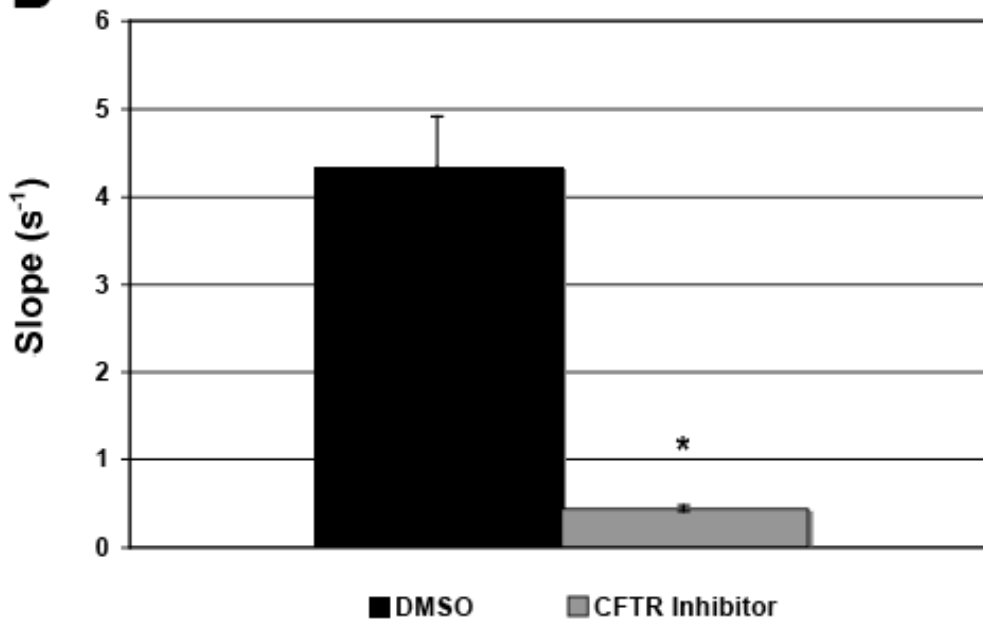


Figure A.1: SPQ fluorescence assays measure CFTR function.

(A) Representative tracing demonstrates the near total inhibition of the increase in SPQ fluorescence for cells perfused in the presence of CFTR inhibitors. T84 cells were loaded with

the SPQ dye, mounted on a heated microscope stage, and perfused with iodide, nitrate, then nitrate buffer with 10 μ M forskolin as described previously. CFTR specific inhibitors CFTR_{inh}172 (10 μ M) and GlyH101 (50 μ M) (grey diamonds) were added to each buffer. Vehicle controls were performed with 60 μ M DMSO (black squares) in each solution. (B) Bars represent the mean normalized slope for the maximum increase in SPQ fluorescence for control DMSO (black bar) or CFTR-inhibited (grey bar) cells from 3 different T84 monolayers and more than 200 cells for each group. * denotes a significant difference with a $p < 0.005$.

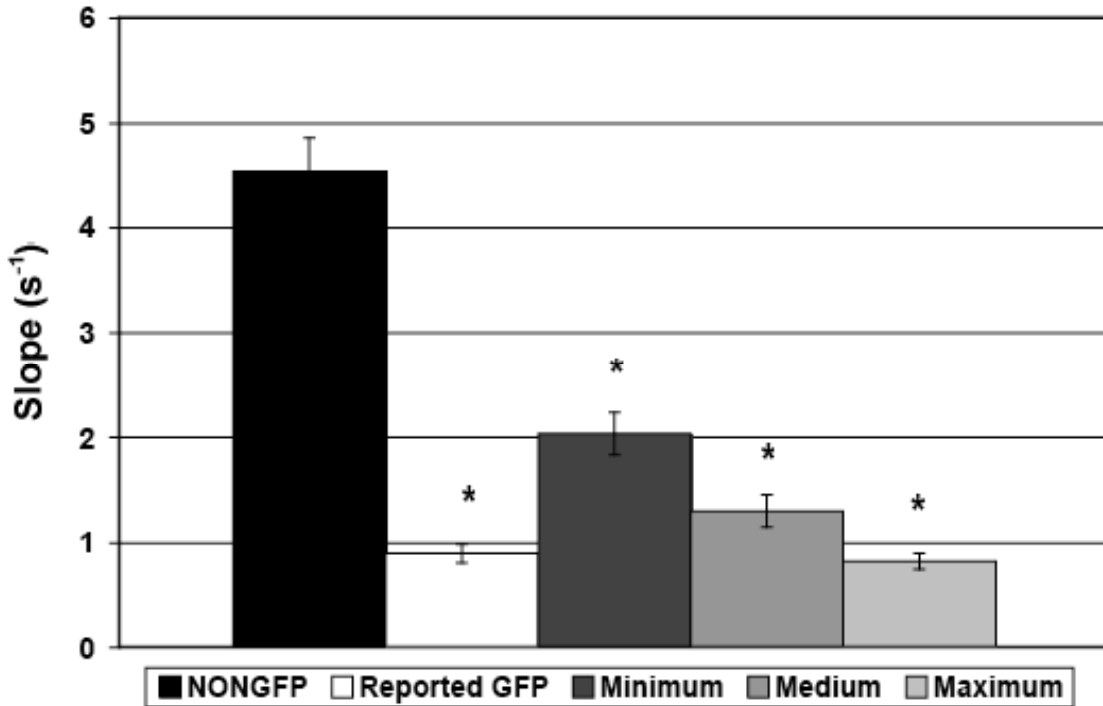


Figure A.2: Dose effect of GFP-Rab11b-S25N expression levels on CFTR-mediated SPQ fluorescence response.

Bars represent additional data obtained from experiments reported in Figure 5. Three additional ROI populations were selected for GFP-Rab11b-S25N expressing cells based on the varying levels of cellular GFP fluorescence intensity as determined by the visual inspection of GFP captures from T84 monolayers (see Figure 5B). The maximum expression (light grey bars) of GFP-Rab11b-S25N (saturated GFP signal) showed the greatest inhibition of CFTR-mediated increases in the SPQ fluorescence response with ~82% inhibition of the slope relative to non-GFP cells within the same field. Intermediate expression inhibited ~72% (grey bar) of the CFTR response while the lowest visually detectable GFP fluorescence signal (minimum) still inhibited ~55% of the CFTR functional response (dark grey bar). * denotes a $p < 0.05$.

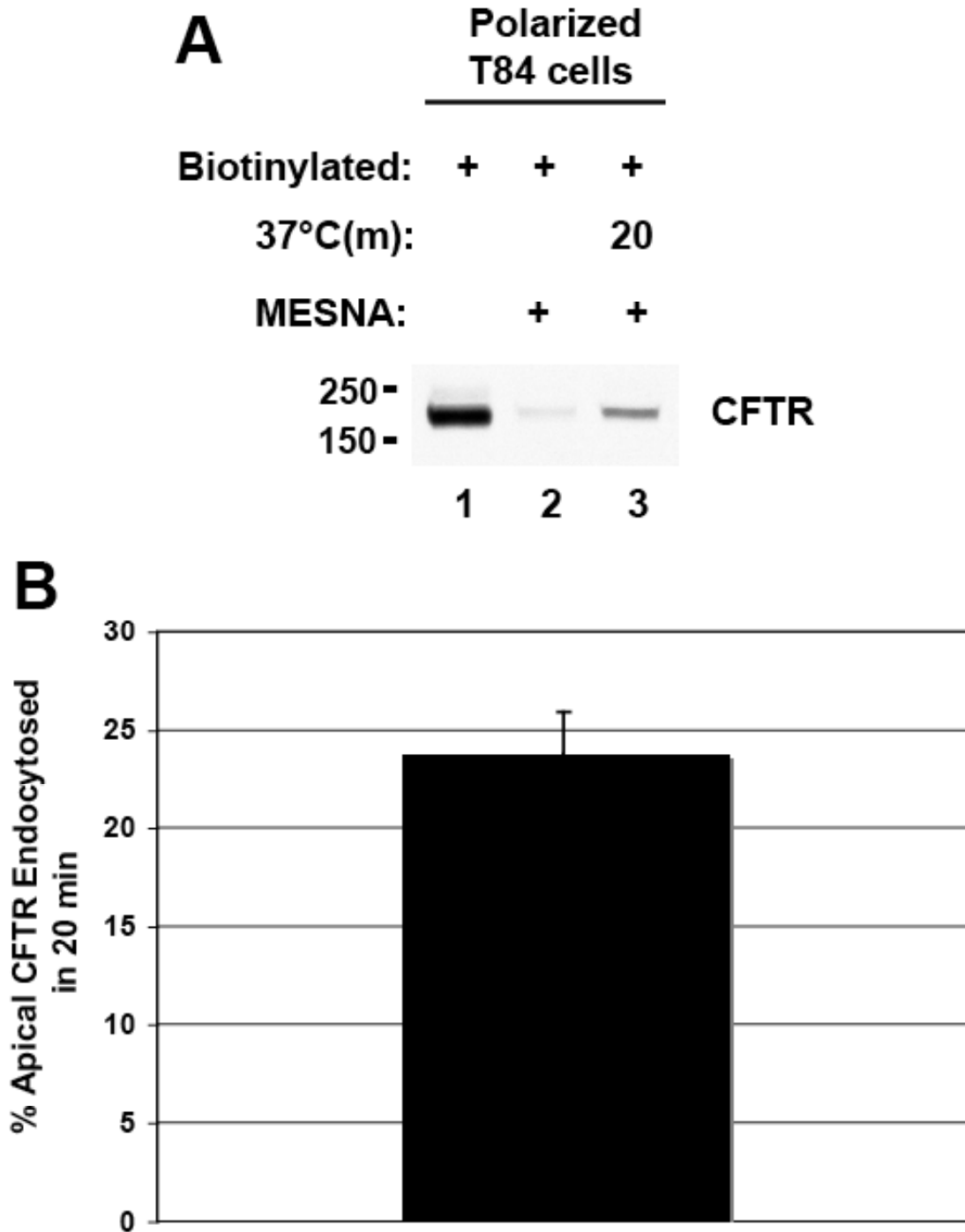


Figure A.3: Endocytosis of CFTR from the apical plasma membrane in polarized T84 cells.

Cell surface biotinylations on T84 cells demonstrating the amount of apical cell surface CFTR internalized after 20 minutes of internalization at 37°C. (A) Representative western blot for CFTR. Lane 1 depicts the amount of CFTR biotinylated at steady state, while lane 2

demonstrates the efficiency of the MESNA to reduce the disulfide bond in the biotinylated CFTR molecules and thereby prevent its streptavidin-mediated isolation. Lane 3 is the amount of CFTR protected from the MESNA treatment through internalization of biotinylated molecules and therefore represents the percentage of CFTR internalized during the 20 minute incubation at 37°C. (B) Bar depicts the mean percentage of CFTR internalized \pm S.E.M. (n=3)

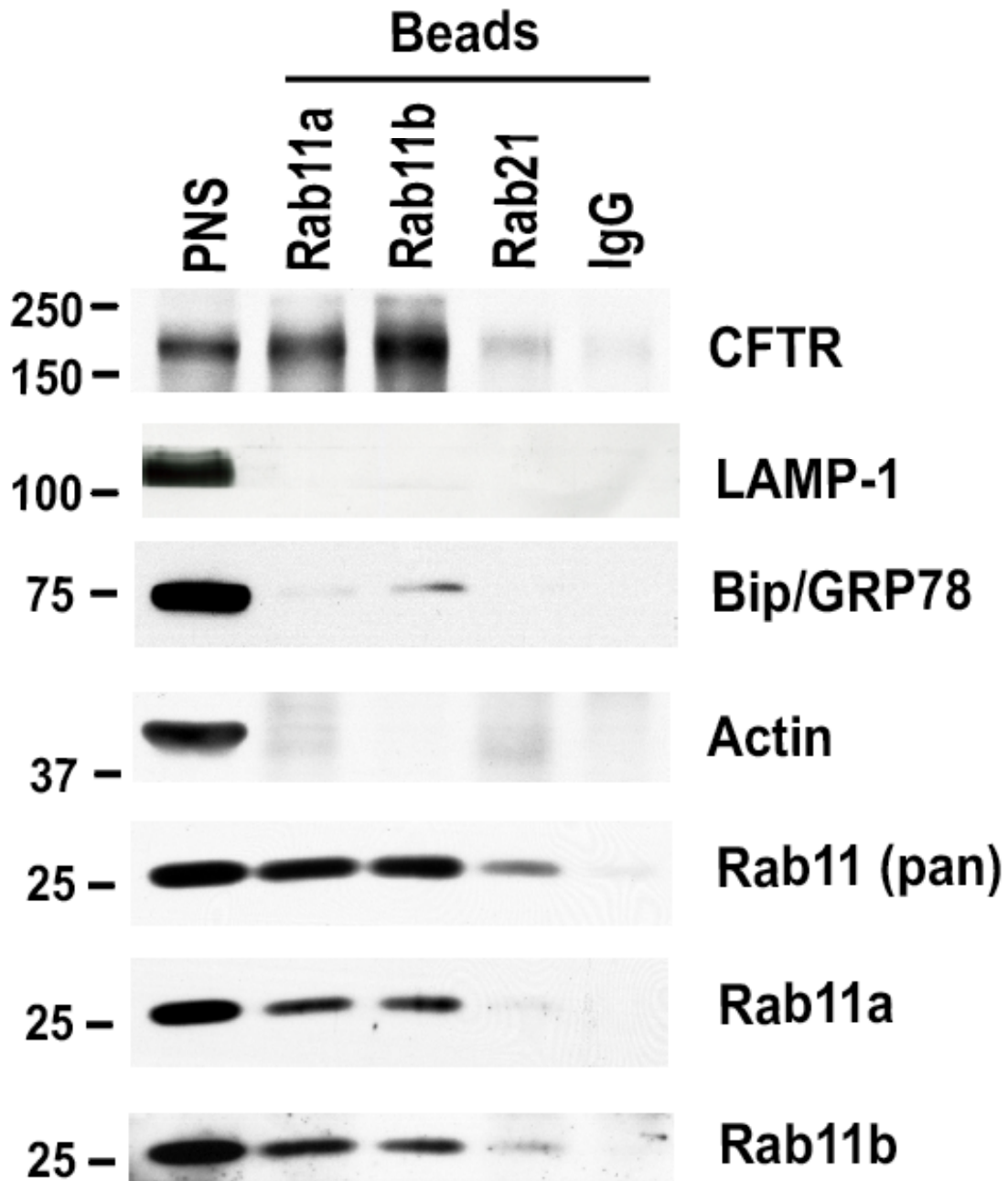


Figure A.4: Immuno-isolation of Rab11a and Rab11b vesicles reveals the overlap of each isoform.

Data from Figure 2.4A showing additional western blots for the Rab11a and Rab11b isoforms (two bottom rows). These data demonstrate the successful isolation of Rab11a and Rab11b vesicles and suggest that Rab11a is present within the Rab11b compartment and vice versa.

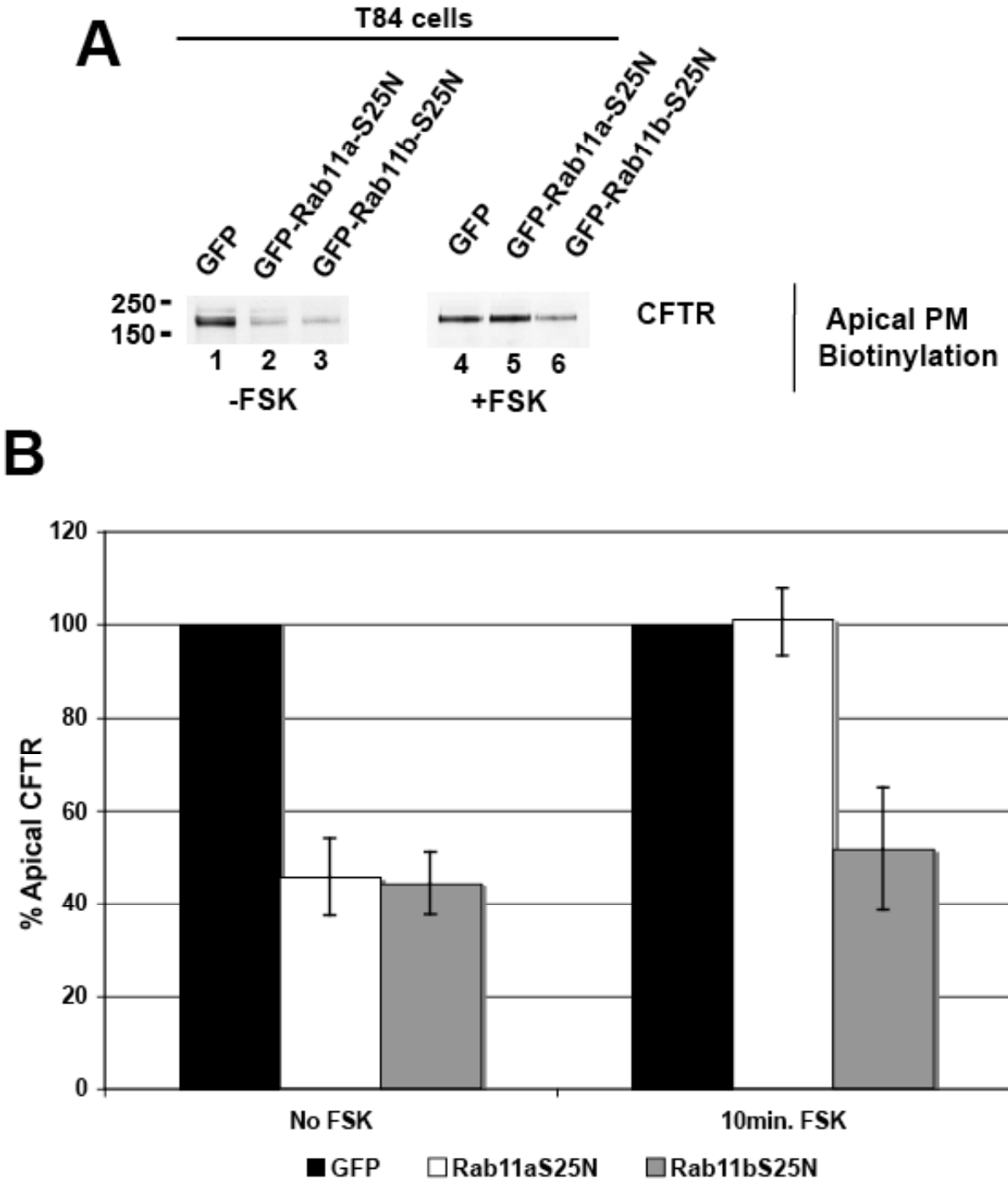


Figure A.5: Comparison of the apical membrane CFTR densities in Rab11a-S25N- and Rab11b-S25N-expressing T84 monolayers with or without cAMP/PKA stimulation.
 (A) Representative western blot for endogenous CFTR after cell surface biotinylations on polarized T84 monolayers expressing GFP, GFP-Rab11a-S25N, or GFP-Rab11b-S25N. The blot on the left demonstrates CFTR PM density in cells without forskolin addition (-FSK), while the right blot depicts CFTR levels after with a ten minute forskolin incubation immediately preceding the biotinylation (+FSK). (B) Bars represent the mean apical PM CFTR levels

normalized to GFP controls \pm S.E.M (n=4). This data suggests that Rab11a-S25N overexpression decreases the steady state membrane levels of endogenous CFTR, while agonist stimulation causes CFTR to traffic to the membrane in the absence of fully functional Rab11a. This suggests that Rab11a may regulate the constitutive levels of CFTR at the apical membrane, but allows additional insertion of CFTR upon cAMP/PKA activation. The grey bars suggests that Rab11b function is required to maintain the steady state levels in addition to the forskolin-stimulated insertion of CFTR at the apical membrane.

6.0 BIBLIOGRAPHY

1. Hossain, Z. and T. Hirata, *Molecular mechanism of intestinal permeability: interaction at tight junctions*. Mol Biosyst, 2008. **4**(12): p. 1181-5.
2. Gasbarrini, G. and M. Montalto, *Structure and function of tight junctions. Role in intestinal barrier*. Ital J Gastroenterol Hepatol, 1999. **31**(6): p. 481-8.
3. Nelson, W.J. and C. Yeaman, *Protein trafficking in the exocytic pathway of polarized epithelial cells*. Trends Cell Biol, 2001. **11**(12): p. 483-6.
4. Groschwitz, K.R. and S.P. Hogan, *Intestinal barrier function: molecular regulation and disease pathogenesis*. J Allergy Clin Immunol, 2009. **124**(1): p. 3-20; quiz 21-2.
5. Kunzelmann, K. and M. Mall, *Electrolyte transport in the mammalian colon: mechanisms and implications for disease*. Physiol Rev, 2002. **82**(1): p. 245-89.
6. Ballard, S.T., J.H. Hunter, and A.E. Taylor, *Regulation of tight-junction permeability during nutrient absorption across the intestinal epithelium*. Annu Rev Nutr, 1995. **15**: p. 35-55.
7. Geibel, J.P., *Secretion and absorption by colonic crypts*. Annu Rev Physiol, 2005. **67**: p. 471-90.
8. Caplan, M.J., *Membrane polarity in epithelial cells: protein sorting and establishment of polarized domains*. Am J Physiol, 1997. **272**(4 Pt 2): p. F425-9.
9. Palade, G., *Intracellular aspects of the process of protein synthesis*. Science, 1975. **189**(4200): p. 347-58.
10. van der Wouden, J.M., et al., *Membrane dynamics and the regulation of epithelial cell polarity*. Int Rev Cytol, 2003. **226**: p. 127-64.
11. Ellis, M.A., et al., *Polarized biosynthetic traffic in renal epithelial cells: sorting, sorting, everywhere*. Am J Physiol Renal Physiol, 2006. **291**(4): p. F707-13.
12. Butterworth, M.B., et al., *Regulation of the epithelial sodium channel by membrane trafficking*. Am J Physiol Renal Physiol, 2009. **296**(1): p. F10-24.
13. Brown, D. and I. Sabolic, *Endosomal pathways for water channel and proton pump recycling in kidney epithelial cells*. J Cell Sci Suppl, 1993. **17**: p. 49-59.
14. Brown, D., *Vesicle recycling and cell-specific function in kidney epithelial cells*. Annu Rev Physiol, 1989. **51**: p. 771-84.
15. Royle, S.J. and R.D. Murrell-Lagnado, *Constitutive cycling: a general mechanism to regulate cell surface proteins*. Bioessays, 2003. **25**(1): p. 39-46.
16. Gallwitz, D., C. Donath, and C. Sander, *A yeast gene encoding a protein homologous to the human c-has/bas proto-oncogene product*. Nature, 1983. **306**(5944): p. 704-7.

17. Schmitt, H.D., et al., *The ras-related YPT1 gene product in yeast: a GTP-binding protein that might be involved in microtubule organization*. Cell, 1986. **47**(3): p. 401-12.
18. Salminen, A. and P.J. Novick, *A ras-like protein is required for a post-Golgi event in yeast secretion*. Cell, 1987. **49**(4): p. 527-38.
19. Goud, B., et al., *A GTP-binding protein required for secretion rapidly associates with secretory vesicles and the plasma membrane in yeast*. Cell, 1988. **53**(5): p. 753-68.
20. Segev, N., J. Mulholland, and D. Botstein, *The yeast GTP-binding YPT1 protein and a mammalian counterpart are associated with the secretion machinery*. Cell, 1988. **52**(6): p. 915-24.
21. Touchot, N., P. Chardin, and A. Tavitian, *Four additional members of the ras gene superfamily isolated by an oligonucleotide strategy: molecular cloning of YPT-related cDNAs from a rat brain library*. Proc Natl Acad Sci U S A, 1987. **84**(23): p. 8210-4.
22. Haubruck, H., et al., *The ras-related ypt protein is an ubiquitous eukaryotic protein: isolation and sequence analysis of mouse cDNA clones highly homologous to the yeast YPT1 gene*. Embo J, 1987. **6**(13): p. 4049-53.
23. Balch, W.E., *Small GTP-binding proteins in vesicular transport*. Trends Biochem Sci, 1990. **15**(12): p. 473-7.
24. Haubruck, H., et al., *The ras-related mouse ypt1 protein can functionally replace the YPT1 gene product in yeast*. Embo J, 1989. **8**(5): p. 1427-32.
25. Zahraoui, A., et al., *The human Rab genes encode a family of GTP-binding proteins related to yeast YPT1 and SEC4 products involved in secretion*. J Biol Chem, 1989. **264**(21): p. 12394-401.
26. Bock, J.B., et al., *A genomic perspective on membrane compartment organization*. Nature, 2001. **409**(6822): p. 839-41.
27. Pereira-Leal, J.B. and M.C. Seabra, *The mammalian Rab family of small GTPases: definition of family and subfamily sequence motifs suggests a mechanism for functional specificity in the Ras superfamily*. J Mol Biol, 2000. **301**(4): p. 1077-87.
28. Schultz, J., et al., *More than 1,000 putative new human signalling proteins revealed by EST data mining*. Nat Genet, 2000. **25**(2): p. 201-4.
29. Takai, Y., T. Sasaki, and T. Matozaki, *Small GTP-binding proteins*. Physiol Rev, 2001. **81**(1): p. 153-208.
30. Deneka, M., M. Neeft, and P. van der Sluijs, *Regulation of membrane transport by rab GTPases*. Crit Rev Biochem Mol Biol, 2003. **38**(2): p. 121-42.
31. Darchen, F., et al., *Association of the GTP-binding protein Rab3A with bovine adrenal chromaffin granules*. Proc Natl Acad Sci U S A, 1990. **87**(15): p. 5692-6.
32. Zacchi, P., et al., *Rab17 regulates membrane trafficking through apical recycling endosomes in polarized epithelial cells*. J Cell Biol, 1998. **140**(5): p. 1039-53.

33. Wada, M., et al., *Isolation and characterization of a GDP/GTP exchange protein specific for the Rab3 subfamily small G proteins*. J Biol Chem, 1997. **272**(7): p. 3875-8.
34. Seabra, M.C. and C. Wasmeier, *Controlling the location and activation of Rab GTPases*. Curr Opin Cell Biol, 2004. **16**(4): p. 451-7.
35. Fukui, K., et al., *Isolation and characterization of a GTPase activating protein specific for the Rab3 subfamily of small G proteins*. J Biol Chem, 1997. **272**(8): p. 4655-8.
36. Pfeffer, S.R., A.B. Dirac-Svejstrup, and T. Soldati, *Rab GDP dissociation inhibitor: putting rab GTPases in the right place*. J Biol Chem, 1995. **270**(29): p. 17057-9.
37. Pfeffer, S. and D. Aivazian, *Targeting Rab GTPases to distinct membrane compartments*. Nat Rev Mol Cell Biol, 2004. **5**(11): p. 886-96.
38. Seabra, M.C., E.H. Mules, and A.N. Hume, *Rab GTPases, intracellular traffic and disease*. Trends Mol Med, 2002. **8**(1): p. 23-30.
39. Seabra, M.C. and E. Coudrier, *Rab GTPases and myosin motors in organelle motility*. Traffic, 2004. **5**(6): p. 393-9.
40. Grosshans, B.L., D. Ortiz, and P. Novick, *Rabs and their effectors: achieving specificity in membrane traffic*. Proc Natl Acad Sci U S A, 2006. **103**(32): p. 11821-7.
41. Christoforidis, S. and M. Zerial, *Purification and identification of novel Rab effectors using affinity chromatography*. Methods, 2000. **20**(4): p. 403-10.
42. Cai, H., K. Reinisch, and S. Ferro-Novick, *Coats, tethers, Rabs, and SNAREs work together to mediate the intracellular destination of a transport vesicle*. Dev Cell, 2007. **12**(5): p. 671-82.
43. McLauchlan, H., et al., *A novel role for Rab5-GDI in ligand sequestration into clathrin-coated pits*. Curr Biol, 1998. **8**(1): p. 34-45.
44. Haas, A.K., et al., *A GTPase-activating protein controls Rab5 function in endocytic trafficking*. Nat Cell Biol, 2005. **7**(9): p. 887-93.
45. Pagano, A., et al., *In vitro formation of recycling vesicles from endosomes requires adaptor protein-1/clathrin and is regulated by rab4 and the connector rabaptin-5*. Mol Biol Cell, 2004. **15**(11): p. 4990-5000.
46. Mallik, R. and S.P. Gross, *Molecular motors: strategies to get along*. Curr Biol, 2004. **14**(22): p. R971-82.
47. Echard, A., et al., *Interaction of a Golgi-associated kinesin-like protein with Rab6*. Science, 1998. **279**(5350): p. 580-5.
48. Nagashima, K., et al., *Melanophilin directly links Rab27a and myosin Va through its distinct coiled-coil regions*. FEBS Lett, 2002. **517**(1-3): p. 233-8.
49. Fukuda, M., T.S. Kuroda, and K. Mikoshiba, *Slac2-a/melanophilin, the missing link between Rab27 and myosin Va: implications of a tripartite protein complex for melanosome transport*. J Biol Chem, 2002. **277**(14): p. 12432-6.

50. Strom, M., et al., *A family of Rab27-binding proteins. Melanophilin links Rab27a and myosin Va function in melanosome transport.* J Biol Chem, 2002. **277**(28): p. 25423-30.
51. Pfeffer, S.R., *Transport vesicle docking: SNAREs and associates.* Annu Rev Cell Dev Biol, 1996. **12**: p. 441-61.
52. Pfeffer, S.R., *Transport-vesicle targeting: tethers before SNAREs.* Nat Cell Biol, 1999. **1**(1): p. E17-22.
53. Sonnichsen, B., et al., *A role for giantin in docking COPI vesicles to Golgi membranes.* J Cell Biol, 1998. **140**(5): p. 1013-21.
54. Nakamura, N., et al., *The vesicle docking protein p115 binds GM130, a cis-Golgi matrix protein, in a mitotically regulated manner.* Cell, 1997. **89**(3): p. 445-55.
55. Chen, Y.A. and R.H. Scheller, *SNARE-mediated membrane fusion.* Nat Rev Mol Cell Biol, 2001. **2**(2): p. 98-106.
56. Ohya, T., et al., *Reconstitution of Rab- and SNARE-dependent membrane fusion by synthetic endosomes.* Nature, 2009. **459**(7250): p. 1091-7.
57. Sivars, U., D. Aivazian, and S.R. Pfeffer, *Yip3 catalyses the dissociation of endosomal Rab-GDI complexes.* Nature, 2003. **425**(6960): p. 856-9.
58. Chavrier, P., et al., *Hypervariable C-terminal domain of rab proteins acts as a targeting signal.* Nature, 1991. **353**(6346): p. 769-72.
59. Calero, M., et al., *Dual prenylation is required for Rab protein localization and function.* Mol Biol Cell, 2003. **14**(5): p. 1852-67.
60. Gomes, A.Q., et al., *Membrane targeting of Rab GTPases is influenced by the prenylation motif.* Mol Biol Cell, 2003. **14**(5): p. 1882-99.
61. Ali, B.R., et al., *Multiple regions contribute to membrane targeting of Rab GTPases.* J Cell Sci, 2004. **117**(Pt 26): p. 6401-12.
62. Seachrist, J.L. and S.S. Ferguson, *Regulation of G protein-coupled receptor endocytosis and trafficking by Rab GTPases.* Life Sci, 2003. **74**(2-3): p. 225-35.
63. Woodman, P.G., *Biogenesis of the sorting endosome: the role of Rab5.* Traffic, 2000. **1**(9): p. 695-701.
64. van der Sluijs, P., et al., *The small GTP-binding protein rab4 controls an early sorting event on the endocytic pathway.* Cell, 1992. **70**(5): p. 729-40.
65. Ullrich, O., et al., *Rab11 regulates recycling through the pericentriolar recycling endosome.* J Cell Biol, 1996. **135**(4): p. 913-24.
66. Schimmoller, F. and H. Riezman, *Involvement of Ypt7p, a small GTPase, in traffic from late endosome to the vacuole in yeast.* J Cell Sci, 1993. **106** (Pt 3): p. 823-30.
67. Riederer, M.A., et al., *Lysosome biogenesis requires Rab9 function and receptor recycling from endosomes to the trans-Golgi network.* J Cell Biol, 1994. **125**(3): p. 573-82.

68. Plutner, H., et al., *Rab1b regulates vesicular transport between the endoplasmic reticulum and successive Golgi compartments*. J Cell Biol, 1991. **115**(1): p. 31-43.
69. Sakurada, K., et al., *Molecular cloning and characterization of a ras p21-like GTP-binding protein (24KG) from rat liver*. Biochem Biophys Res Commun, 1991. **177**(3): p. 1224-32.
70. Lai, F., L. Stubbs, and K. Artzt, *Molecular analysis of mouse Rab11b: a new type of mammalian YPT/Rab protein*. Genomics, 1994. **22**(3): p. 610-6.
71. Goldenring, J.R., et al., *Identification of a small GTP-binding protein, Rab25, expressed in the gastrointestinal mucosa, kidney, and lung*. J Biol Chem, 1993. **268**(25): p. 18419-22.
72. Chen, W., et al., *Rab11 is required for trans-golgi network-to-plasma membrane transport and a preferential target for GDP dissociation inhibitor*. Mol Biol Cell, 1998. **9**(11): p. 3241-57.
73. Ren, M., et al., *Hydrolysis of GTP on rab11 is required for the direct delivery of transferrin from the pericentriolar recycling compartment to the cell surface but not from sorting endosomes*. Proc Natl Acad Sci U S A, 1998. **95**(11): p. 6187-92.
74. Wilcke, M., et al., *Rab11 regulates the compartmentalization of early endosomes required for efficient transport from early endosomes to the trans-golgi network*. J Cell Biol, 2000. **151**(6): p. 1207-20.
75. Goldenring, J.R., et al., *Rab11 is an apically located small GTP-binding protein in epithelial tissues*. Am J Physiol, 1996. **270**(3 Pt 1): p. G515-25.
76. Goldenring, J.R., et al., *Enrichment of rab11, a small GTP-binding protein, in gastric parietal cells*. Am J Physiol, 1994. **267**(2 Pt 1): p. G187-94.
77. Kikuchi, A., et al., *Purification and characterization of a novel GTP-binding protein with a molecular weight of 24,000 from bovine brain membranes*. J Biol Chem, 1988. **263**(6): p. 2897-904.
78. Chavrier, P., et al., *Molecular cloning of YPT1/SEC4-related cDNAs from an epithelial cell line*. Mol Cell Biol, 1990. **10**(12): p. 6578-85.
79. Chavrier, P., K. Simons, and M. Zerial, *The complexity of the Rab and Rho GTP-binding protein subfamilies revealed by a PCR cloning approach*. Gene, 1992. **112**(2): p. 261-4.
80. Sonnichsen, B., et al., *Distinct membrane domains on endosomes in the recycling pathway visualized by multicolor imaging of Rab4, Rab5, and Rab11*. J Cell Biol, 2000. **149**(4): p. 901-14.
81. Trischler, M., W. Stoorvogel, and O. Ullrich, *Biochemical analysis of distinct Rab5- and Rab11-positive endosomes along the transferrin pathway*. J Cell Sci, 1999. **112** (Pt 24): p. 4773-83.
82. Mostov, K., et al., *Plasma membrane protein sorting in polarized epithelial cells*. J Cell Biol, 1992. **116**(3): p. 577-83.

83. Apodaca, G., L.A. Katz, and K.E. Mostov, *Receptor-mediated transcytosis of IgA in MDCK cells is via apical recycling endosomes*. J Cell Biol, 1994. **125**(1): p. 67-86.
84. Casanova, J.E., et al., *Association of Rab25 and Rab11a with the apical recycling system of polarized Madin-Darby canine kidney cells*. Mol Biol Cell, 1999. **10**(1): p. 47-61.
85. Hunziker, W. and P.J. Peters, *Rab17 localizes to recycling endosomes and regulates receptor-mediated transcytosis in epithelial cells*. J Biol Chem, 1998. **273**(25): p. 15734-41.
86. Leung, S.M., W.G. Ruiz, and G. Apodaca, *Sorting of membrane and fluid at the apical pole of polarized Madin-Darby canine kidney cells*. Mol Biol Cell, 2000. **11**(6): p. 2131-50.
87. Schlierf, B., et al., *Rab11b is essential for recycling of transferrin to the plasma membrane*. Exp Cell Res, 2000. **259**(1): p. 257-65.
88. Prigozhina, N.L. and C.M. Waterman-Storer, *Decreased polarity and increased random motility in PtK1 epithelial cells correlate with inhibition of endosomal recycling*. J Cell Sci, 2006. **119**(Pt 17): p. 3571-82.
89. Lapierre, L.A., et al., *Rab11b resides in a vesicular compartment distinct from Rab11a in parietal cells and other epithelial cells*. Exp Cell Res, 2003. **290**(2): p. 322-31.
90. Khvotchev, M.V., et al., *Divergent functions of neuronal Rab11b in Ca²⁺-regulated versus constitutive exocytosis*. J Neurosci, 2003. **23**(33): p. 10531-9.
91. Calhoun, B.C., et al., *Rab11a redistributes to apical secretory canaliculus during stimulation of gastric parietal cells*. Am J Physiol, 1998. **275**(1 Pt 1): p. C163-70.
92. Duman, J.G., et al., *Expression of rab11a N124I in gastric parietal cells inhibits stimulatory recruitment of the H⁺-K⁺-ATPase*. Am J Physiol, 1999. **277**(3 Pt 1): p. C361-72.
93. Wang, X., et al., *Regulation of vesicle trafficking in madin-darby canine kidney cells by Rab11a and Rab25*. J Biol Chem, 2000. **275**(37): p. 29138-46.
94. Wakabayashi, Y., J. Lippincott-Schwartz, and I.M. Arias, *Intracellular trafficking of bile salt export pump (ABCB11) in polarized hepatic cells: constitutive cycling between the canalicular membrane and rab11-positive endosomes*. Mol Biol Cell, 2004. **15**(7): p. 3485-96.
95. Swiatecka-Urban, A., et al., *The short apical membrane half-life of rescued uF508-CFTR results from accelerated endocytosis uF508-CFTR in polarized human airway epithelial cells*. J Biol Chem, 2005.
96. Sugawara, K., et al., *Rab11 and its effector Rip11 participate in regulation of insulin granule exocytosis*. Genes Cells, 2009. **14**(4): p. 445-56.
97. Kerem, B., et al., *Identification of the cystic fibrosis gene: genetic analysis*. Science, 1989. **245**(4922): p. 1073-80.
98. Riordan, J.R., et al., *Identification of the cystic fibrosis gene: cloning and characterization of complementary DNA*. Science, 1989. **245**(4922): p. 1066-73.

99. Kopito, R.R., *Biosynthesis and degradation of CFTR*. *Physiol Rev*, 1999. **79**(1 Suppl): p. S167-73.
100. Cheng, S.H., et al., *Defective intracellular transport and processing of CFTR is the molecular basis of most cystic fibrosis*. *Cell*, 1990. **63**(4): p. 827-34.
101. Lewis, M.J., et al., *Cystic fibrosis*. *Am J Clin Pathol*, 2003. **120 Suppl**: p. S3-13.
102. Hanrahan, J.W. and M.A. Wioland, *Revisiting cystic fibrosis transmembrane conductance regulator structure and function*. *Proc Am Thorac Soc*, 2004. **1**(1): p. 17-21.
103. Cheng, S.H., et al., *Phosphorylation of the R domain by cAMP-dependent protein kinase regulates the CFTR chloride channel*. *Cell*, 1991. **66**(5): p. 1027-36.
104. Anderson, M.P., et al., *Nucleoside triphosphates are required to open the CFTR chloride channel*. *Cell*, 1991. **67**(4): p. 775-84.
105. Chang, X.B., et al., *Mapping of cystic fibrosis transmembrane conductance regulator membrane topology by glycosylation site insertion*. *J Biol Chem*, 1994. **269**(28): p. 18572-5.
106. Chang, X.B., et al., *Role of N-linked oligosaccharides in the biosynthetic processing of the cystic fibrosis membrane conductance regulator*. *J Cell Sci*, 2008. **121**(Pt 17): p. 2814-23.
107. Gluzman, R., et al., *N-glycans are direct determinants of CFTR folding and stability in secretory and endocytic membrane traffic*. *J Cell Biol*, 2009. **184**(6): p. 847-62.
108. Picciotto, M.R., et al., *Phosphorylation of the cystic fibrosis transmembrane conductance regulator*. *J Biol Chem*, 1992. **267**(18): p. 12742-52.
109. Hanrahan, J.W., et al., *Regulation of the CFTR chloride channel from humans and sharks*. *J Exp Zool*, 1996. **275**(4): p. 283-91.
110. Crawford, I., et al., *Immunocytochemical localization of the cystic fibrosis gene product CFTR*. *Proc Natl Acad Sci U S A*, 1991. **88**(20): p. 9262-6.
111. Webster, P., et al., *Subcellular localization of CFTR to endosomes in a ductal epithelium*. *Am J Physiol*, 1994. **267**(2 Pt 1): p. C340-8.
112. Cohn, J.A., et al., *Characterization of the cystic fibrosis transmembrane conductance regulator in a colonocyte cell line*. *Proc Natl Acad Sci U S A*, 1992. **89**(6): p. 2340-4.
113. Denning, G.M., et al., *Localization of cystic fibrosis transmembrane conductance regulator in chloride secretory epithelia*. *J Clin Invest*, 1992. **89**(1): p. 339-49.
114. Prince, L.S., A. Tousson, and R.B. Marchase, *Cell surface labeling of CFTR in T84 cells*. *Am J Physiol*, 1993. **264**(2 Pt 1): p. C491-8.
115. Lukacs, G.L., et al., *The cystic fibrosis transmembrane regulator is present and functional in endosomes. Role as a determinant of endosomal pH*. *J Biol Chem*, 1992. **267**(21): p. 14568-72.

116. Biwersi, J. and A.S. Verkman, *Functional CFTR in endosomal compartment of CFTR-expressing fibroblasts and T84 cells*. Am J Physiol, 1994. **266**(1 Pt 1): p. C149-56.
117. Bradbury, N.A., et al., *Biochemical and biophysical identification of cystic fibrosis transmembrane conductance regulator chloride channels as components of endocytic clathrin-coated vesicles*. J Biol Chem, 1994. **269**(11): p. 8296-302.
118. Bertrand, C.A. and R.A. Frizzell, *The role of regulated CFTR trafficking in epithelial secretion*. Am J Physiol Cell Physiol, 2003. **285**(1): p. C1-18.
119. Varga, K., et al., *Efficient Intracellular processing of the endogenous cystic fibrosis transmembrane conductance regulator in epithelial cell lines*. J Biol Chem, 2004.
120. Sun, F., et al., *E3KARP mediates the association of ezrin and protein kinase A with the cystic fibrosis transmembrane conductance regulator in airway cells*. J Biol Chem, 2000. **275**(38): p. 29539-46.
121. Weixel, K.M. and N.A. Bradbury, *The carboxyl terminus of the cystic fibrosis transmembrane conductance regulator binds to AP-2 clathrin adaptors*. J Biol Chem, 2000. **275**(5): p. 3655-60.
122. Prince, L.S., R.B. Workman, Jr., and R.B. Marchase, *Rapid endocytosis of the cystic fibrosis transmembrane conductance regulator chloride channel*. Proc Natl Acad Sci U S A, 1994. **91**(11): p. 5192-6.
123. Swiatecka-Urban, A., et al., *Myosin Vb is required for trafficking of the cystic fibrosis transmembrane conductance regulator in Rab11a-specific apical recycling endosomes in polarized human airway epithelial cells*. J Biol Chem, 2007. **282**(32): p. 23725-36.
124. Bilan, F., et al., *Endosomal SNARE proteins regulate CFTR activity and trafficking in epithelial cells*. Exp Cell Res, 2008. **314**(11-12): p. 2199-211.
125. Ganeshan, R., et al., *CFTR surface expression and chloride currents are decreased by inhibitors of N-WASP and actin polymerization*. Biochim Biophys Acta, 2007. **1773**(2): p. 192-200.
126. Ameen, N.A., et al., *CFTR channel insertion to the apical surface in rat duodenal villus epithelial cells is upregulated by VIP in vivo*. J Cell Sci, 1999. **112** (Pt 6): p. 887-94.
127. Chappe, F., et al., *Vasoactive intestinal peptide increases cystic fibrosis transmembrane conductance regulator levels in the apical membrane of Calu-3 cells through a protein kinase C-dependent mechanism*. J Pharmacol Exp Ther, 2008. **327**(1): p. 226-38.
128. Dharmasathaphorn, K., et al., *A human colonic tumor cell line that maintains vectorial electrolyte transport*. Am J Physiol, 1984. **246**(2 Pt 1): p. G204-8.
129. Nataro, J.P., et al., *T84 cells in culture as a model for enteroaggregative Escherichia coli pathogenesis*. Infect Immun, 1996. **64**(11): p. 4761-8.
130. Dharmasathaphorn, K., et al., *Vasoactive intestinal polypeptide-induced chloride secretion by a colonic epithelial cell line. Direct participation of a basolaterally localized Na⁺,K⁺,Cl⁻ cotransport system*. J Clin Invest, 1985. **75**(2): p. 462-71.

131. Cartwright, C.A., et al., *Synergistic action of cyclic adenosine monophosphate- and calcium-mediated chloride secretion in a colonic epithelial cell line*. J Clin Invest, 1985. **76**(5): p. 1837-42.
132. Mandel, K.G., K. Dharmasathaphorn, and J.A. McRoberts, *Characterization of a cyclic AMP-activated Cl-transport pathway in the apical membrane of a human colonic epithelial cell line*. J Biol Chem, 1986. **261**(2): p. 704-12.
133. Bell, C.L. and P.M. Quinton, *T84 cells: anion selectivity demonstrates expression of Cl-conductance affected in cystic fibrosis*. Am J Physiol, 1992. **262**(3 Pt 1): p. C555-62.
134. Gregory, R.J., et al., *Expression and characterization of the cystic fibrosis transmembrane conductance regulator*. Nature, 1990. **347**(6291): p. 382-6.
135. Barrett, K.E., *Positive and negative regulation of chloride secretion in T84 cells*. Am J Physiol, 1993. **265**(4 Pt 1): p. C859-68.
136. Barrett, K.E. and S.J. Keely, *Chloride secretion by the intestinal epithelium: molecular basis and regulatory aspects*. Annu Rev Physiol, 2000. **62**: p. 535-72.
137. Bradbury, N.A. and R.J. Bridges, *Role of membrane trafficking in plasma membrane solute transport*. Am J Physiol, 1994. **267**(1 Pt 1): p. C1-24.
138. Chan, H.C., et al., *Antibody against a cystic fibrosis transmembrane conductance regulator-derived synthetic peptide inhibits anion currents in human colonic cell line T84*. J Biol Chem, 1992. **267**(12): p. 8411-6.
139. Berger, H.A., et al., *Identification and regulation of the cystic fibrosis transmembrane conductance regulator-generated chloride channel*. J Clin Invest, 1991. **88**(4): p. 1422-31.
140. Wagner, J.A., et al., *Antisense oligodeoxynucleotides to the cystic fibrosis transmembrane conductance regulator inhibit cAMP-activated but not calcium-activated chloride currents*. Proc Natl Acad Sci U S A, 1992. **89**(15): p. 6785-9.
141. Clarke, L.L., et al., *Relationship of a non-cystic fibrosis transmembrane conductance regulator-mediated chloride conductance to organ-level disease in Cftr(-/-) mice*. Proc Natl Acad Sci U S A, 1994. **91**(2): p. 479-83.
142. Rogers, C.S., et al., *Disruption of the CFTR gene produces a model of cystic fibrosis in newborn pigs*. Science, 2008. **321**(5897): p. 1837-41.
143. Ameen, N.A., et al., *Subcellular distribution of CFTR in rat intestine supports a physiologic role for CFTR regulation by vesicle traffic*. Histochem Cell Biol, 2000. **114**(3): p. 219-28.
144. Zeitlin, P.L., et al., *CFTR protein expression in primary and cultured epithelia*. Proc Natl Acad Sci U S A, 1992. **89**(1): p. 344-7.
145. Ameen, N. and G. Apodaca, *Defective CFTR apical endocytosis and enterocyte brush border in myosin VI-deficient mice*. Traffic, 2007(8): p. 998-1006.

146. Swiatecka-Urban, A., et al., *Myosin VI regulates endocytosis of the cystic fibrosis transmembrane conductance regulator*. J Biol Chem, 2004. **279**(36): p. 38025-31.
147. Zerial, M. and H. McBride, *Rab proteins as membrane organizers*. Nat Rev Mol Cell Biol, 2001. **2**(2): p. 107-17.
148. Chao, A.C., et al., *Fluorescence measurement of chloride transport in monolayer cultured cells. Mechanisms of chloride transport in fibroblasts*. Biophys J, 1989. **56**(6): p. 1071-81.
149. Tousson, A., C.M. Fuller, and D.J. Benos, *Apical recruitment of CFTR in T-84 cells is dependent on cAMP and microtubules but not Ca²⁺ or microfilaments*. J Cell Sci, 1996. **109** (Pt 6): p. 1325-34.
150. Simpson, J.C., et al., *A role for the small GTPase Rab21 in the early endocytic pathway*. J Cell Sci, 2004. **117**(Pt 26): p. 6297-311.
151. Opdam, F.J., et al., *Expression of Rab small GTPases in epithelial Caco-2 cells: Rab21 is an apically located GTP-binding protein in polarised intestinal epithelial cells*. Eur J Cell Biol, 2000. **79**(5): p. 308-16.
152. Gorvel, J.P., et al., *rab5 controls early endosome fusion in vitro*. Cell, 1991. **64**(5): p. 915-25.
153. Junutula, J.R., et al., *Molecular characterization of Rab11 interactions with members of the family of Rab11-interacting proteins*. J Biol Chem, 2004. **279**(32): p. 33430-7.
154. Ameen, N., M. Silvis, and N.A. Bradbury, *Endocytic trafficking of CFTR in health and disease*. J Cyst Fibros, 2007. **6**(1): p. 1-14.
155. Uzan-Gafsou, S., et al., *Rab11A controls the biogenesis of Birbeck granules by regulating Langerin recycling and stability*. Mol Biol Cell, 2007. **18**(8): p. 3169-79.
156. Scapin, S.M., et al., *The crystal structure of the small GTPase Rab11b reveals critical differences relative to the Rab11a isoform*. J Struct Biol, 2006. **154**(3): p. 260-8.
157. Tuma, P.L., L.K. Nyasae, and A.L. Hubbard, *Nonpolarized cells selectively sort apical proteins from cell surface to a novel compartment, but lack apical retention mechanisms*. Mol Biol Cell, 2002. **13**(10): p. 3400-15.
158. Gentsch, M., et al., *Endocytic trafficking routes of wild-type and {Delta}F508 CFTR*. Mol Biol Cell, 2004.
159. Bilan, F., et al., *Syntaxin 8 impairs trafficking of cystic fibrosis transmembrane conductance regulator (CFTR) and inhibits its channel activity*. J Cell Sci, 2004. **Pt.**
160. Bebok, Z., et al., *Failure of cAMP agonists to activate rescued deltaF508 CFTR in CFBE41o- airway epithelial monolayers*. J Physiol, 2005. **569**(Pt 2): p. 601-15.
161. Guggino, W.B. and B.A. Stanton, *New insights into cystic fibrosis: molecular switches that regulate CFTR*. Nat Rev Mol Cell Biol, 2006. **7**(6): p. 426-36.
162. Lapierre, L.A., et al., *Myosin vb is associated with plasma membrane recycling systems*. Mol Biol Cell, 2001. **12**(6): p. 1843-57.

163. Sharma, M., et al., *Misfolding diverts CFTR from recycling to degradation: quality control at early endosomes*. J Cell Biol, 2004. **164**(6): p. 923-33.
164. Prince, L.S., et al., *Efficient endocytosis of the cystic fibrosis transmembrane conductance regulator requires a tyrosine-based signal*. J Biol Chem, 1999. **274**(6): p. 3602-9.
165. Ivanov, A.I., *Actin motors that drive formation and disassembly of epithelial apical junctions*. Front Biosci, 2008. **13**: p. 6662-81.
166. Yeaman, C., K.K. Grindstaff, and W.J. Nelson, *New perspectives on mechanisms involved in generating epithelial cell polarity*. Physiol Rev, 1999. **79**(1): p. 73-98.
167. Prat, A.G., et al., *Actin filament organization is required for proper cAMP-dependent activation of CFTR*. Am J Physiol, 1999. **277**(6 Pt 1): p. C1160-9.
168. Chasan, B., et al., *Evidence for direct interaction between actin and the cystic fibrosis transmembrane conductance regulator*. Eur Biophys J, 2002. **30**(8): p. 617-24.
169. Thelin, W.R., et al., *Direct interaction with filamins modulates the stability and plasma membrane expression of CFTR*. J Clin Invest, 2007. **117**(2): p. 364-74.
170. Okiyoneda, T. and G.L. Lukacs, *Cell surface dynamics of CFTR: the ins and outs*. Biochim Biophys Acta, 2007. **1773**(4): p. 476-9.
171. Haggie, P.M., et al., *Tracking of quantum dot-labeled CFTR shows near immobilization by C-terminal PDZ interactions*. Mol Biol Cell, 2006. **17**(12): p. 4937-45.
172. Wittmann, J.G. and M.G. Rudolph, *Crystal structure of Rab9 complexed to GDP reveals a dimer with an active conformation of switch II*. FEBS Lett, 2004. **568**(1-3): p. 23-9.
173. Pasqualato, S., et al., *The structural GDP/GTP cycle of Rab11 reveals a novel interface involved in the dynamics of recycling endosomes*. J Biol Chem, 2004. **279**(12): p. 11480-8.
174. Wallace, D.M., et al., *The novel Rab11-FIP/Rip/RCP family of proteins displays extensive homo- and hetero-interacting abilities*. Biochem Biophys Res Commun, 2002. **292**(4): p. 909-15.
175. Lapierre, L.A. and J.R. Goldenring, *Interactions of myosin vb with rab11 family members and cargoes traversing the plasma membrane recycling system*. Methods Enzymol, 2005. **403**: p. 715-23.
176. Ding, J., et al., *Tyrosine phosphorylation of the Rab24 GTPase in cultured mammalian cells*. Biochem Biophys Res Commun, 2003. **312**(3): p. 670-5.
177. Prekeris, R., J. Klumperman, and R.H. Scheller, *A Rab11/Rip11 protein complex regulates apical membrane trafficking via recycling endosomes*. Mol Cell, 2000. **6**(6): p. 1437-48.
178. Hamelin, E., et al., *The intracellular trafficking of the G protein-coupled receptor TPbeta depends on a direct interaction with Rab11*. J Biol Chem, 2005.

179. Smythe, E., *Direct interactions between rab GTPases and cargo*. Mol Cell, 2002. **9**(2): p. 205-6.
180. van, I.S.C., et al., *Direct interaction between Rab3b and the polymeric immunoglobulin receptor controls ligand-stimulated transcytosis in epithelial cells*. Dev Cell, 2002. **2**(2): p. 219-28.
181. Wikstrom, K., et al., *Recycling of the human prostacyclin receptor is regulated through a direct interaction with Rab11a GTPase*. Cell Signal, 2008. **20**(12): p. 2332-46.
182. van de Graaf, S.F., et al., *Direct interaction with Rab11a targets the epithelial Ca²⁺ channels TRPV5 and TRPV6 to the plasma membrane*. Mol Cell Biol, 2006. **26**(1): p. 303-12.
183. Hallows, K.R., et al., *Physiological modulation of CFTR activity by AMP-activated protein kinase in polarized T84 cells*. Am J Physiol Cell Physiol, 2003. **284**(5): p. C1297-308.
184. Ameen, N.A., et al., *A unique subset of rat and human intestinal villus cells express the cystic fibrosis transmembrane conductance regulator*. Gastroenterology, 1995. **108**(4): p. 1016-23.
185. Ameen, N.A., C. Marino, and P.J. Salas, *cAMP-dependent exocytosis and vesicle traffic regulate CFTR and fluid transport in rat jejunum in vivo*. Am J Physiol Cell Physiol, 2003. **284**(2): p. C429-38.
186. Howard, M., et al., *Epitope tagging permits cell surface detection of functional CFTR*. Am J Physiol, 1995. **269**(6 Pt 1): p. C1565-76.
187. Yang, Y., et al., *Molecular basis of defective anion transport in L cells expressing recombinant forms of CFTR*. Hum Mol Genet, 1993. **2**(8): p. 1253-61.
188. Butterworth, M.B., et al., *Acute ENaC stimulation by cAMP in a kidney cell line is mediated by exocytic insertion from a recycling channel pool*. J Gen Physiol, 2005. **125**(1): p. 81-101.
189. Elferink, L.A. and D.J. Strick, *Functional properties of rab15 effector protein in endocytic recycling*. Methods Enzymol, 2005. **403**: p. 732-43.